

Extracellular vesicle therapeutics

A translational perspective

Proefschrift

ter verkrijging van
de graad van Doctor aan de Universiteit Leiden
op gezag van Rector Magnificus ...,
volgens besluit van het College voor Promoties
te verdedigen op dag
klokke uur

... des middags te ... uur

door

Emma Alise Mol

geboren op 3 oktober 1992
te Nunspeet

Promotoren:

Prof. Dr. M.J. Goumans

Prof. Dr. J.P.G. Sluijter

Copromotoren:

Dr. P. Vader

Promotiecommissie:

Table of content

Chapter 1	Cardiac progenitor-cell derived exosomes as cell-free therapeutic for cardiac repair	4
Chapter 2	Higher functionality of extracellular vesicles isolated using size-exclusion chromatography compared to ultracentrifugation	19
Chapter 3	Cardiac progenitor-derived extracellular vesicles do not reduce infarct size after myocardial infarction in mice, independently of isolation method	30
Chapter 4	Injectable supramolecular ureidopyrimidinone hydrogels provide sustained release of extracellular vesicle therapeutics	45
Chapter 5	Effect of storage conditions on extracellular vesicle functionality <i>in vitro</i> and <i>in vivo</i>	63
Chapter 6	Summary and general discussion	80

Nederlandse Samenvatting

Dankwoord

Curriculum Vitae

List of Publications

Chapter 1

Cardiac progenitor-cell derived exosomes as cell-free therapeutic for cardiac repair

Emma A. Mol MSc^{1,2}, Marie-José Goumans PhD², Joost P.G. Sluijter PhD^{1,3,4}

In: Exosomes in Cardiovascular Disease. Advances in Experimental Medicine and Biology 2017

¹Department of Cardiology, Laboratory of Experimental Cardiology, University Medical Center Utrecht, Utrecht 3584CX, The Netherlands

²Department of Cardiovascular Cell Biology, Department of Cell and Chemical Biology, Leiden University Medical Center, Leiden 2333ZA, The Netherlands

³UMC Utrecht Regenerative Medicine Center, University Medical Center, Utrecht 3584CT, The Netherlands

⁴Netherlands Heart Institute, Utrecht 3584CX, The Netherlands

Introduction

Myocardial infarction (MI) is one of the leading causes of death in the western world¹. MI is induced by occlusion of one or more coronary arteries that supply oxygen to the heart, resulting in necrosis and apoptosis of cardiomyocytes that are highly dependent of oxygen. As a result, different molecular and cellular mechanisms are activated roughly in two phases. First, as necrotic cardiomyocytes release danger signals into the myocardium, the immune system is activated via toll-like receptors and complement activation². This inflammatory response causes the attraction of neutrophils and monocytes to the infarcted area and is necessary to remove cellular debris. An overactive immune system can promote further tissue damage and infarct expansion³. The second step is a reparative phase characterized by activated fibroblasts (myofibroblasts) that produce excessive amounts of extracellular matrix, resulting in the formation of scar tissue⁴. Initially this scar tissue replaces the lost cardiomyocytes and provides strength to the heart to maintain its integrity, however, later progressive matrix deposition by activated myofibroblasts might lead to myocardial stiffening and impaired contraction. Since the initial myocardial damage is caused by a perfusion defect, stimulating neovessel formation or promoting arteriogenesis could contribute to cardiac regeneration^{5,6}. Cardiac repair mechanisms may be improved by interfering in these reparative mechanisms that play a role after MI by down-tuning the detrimental processes, such as cardiomyocyte apoptosis, the inflammatory response, and fibrosis, and promoting further reparative signals like angiogenesis (Figure 1).

Of all patients that suffer from MI, approximately 25% will develop heart failure within one year⁷. Currently, the only long-term treatment option for heart failure patients is heart transplantation, but donor availability is limited. Although patients waiting for heart transplantation can benefit from a left ventricular assist device (LVAD) taking over the pump function of the heart, this is usually a temporary solution⁸. Therefore, new treatment options are explored to replace the lost cardiomyocytes and improve contractility in cardiac diseases, especially for heart failure patients.

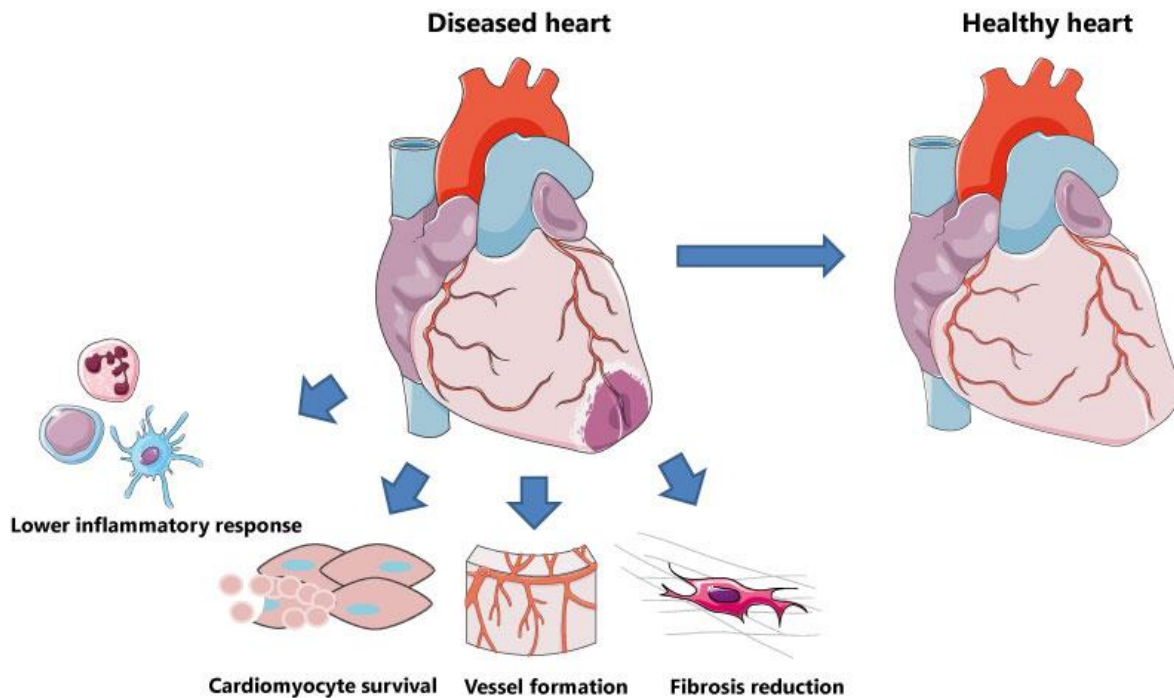


Figure 1 Processes that need additional adaptations to further induce cardiac repair after myocardial infarction. Adjusted from Servier Medical Art at www.Servier.com, licensed under a Creative Commons Attribution 3.0 Unported License.

Cardiac progenitor cells as potent potential cell type for myocardial repair

One of the first authors describing the existence of cardiomyocyte regeneration was Oberpriller et al⁹. Amputation of the ventricular apex of the newt heart resulted in the renewal of cardiomyocytes by re-entry into the cell cycle and proper engraftment in the myocardium. Also resection of the ventricular apex in zebrafish resulted in complete apical regeneration, mainly due to proliferation of progenitor cells in the heart and possibly also by dedifferentiation of residing cardiomyocytes^{10,11}.

For decades it was believed that the mammalian heart had no regenerative capacity. Recent studies provided evidence for a limited but true regenerative potential of the heart¹²⁻¹⁴. Bergmann et al. demonstrated the ability of the heart to regenerate by quantifying carbon-14 incorporation into the DNA of human cardiomyocytes¹³. Approximately 1% of the cardiomyocytes is renewed at an age of 25; this capacity is fast reduced upon aging and in sharp contrast to cardiac resident non-cardiomyocytes with a renewel rate of approximately 15%¹⁵.

Recently, a human case study of a newborn reported functional recovery of the human heart suffering from MI at this early age¹⁶. As a result of these observations, several new strategies have been explored to stimulate the regenerative capacity of the mammalian heart.

One of the strategies is the use of progenitor cell treatment as potential therapy to improve cardiac repair and prevent further damage in cardiac diseases. Several cell sources have been studied over the years and used to stimulate myocardial repair; these so-called first generation patient-derived cells include bone-marrow mononuclear cells (BM-MNCs)¹⁷⁻¹⁹ and mesenchymal progenitor cells (MSCs)^{20,21}. The use of BM-MNCs and MSCs for cardiac repair are explored extensively due to their quick and relative easy clinical application. Furthermore, large numbers of cells could be achieved by culturing MSCs under good manufacturing practice conditions for clinical use^{21,22}. Meta-analysis of pre-clinical and clinical studies showed that injection of MSCs, in contrast to BM-MNCs, resulted in beneficial effects on cardiac function^{23,24}. MSC therapy was, however, limited to its potential to activate endogenous repair systems in the heart²⁵. More recently, second-generation cells, including cardiac-derived progenitor cells (CPCs)²⁶⁻³⁰ and induced pluripotent stem cell (iPSC)-derived cardiomyocytes^{31,32}, have gained interest as a cell source for myocardial repair, mainly because of their promising regeneration capacity and their intrinsic ability to form contractile cells. iPSC-derived cardiomyocytes are cardiomyocytes generated by reprogramming fibroblasts to pluripotent stem cells using several transcription factors^{31,32}. Despite their true potential to form cardiomyocytes, the main effect of second-generation cells, observed upon cardiac transplantation, has been of paracrine origin. Excellent recent reviews describing the most relevant results and current limitations of cell-based therapies have been recently reported^{33,34}.

The existence of progenitor cells in the heart was first described by Beltrami et al.²⁸, but since then several cardiac progenitor cell populations have been identified²⁶⁻³⁰. CPCs are potentially the most promising adult cells for cardiac therapy as they can generate all cardiovascular lineages *in vitro* and *in vivo*^{27,35,36}. Since they originate from the heart itself, CPCs may be destined to activate endogenous repair mechanisms. Therefore, CPCs hold greater cardiac regeneration potential compared to BM-MNCs or MSCs.

In different animal models for myocardial infarction, injection of CPCs increased cardiac performance³⁷⁻⁴⁰. However, although cardiac function was improved, cell engraftment of the injected cells in the myocardium was low, as indicated before for BM-MNC and MSCs. To stimulate cell survival upon myocardial injection, pre-treatment of CPCs with e.g. pim-1 or necrostatin-1 before CPC injection has been investigated^{41,42}. To further improve cell retention and prevent immediate flush-out⁴³, different approaches have been investigated, e.g. the use of cell clusters or a combination of cells with microcarriers^{44,45}. These approaches resulted in

increased cell retention and survival, however, the additional beneficial effects on cardiac function was minimal.

Comparison of CPC types

Although the heart has poor regenerative potential, many cardiac progenitor cell types have been identified based on marker expression/morphology, including Sca1+, c-kit+, cardiosphere-derived cells (CDCs) and cardiospheres (CSPs), and all these types can be isolated from the heart successfully²⁶⁻³⁰. As the existence of so many CPC populations is counterintuitive, Gaetani et al. have compared the different CPC types⁴⁶. Using their individual isolation methods, several of these progenitor cell types have been cultured and the gene expression profiles were compared to define differences between culture propagated CPCs. The gene expression profile of CSPs was most distinct from the Sca1+, c-kit+, and CDCs, most likely due to the monolayer and 3D culture conditions. Additionally, the difference between individual patients was larger than differences between different cell types from a single individual and expression partners are highly overlapping. Interestingly, when these cells were freshly isolated directly from the rodent heart some differences could be observed, indicating that c-kit positive cells were the most primitive progenitor cell⁴⁷. However, this difference is abolished upon culture propagation. Furthermore, Zwetsloot et al. recently compared effect sizes of different types of CPCs⁴⁸, and observed that small differences in effect size can be found based on cell type; CSP treatment resulted in the largest increase in ejection fraction after injection in different animal models compared to e.g. Sca1+ and c-kit+ CPCs, that showed a lower increase in cardiac function. Therefore, the mode of action of different CPC types on the myocardium is largely similar, although slight variations in effect size and transcriptome are described. Interestingly, a strong drop in functional benefit was observed upon their use in rodent and preclinical large animal models.

To date, two clinical trials have used CPCs as cell type for cardiac repair after MI. The SCIPIO (c-kit+ CPC)s and CADUCEUS trial (CDCs) showed that intracoronary infusion of CPCs is safe in patients and led to enhanced cardiac function^{49,50}. Therefore, CPCs are a promising cell type for stem cell therapeutics.

Paracrine secretion

Originally, the concept for myocardial repair by progenitor cells was that they would engraft in the infarcted area and differentiate into functional cardiomyocytes upon injection. Recently, it has become more and more clear from both animal studies and clinical trials that injected progenitor cells do not engraft properly in the cardiac tissue, despite beneficial effects on cardiac function^{37,44,49,50}. Moreover, cardiomyocyte, endothelial, and blood vessel numbers were increased, which led to the hypothesis that the injected progenitor cells exert their effect via release of factors into their environment, called paracrine factors^{37,42,51}. To study the effect of

paracrine secretions, Timmers et al. injected MSC conditioned medium intravenously at the moment of reperfusion in pigs after MI and showed that MSC secretions could mimic the increased cardiac function⁵². This paracrine effect was observed for bone-marrow derived-, and mesenchymal progenitors, but also CPC secretions have these effects. CPC conditioned medium lowered cardiomyocyte apoptosis, stimulated endothelial cell migration, and increased tube formation of endothelial cells *in vitro*^{40,44,53,54}.

In addition to paracrine molecules, the release of extracellular membrane vesicles such as exosomes are of increasing interest. Besides their use as biomarkers to detect early diseases⁵⁵, these nano-sized vesicles have also shown to be important mediators in repair after cardiac injury. Upon receiving stress signals, cells can influence their communication to other cells by adjusting membrane markers and vesicle content. Interestingly, Lai et al. identified the active cardioprotective component in the conditioned medium of MSCs to be exosomes⁵⁶. They showed that upon separation of MSC conditioned medium in fractions of different sizes, the beneficial effects on ischemia/reperfusion injury observed after injection with fractionated MSC conditioned medium could only be reproduced by injecting the fraction containing complexes larger than 1000 kDa. Since progenitor-derived exosomes were found to be the paracrine factors mainly responsible for the observed beneficial effects after progenitor cell injection⁵⁶⁻⁵⁹, the idea that CPC exosomes could be used for this purposes have emerged as potential off-the-shelf therapeutics.

CPC exosomes carry a variety of different proteins, growth factors, mRNAs, and microRNAs (miRNAs). MiRNAs are small non-coding RNAs that can inhibit or degrade mRNA, thereby preventing protein translation. Studies that investigate the effect of CPC exosomes on cardiac repair *in vitro* and *in vivo* are described below.

Functional benefits of CPC exosome treatment

To study the functional benefits of CPC exosomes, CPC exosomes were intramyocardially injected in mice undergoing ischemia-reperfusion of the left coronary artery³⁹. Injection of CPC exosomes reduced cardiomyocyte apoptosis by 53%. In addition, Barile et al. showed that intramyocardial injection of CPC exosomes in mice improved cardiac function after MI⁴⁰. Morphological analysis after CPC exosome treatment in the myocardium revealed reduced scar tissue, lowered cardiomyocyte apoptosis, and increased blood vessel density.

Injection of exosomes from autologous CPCs requires cell expansion *in vitro*, therefore, injection in the chronic phase is more clinically relevant. Therefore, while most studies investigate the effect of CPC exosomes in the acute setting after MI (within a few hours), Tang et al. studied the effect of CPC exosome treatment of an old infarct³⁸. Intracoronary infusion of autologous CPC exosomes in rats one month after MI resulted in less fibrotic tissue and improved cardiac

function. The fact that CPC exosomes still seem to have regenerative effects after a longer time period is promising for patients with chronic cardiac diseases.

To investigate if the release of exosomes from CPCs is critical for cardiac repair *in vivo*, Ibrahim et al. treated CPCs with GW4869, a reversible inhibitor of neutral sphingomyelinase that blocks, among others, exosome production⁵⁴. The CPC-mediated benefits in mice after MI were completely abolished after treatment with GW4869, indicating that exosome release from CPCs is necessary to accomplish the beneficial effects on cardiac function. Altogether, these *in vivo* studies suggest that CPC exosomes induce cardiac repair, by interfering in processes such as cardiomyocyte apoptosis, fibrosis, and vessel formation. The following *in vitro* studies aim to identify the key cardioprotective processes stimulated by CPC exosomes.

Key mechanisms targeted by CPC exosomes

Targeting the different processes that either prevent or reduce cardiac injury or contribute to cardiac regeneration after MI might lead to new treatment options. As described before, MI induces a cascade of molecular and cellular mechanisms in mainly two phases. The first phase is characterized by cardiomyocyte apoptosis and subsequent activation of the immune system. Cardiomyocyte apoptosis is a large contributor to impaired cardiac function after MI, as the major loss of contracting cells is responsible for the reduced contraction capacity of the heart. Preventing cardiomyocyte apoptosis could therefore be one of the mechanisms to improve cardiac injury. Interestingly, CPC exosomes have shown to have anti-apoptotic effects. Chen et al., for example, showed that CPC exosomes prevent apoptosis of H₂O₂-treated cardiomyocytes *in vitro*³⁹. Caspase 3/7 activity in cardiomyocytes was lowered after treatment with CPC exosomes, which is an important mediator of H₂O₂-induced apoptosis. To further identify how CPC exosomes affect oxidative-stress related apoptosis of cardiomyocytes, Xiao et al. focused on exosomal-derived miRNAs⁶⁰. They found that miRNA-21 is upregulated in CPC exosomes exposed to oxidative stress compared to non-exposed CPC exosomes. Interestingly, miRNA-21 targets programmed cell death 4 (PDCD4) in cardiomyocytes, thereby reducing oxidative-stress related apoptosis. Furthermore, miRNA analysis revealed that miRNA-210, miRNA-132, and miRNA-146a are highly enriched in CPC exosomes compared to fibroblast exosomes⁴⁰. By inhibiting downstream targets such as RasGAP-p120, ephrin A3, and PTP1b, these miRNAs inhibit cardiomyocyte apoptosis and enhance endothelial migration after MI. Likewise, CDC and CSP-derived exosomes promote cardiac regeneration, as was shown after injection of these exosomes in the ischemic myocardium⁵⁴. MiRNA analysis comparing CDC exosomes to fibroblast-derived exosomes revealed that miRNA-146a was the most highly enriched in CDC exosomes. Reduced cardiac function after MI was observed for miRNA-146a knockout mice compared to wild-type mice, indicating a role for miRNA-146a in cardiac repair. Pathway

analysis revealed that miRNA-146a is involved in cell survival, cell cycle, and cellular organization, which are important processes involved in cardiac injury.

Upon MI, necrotic/apoptotic cardiomyocytes release danger signals into the environment, thereby activating the immune system via complement activation and toll-like receptors². Although the immune response is required to clear tissue debris after MI, an overactive immune system might aggravate cardiac damage and infarct size³. Therefore, modulating the immune response might prevent/reduce cardiac injury. Progenitor exosomes might be able to modulate this balance in immune responses after MI by delivery of miRNAs, anti-inflammatory cytokines, or other molecules involved in inflammation. This anti-inflammatory response was described for MSC exosomes, as MSC exosomes were capable of switching the macrophage phenotype from the pro-inflammatory M1 to the anti-inflammatory M2 phenotype and suppress T-cell activation⁶¹. Until now, the immune-modulating properties of CPC exosomes have not been described in literature yet.

The second phase after MI involves myofibroblasts that are responsible for reorganizing the structure of the heart, a process called remodeling. Reducing the fibrotic tissue may be a promising way to improve cardiac repair, however, as fibrosis is initially a reparative response, a fine balance between pro- and anti-fibrotic factors is needed. Interestingly, the physiological state of CPCs can influence the secretion and cargo of CPC exosomes. Culturing CPC exosomes under hypoxic conditions resulted in higher tube formation and lowered pro-fibrotic gene expression compared to exosomes cultured under normoxic conditions⁶². Indeed, administration of hypoxic CPC exosomes in mice reduced fibrosis and increased cardiac function compared to normoxic CPC exosomes in an ischemia-reperfusion model. Microarray analysis revealed that eleven miRNAs with anti-fibrotic and pro-angiogenic properties were upregulated compared to normoxic exosomes. Whether the observed beneficial effects of hypoxic CPC exosomes on cardiac function are established through these miRNAs only or if other molecules are also involved needs to be investigated⁶³. Although several *in vivo* studies indeed observed anti-fibrotic effects of CPC exosome treatment after MI^{38,62}, to our knowledge there are no further studies addressing the possible anti-fibrotic mechanism of CPC exosomes so far.

Other cardioprotective mechanisms that could be important for cardiac regeneration are stimulating angiogenesis or arteriogenesis, since the initial myocardial injury is due to a perfusion defect^{5,6}. Progenitor exosomes derived from several cell sources have been described to have pro-angiogenic effects. Sahoo et al., for example, showed that exosomes from human CD34+ progenitor cells mediate their pro-angiogenic activity⁵⁷. After adding exosomes, derived from CD34+ progenitor cells to endothelial cells *in vitro*, they observed increased viability, proliferation, and tube formation of endothelial cells. Furthermore, subcutaneous injection of a matrigel plug containing CD34+ exosomes in mice showed higher vessel formation compared

to injection of a matrigel plug alone. They found that the presence of a pro-angiogenic protein in CD34+ exosomes, sonic hedgehog, was largely responsible for the preserved cardiac function after MI⁵⁸.

This pro-angiogenic property of exosomes was also observed for CPC-derived exosomes. Vrijssen et al. reported that CPC exosomes stimulated migration of endothelial cells in a wound scratch assay⁵³. Analyzing the presence of pro-angiogenic factors in CPC exosomes revealed high expression levels of extracellular matrix metalloproteinase inducer (EMMPRIN), which is present on the exosomal membrane. The migration of endothelial cells upon stimulation with CPC exosomes was not observed upon stimulation with exosomes depleted for EMMPRIN (KD EMMPRIN exosomes). Furthermore, KD EMMPRIN exosomes also inhibited angiogenesis *in vivo*, demonstrated by a reduced influx of cells into a matrigel plug compared to control exosomes after application in mice⁶⁴. Therefore, EMMPRIN is an important mediator of the pro-angiogenic effect of CPC exosomes.

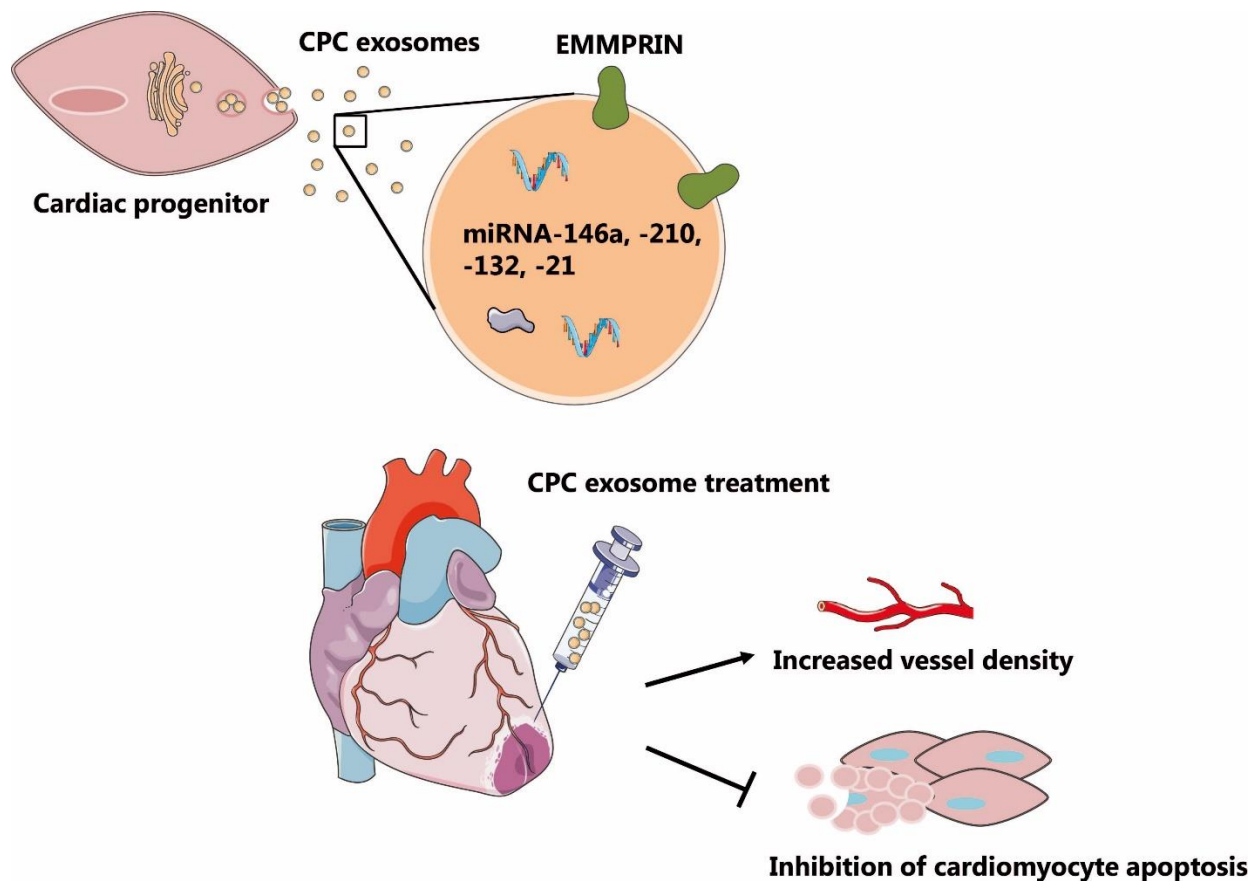


Figure 2 Key mechanisms targeted by CPC exosomes. Adjusted from Servier Medical Art at www.Servier.com, licensed under a Creative Commons Attribution 3.0 Unported License.

Future perspectives

Altogether, these studies provide insights into the ability of CPC exosomes to enhance cardiac repair after injury and the involved mechanisms. The key mechanisms that are influenced by CPC exosomes described so far are neovessel formation and cardiomyocyte apoptosis (Figure 2). Despite considerable efforts have been made to study the effect of CPC exosomes on cardiac repair, many challenges have to be overcome before deployment of exosomes in clinical trials. Firstly, most of the described studies investigated the effect of CPC exosomes on the acute setting after MI^{39,40}. Due to better revascularization therapy and medication planning, the survival of patients after acute MI is increased last decades. These surviving patients, however, have a higher chance to develop a more chronic disease like heart failure. From a clinical perspective it would therefore be useful to study regeneration by CPC exosomes in these more chronic phases after cardiac injury. Another important challenge is retention of exosomes after injection. van den Akker et al. performed intramyocardial injection of stem cells and observed immediate flush-out of the cells upon injection⁴³. It is thus likely that the same flush-out can be expected upon exosome injection into the myocardium, since the exosomes sizes are even smaller (30-100 nm) compared to cells (8-12 μm). Furthermore, accurate mapping of the *in vivo* biodistribution of exosomes after systemic injection is also an important objective before using exosomes in clinical trials. Lai et al. developed an excellent technique to allow multimodal imaging of exosomes *in vivo*. Membrane-bound Gaussia luciferase was combined with metabolic biotinylation to visualize exosomes after systemic injection in athymic nude mice via bioluminescent signals⁶⁵. The highest uptake of exosomes was observed in the liver and spleen, therefore, systemic administration of exosomes might require targeted therapy towards the injured heart. Aiming to target exosomes to the brain, Alvarez-Erviti et al., engineered cells to express an exosomal membrane protein (lysosome-associated membrane glycoprotein 2b) fused to a brain-specific peptide that targets the acetylcholine receptor⁶⁶. They showed increased delivery of functional exosomes to the brain. Thus, although some achievements have been made to engineer exosomes in a way that they target tissues aimed for, by using specific ligands, non-specific accumulation of exosomes in other tissues remains an issue to be solved⁶⁵⁻⁶⁷. Lastly, to cover the high demand of exosomes needed for clinical application, a reproducible and standardized exosome isolation technique is required that allows for upscaling⁶⁸. In addition, the characteristics of exosome-based therapeutics have to be defined properly, which requires more in-depth research into the mechanism of how exosomes exert their therapeutic effects. Nonetheless, CPC exosomes can be considered as potential off-the-shelf therapeutics, as they are able to stimulate the regenerative capacity of the heart mainly by increasing vessel density and lowering apoptosis of cardiomyocytes.

Thesis outline

Extracellular vesicles (EVs) are nano-sized lipid bilayer-enclosed particles that are released by every cell type of the human body studied to date. Mammalian EVs can be classified in three major subclasses according to their intracellular origin⁶⁹. Larger vesicles are generally more heterogeneous in size (50-1000 nm) and are referred to as microvesicles or ectosomes. These microvesicles are formed through direct budding from the plasma membrane. The smaller vesicle population (40-100 nm) is referred to as exosomes, which originate from intraluminal budding of multivesicular endosomes (MVE) and are released upon fusion with the plasma membrane. The last subclass is also more heterogeneous in size (50 nm – 5000 nm) and consists of vesicles that are released when cells are compelled to undergo apoptosis, which are named apoptotic bodies. Despite differences in origin, these subclasses show overlapping characteristics in terms of size, and they lack subtype-specific markers as of yet. As a result, it remains difficult to purify these subpopulations and therefore no uniform nomenclature is currently used⁷⁰. In this thesis, we will use the term 'extracellular vesicles' from now on, to refer to all vesicle subtypes.

The aim of this thesis was to investigate if CPC-derived extracellular vesicles (CPC-EVs) can be used for cardiac repair, and to optimize EV production and delivery processes that could allow for faster clinical application of EV therapeutics.

An overview describing the potential of CPC-EVs as therapeutics post MI was provided in **chapter 1**. Moving towards the use of EVs for therapeutic applications, several aspects need to be addressed that will accelerate their clinical adoption. First, we need a standardized and scalable isolation method that yields sufficient amounts of EVs with maintained functionality. We hypothesized that EV isolation method could affect their functionality. Therefore, in **chapter 2** we compared physicochemical characteristics, as well as *in vitro* functionality of ultracentrifugation-isolated EVs (UC-EV) and ultrafiltration combined with size-exclusion chromatography-isolated EVs (SEC-EV). To validate our *in vitro* findings, we compared UC-EV and SEC-EV in a permanent ligation mouse model, as well as an I/R injury mouse model, in **chapter 3**. We assessed short term infarct size, myocardial deformation parameters, and plasma levels of troponin I after treatment with UC-EV or SEC-EV when compared to PBS treatment.

Strategies are being developed to prolong EV exposure to target organs in order to achieve optimal therapeutic effects. One promising approach to achieve this is using EV-loaded injectable hydrogels. In **chapter 4** we investigated if EV release can be prolonged using a pH switchable ureidopyrimidinone (UPy) hydrogel. First, we investigated the kinetics of EV release from UPy-hydrogel *in vitro*. Next, we explored if this UPy-hydrogel can be used to increase EV retention *in vivo*.

For clinical application of EV therapeutics, the ability to store EVs at different conditions is an important aspect. Currently, there is little information on the effect of storage on EV functionality. Therefore, in **chapter 5** we directly compared the functionality of CPC-EV that were stored at 4°C and -80°C. We first compared physiochemical characteristics of freshly isolated EVs to EVs stored at 4°C or -80°C. Additionally, we assessed EV functionality after different storage temperatures using *in vitro* and *in vivo* angiogenesis assays. Finally, **chapter 6** provides a summary and general discussion of the work presented in this thesis.

Acknowledgements

EAM is funded by the Project SMARTCARE-II of the BioMedicalMaterials institute, co-funded by the ZonMw-TAS program (#116002016), the Netherlands Organization for Health Research and Development, the Dutch Ministry of Economic Affairs, Agriculture and Innovation and the Netherlands CardioVascular Research Initiative (CVON): the Dutch Heart Foundation, Royal Netherlands Academy of Sciences, and the Dutch Federations of University Medical Centers. JS received a Horizon2020 ERC-2016-COG grant, called EVICARE (725229).

References

1. Thom, T. *et al.* Heart disease and stroke statistics - 2006 Update: A report from the American Heart Association Statistics Committee and Stroke Statistics Subcommittee. *Circulation* **113**, (2006).
2. Frangogiannis, N. G. Regulation of the inflammatory response in cardiac repair. *Circ. Res.* **110**, 159–73 (2012).
3. Kain, V., Prabhu, S. D. & Halade, G. V. Inflammation revisited: inflammation versus resolution of inflammation following myocardial infarction. *Basic Res. Cardiol.* **109**, 444 (2014).
4. van Nieuwenhoven, F. A. & Turner, N. A. The role of cardiac fibroblasts in the transition from inflammation to fibrosis following myocardial infarction. *Vascul. Pharmacol.* **58**, 182–8 (2013).
5. Tonnesen, M. G., Feng, X. & Clark, R. A. F. Angiogenesis in wound healing. *J. Investig. Dermatology Symp. Proc.* **5**, 40–46 (2000).
6. van der Laan, A. M., Piek, J. J. & van Royen, N. Targeting angiogenesis to restore the microcirculation after reperfused MI. *Nat. Rev. Cardiol.* **6**, 515–23 (2009).
7. Velagaleti, R. S. *et al.* Long-term trends in the incidence of heart failure after myocardial infarction. *Circulation* **118**, 2057–2062 (2008).
8. Birks, E. J. Left ventricular assist devices. *Heart* **96**, 63–71 (2010).
9. Oberpriller, J., Oberpriller, J. & Mauro, A. Cell division in adult newt cardiac myocytes. In *The development and regenerative potential of cardiac muscle.* 293–312 (1991).
10. Poss, K. D., Wilson, L. G. & Keating, M. T. Heart regeneration in zebrafish. *Science (80-.).* **298**, 2188–2190 (2002).
11. Lepilina, A. *et al.* A dynamic epicardial injury response supports progenitor cell activity during zebrafish heart regeneration. *Cell* **127**, 607–19 (2006).

12. Beltrami, A. P. *et al.* Evidence that human cardiac myocytes divide after myocardial infarction. *N. Engl. J. Med.* **344**, 1750–7 (2001).
13. Bergmann, O. *et al.* Evidence for cardiomyocyte renewal in humans. *Science* **324**, 98–102 (2009).
14. Bergmann, O. *et al.* Identification of cardiomyocyte nuclei and assessment of ploidy for the analysis of cell turnover. *Exp. Cell Res.* **317**, 188–194 (2011).
15. Bergmann, O. *et al.* Dynamics of Cell Generation and Turnover in the Human Heart. *Cell* **161**, 1566–1575 (2015).
16. Haubner, B. J. *et al.* Functional Recovery of a Human Neonatal Heart after Severe Myocardial Infarction. *Circ. Res.* **118**, 216–221 (2016).
17. Tomita, S. *et al.* Autologous transplantation of bone marrow cells improves damaged heart function. *Circulation* **100**, II247-56 (1999).
18. Orlic, D. *et al.* Bone marrow cells regenerate infarcted myocardium. *Nature* **410**, 701–5 (2001).
19. Strauer, B. E. *et al.* Repair of infarcted myocardium by autologous intracoronary mononuclear bone marrow cell transplantation in humans. *Circulation* **106**, 1913–8 (2002).
20. Friedenstein, A. J., Chailakhyan, R. K. & Gerasimov, U. V. Bone marrow osteogenic stem cells: in vitro cultivation and transplantation in diffusion chambers. *Cell Prolif.* **20**, 263–272 (1987).
21. Pittenger, M. F. *et al.* Multilineage potential of adult human mesenchymal stem cells. *Science* **284**, 143–7 (1999).
22. Sensebé, L., Bourin, P. & Tarte, K. Good manufacturing practices production of mesenchymal stem/stromal cells. *Hum. Gene Ther.* **22**, 19–26 (2011).
23. Van Der Spoel, T. I. G. *et al.* Human relevance of pre-clinical studies in stem cell therapy: Systematic review and meta-analysis of large animal models of ischaemic heart disease. *Cardiovasc. Res.* **91**, 649–658 (2011).
24. de Jong, R., Houtgraaf, J. H., Samiei, S., Boersma, E. & Duckers, H. J. Intracoronary stem cell infusion after acute myocardial infarction: a meta-analysis and update on clinical trials. *Circ. Cardiovasc. Interv.* **7**, 156–67 (2014).
25. Noort, W. A. *et al.* Mesenchymal stromal cells to treat cardiovascular disease: Strategies to improve survival and therapeutic results. *Panminerva Med.* **52**, 27–40 (2010).
26. Oh, H. *et al.* Cardiac progenitor cells from adult myocardium: Homing, differentiation, and fusion after infarction. *Proc. Natl. Acad. Sci. U. S. A.* **100**, 12313–12318 (2003).
27. Goumans, M. *et al.* Human cardiomyocyte progenitor cells differentiate into functional mature cardiomyocytes: an in vitro model for studying human cardiac physiology and pathophysiology. *Nat. Protoc.* **4**, 232–43 (2009).
28. Beltrami, A. P. *et al.* Adult cardiac stem cells are multipotent and support myocardial regeneration. *Cell* **114**, 763–776 (2003).
29. Smith, R. R. *et al.* Regenerative potential of cardiosphere-derived cells expanded from percutaneous endomyocardial biopsy specimens. *Circulation* **115**, 896–908 (2007).
30. Messina, E. *et al.* Isolation and expansion of adult cardiac stem cells from human and murine heart. *Circ. Res.* **95**, 911–921 (2004).
31. Zwi, L. *et al.* Cardiomyocyte differentiation of human induced pluripotent stem cells. *Circulation* **120**, 1513–23 (2009).
32. Singla, D. K., Long, X., Glass, C., Singla, R. D. & Yan, B. Induced pluripotent stem (iPS) cells repair and regenerate infarcted myocardium. *Mol. Pharm.* **8**, 1573–81 (2011).
33. Madonna, R. *et al.* ESC Working Group on Cellular Biology of the Heart: position paper for Cardiovascular Research: tissue engineering strategies combined with cell therapies for cardiac repair in ischaemic heart disease and heart failure. *Cardiovasc. Res.* **115**, 488–500 (2019).
34. Feyen, D. A. M., Gaetani, R., Doevendans, P. A. & Sluijter, J. P. G. Stem cell-based therapy: Improving myocardial cell delivery. *Adv. Drug Deliv. Rev.* **106**, 104–115 (2016).

35. van Vliet, P. *et al.* Progenitor cells isolated from the human heart: a potential cell source for regenerative therapy. *Neth. Heart J.* **16**, 163–9 (2008).
36. Smits, A. M. *et al.* Human cardiomyocyte progenitor cells differentiate into functional mature cardiomyocytes: an in vitro model for studying human cardiac physiology and pathophysiology. *Nat. Protoc.* **4**, 232–243 (2009).
37. Smits, A. M. *et al.* Human cardiomyocyte progenitor cell transplantation preserves long-term function of the infarcted mouse myocardium. *Cardiovasc. Res.* **83**, 527–35 (2009).
38. Tang, X.-L. *et al.* Intracoronary administration of cardiac progenitor cells alleviates left ventricular dysfunction in rats with a 30-day-old infarction. *Circulation* **121**, 293–305 (2010).
39. Chen, L. *et al.* Cardiac progenitor-derived exosomes protect ischemic myocardium from acute ischemia/reperfusion injury. *Biochem. Biophys. Res. Commun.* **431**, 566–71 (2013).
40. Barile, L. *et al.* Extracellular vesicles from human cardiac progenitor cells inhibit cardiomyocyte apoptosis and improve cardiac function after myocardial infarction. *Cardiovasc. Res.* **103**, 530–541 (2014).
41. Fischer, K. M. *et al.* Enhancement of myocardial regeneration through genetic engineering of cardiac progenitor cells expressing Pim-1 kinase. *Circulation* **120**, 2077–87 (2009).
42. Feyen, D. *et al.* Increasing short-term cardiomyocyte progenitor cell (CMPC) survival by necrostatin-1 did not further preserve cardiac function. *Cardiovasc. Res.* **99**, 83–91 (2013).
43. van den Akker, F. *et al.* Intramyocardial stem cell injection: go(ne) with the flow. *Eur. Heart J.* **38**, 184–186 (2017).
44. Chimenti, I. *et al.* Relative roles of direct regeneration versus paracrine effects of human cardiosphere-derived cells transplanted into infarcted mice. *Circ. Res.* **106**, 971–980 (2010).
45. Feyen, D. A. M. *et al.* Gelatin Microspheres as Vehicle for Cardiac Progenitor Cells Delivery to the Myocardium. *Adv. Healthc. Mater.* **5**, 1071–9 (2016).
46. Gaetani, R. *et al.* Different types of cultured human adult cardiac progenitor cells have a high degree of transcriptome similarity. *J. Cell. Mol. Med.* **18**, 2147–51 (2014).
47. Dey, D. *et al.* Dissecting the molecular relationship among various cardiogenic progenitor cells. *Circ. Res.* **112**, 1253–62 (2013).
48. Zwetsloot, P. P. *et al.* Cardiac stem cell treatment in myocardial infarction: A systematic review and meta-analysis of preclinical studies. *Circ. Res.* **118**, 1223–1232 (2016).
49. Bolli, R. *et al.* Cardiac stem cells in patients with ischaemic cardiomyopathy (SCIPIO): Initial results of a randomised phase 1 trial. *Lancet* **378**, 1847–1857 (2011).
50. Malliaras, K. *et al.* Intracoronary cardiosphere-derived cells after myocardial infarction: evidence of therapeutic regeneration in the final 1-year results of the CADUCEUS trial (Cardiosphere-Derived aUtologous stem CElls to reverse ventricUlar dySfunction). *J. Am. Coll. Cardiol.* **63**, 110–22 (2014).
51. Haubner, B. J. *et al.* Functional Recovery of a Human Neonatal Heart After Severe Myocardial Infarction. *Circ. Res.* **118**, 216–21 (2016).
52. Timmers, L. *et al.* Human mesenchymal stem cell-conditioned medium improves cardiac function following myocardial infarction. *Stem Cell Res.* **6**, 206–14 (2011).
53. Vrijssen, K. R. *et al.* Cardiomyocyte progenitor cell-derived exosomes stimulate migration of endothelial cells. *J. Cell. Mol. Med.* **14**, 1064–1070 (2010).
54. Ibrahim, A. G. E., Cheng, K. & Marbán, E. Exosomes as critical agents of cardiac regeneration triggered by cell therapy. *Stem Cell Reports* **2**, 606–619 (2014).
55. Deddens, J. C. *et al.* Circulating microRNAs as novel biomarkers for the early diagnosis of acute coronary syndrome. *J. Cardiovasc. Transl. Res.* **6**, 884–98 (2013).
56. Lai, R. C. *et al.* Exosome secreted by MSC reduces myocardial ischemia/reperfusion injury. *Stem Cell Res.* **4**, 214–22 (2010).

57. Sahoo, S. *et al.* Exosomes from human CD34(+) stem cells mediate their proangiogenic paracrine activity. *Circ. Res.* **109**, 724–8 (2011).
58. Mackie, A. R. *et al.* Sonic hedgehog-modified human CD34+ cells preserve cardiac function after acute myocardial infarction. *Circ. Res.* **111**, 312–21 (2012).
59. Arslan, F. *et al.* Mesenchymal stem cell-derived exosomes increase ATP levels, decrease oxidative stress and activate PI3K/Akt pathway to enhance myocardial viability and prevent adverse remodeling after myocardial ischemia/reperfusion injury. *Stem Cell Res.* **10**, 301–312 (2013).
60. Xiao, J. *et al.* Cardiac progenitor cell-derived exosomes prevent cardiomyocytes apoptosis through exosomal miR-21 by targeting PDCD4. *Cell Death Dis.* **7**, (2016).
61. François, M., Romieu-Mourez, R., Li, M. & Galipeau, J. Human MSC suppression correlates with cytokine induction of indoleamine 2,3-dioxygenase and bystander M2 macrophage differentiation. *Mol. Ther.* **20**, 187–95 (2012).
62. Gray, W. D. *et al.* Identification of therapeutic covariant microRNA clusters in hypoxia-treated cardiac progenitor cell exosomes using systems biology. *Circ. Res.* **116**, 255–63 (2015).
63. Sluijter, J. P. G. & van Rooij, E. Exosomal microRNA clusters are important for the therapeutic effect of cardiac progenitor cells. *Circ. Res.* **116**, 219–21 (2015).
64. Vrijssen, K. R. *et al.* Exosomes from Cardiomyocyte Progenitor Cells and Mesenchymal Stem Cells Stimulate Angiogenesis Via EMMPRIN. *Adv. Healthc. Mater.* **5**, 2555–2565 (2016).
65. Lai, C. P. *et al.* Dynamic biodistribution of extracellular vesicles in vivo using a multimodal imaging reporter. *ACS Nano* **8**, 483–494 (2014).
66. Alvarez-Erviti, L. *et al.* Delivery of siRNA to the mouse brain by systemic injection of targeted exosomes. *Nat. Biotechnol.* **29**, 341–5 (2011).
67. Zhuang, X. *et al.* Treatment of brain inflammatory diseases by delivering exosome encapsulated anti-inflammatory drugs from the nasal region to the brain. *Mol. Ther.* **19**, 1769–1779 (2011).
68. Mol, E. A., Goumans, M. J., Doevendans, P. A., Sluijter, J. P. G. & Vader, P. Higher functionality of extracellular vesicles isolated using size-exclusion chromatography compared to ultracentrifugation. *Nanomedicine Nanotechnology, Biol. Med.* **13**, 2061–2065 (2017).
69. Raposo, G. & Stoorvogel, W. Extracellular vesicles: Exosomes, microvesicles, and friends. *J. Cell Biol.* **200**, 373–383 (2013).
70. Gould, S. J. & Raposo, G. As we wait: coping with an imperfect nomenclature for extracellular vesicles. *J. Extracell. vesicles* **2**, 3–5 (2013).

Higher functionality of extracellular vesicles isolated using size-exclusion chromatography compared to ultracentrifugation

Emma A. Mol MSc^{1,2}, Marie-José Goumans PhD², Pieter A. Doevendans PhD^{1,3,4}, Joost P.G. Sluiter PhD^{1,3,4}, Pieter Vader PhD⁵

Nanomedicine 2017; 13: 2061-2065

¹Department of Cardiology, Laboratory of Experimental Cardiology, University Medical Center Utrecht, Utrecht 3584CX, The Netherlands

²Department of Cardiovascular Cell Biology, Department of Cell and Chemical Biology, Leiden University Medical Center, Leiden 2333ZA, The Netherlands

³UMC Utrecht Regenerative Medicine Center, University Medical Center, Utrecht 3584CT, The Netherlands

⁴Netherlands Heart Institute (ICIN), Utrecht 3584CX, The Netherlands

⁵Laboratory of Clinical Chemistry and Haematology, University Medical Center Utrecht, Utrecht 3584, The Netherlands

Abstract

Extracellular vesicles (EVs) are nano-sized, lipid bilayer-enclosed particles involved in intercellular communication. EVs are increasingly being considered as drug delivery vehicles or as cell-free approach to regenerative medicine. However, one of the major challenges for their clinical application is finding a scalable EV isolation method that yields functional EVs. Although the golden standard for EV isolation is ultracentrifugation (UC), a recent study suggested that isolation using size-exclusion chromatography (SEC) yielded EVs with more intact biophysical properties. Whether this also leads to differences in functionality remained to be investigated. Therefore, we investigated possible differences in functionality of cardiomyocyte progenitor cell-derived EVs isolated using UC and SEC. Western blot analysis showed higher pERK/ERK ratios after stimulation with SEC-EVs compared to UC-EVs, indicating that SEC-EVs bear higher functionality. Therefore, we propose to use SEC-EVs for further investigation of EVs' therapeutic potential. Further optimization of isolation protocols may accelerate clinical adoption of therapeutic EVs.

Background

Extracellular vesicles (EVs) are nano-sized endogenous messengers containing a plethora of biological cargo including proteins and RNA, reflecting the content of the secreting cell. By mediating intercellular communication, EVs can influence recipient cell behavior, and affect physiological and pathological processes¹⁻³. For this reason, EVs are increasingly being considered for therapeutic purposes, including cell-free approaches for regenerative medicine and drug delivery⁴⁻⁶. The interest in using EVs for cardiac therapy increased after it became clear that the beneficial effects of stem cell therapy after a myocardial infarction (MI) were mainly due to paracrine actions⁷. EVs were identified to be the major component of the stem cell secretome responsible for the observed increase in cardiac function⁸. Therefore, using EVs as an off-the-shelf therapeutic may circumvent some of the drawbacks of cell based therapy, such as cell survival, retention, rejection, and the use of replicating cells.

One of the major challenges for implementation of EVs as therapeutics is the development of a scalable, reproducible, and standardisable isolation method that results in an acceptable yield of EVs. To date, the most common EV isolation method is differential ultracentrifugation (UC). This method relies on sedimentation at high speed for separating EVs from other (extra)cellular components. Although the UC protocol is relatively straightforward, it is also time consuming, and may yield aggregated EVs after pelleting^{9,10}. Furthermore, UC isolation results in low and operator-dependent yields and EVs can be damaged due to shearing forces, as a result of centrifugation at high speeds^{11,12}. An additional method for EV isolation, based on ultrafiltration and size-exclusion chromatography (SEC) to separate EVs from other media components, was recently suggested by Nordin et al¹³. EVs isolated using chromatography (SEC-EVs) are more intact than EVs isolated using UC (UC-EVs), likely due to the absence of centrifugation at high speeds. Whether this also leads to differences in functionality of SEC- and UC-EVs remained to be investigated.

Results

In order to investigate whether the isolation protocol affects EV functionality, EVs derived from cardiomyocyte progenitor cells (CPCs) were isolated using UC and SEC. CPCs are being intensively investigated for cardiac-related therapies, and CPC-derived EVs have previously been shown to bear pro-angiogenic properties¹⁴⁻¹⁶. A schematic representation of the UC and SEC isolation protocols used in this study is shown in Figure 1.

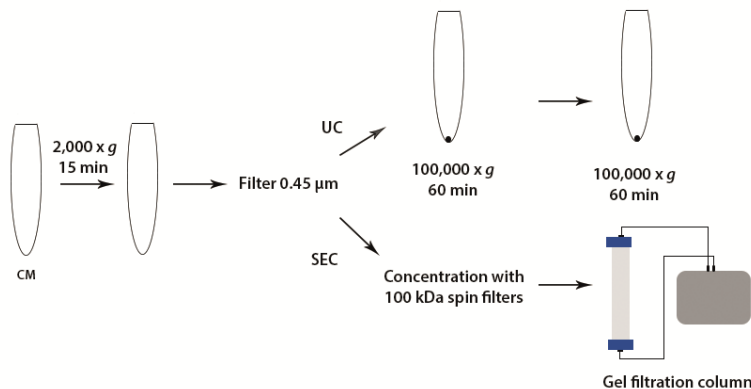


Figure 1 Schematic overview of EV isolation protocols used in this study. Abbreviations: CM = conditioned medium, SEC = size-exclusion chromatography, UC = ultracentrifugation.

First, EV yield was compared by quantification of EV protein content and number of particles, as shown in Figure 2A. No significant differences in total EV protein or particle yield between UC and SEC were found. This is in contrast with previous observations showing that SEC isolation results in a higher EV yield compared to UC isolation.^[13] This may be explained by variation between cell types or due to slight differences in UC or SEC isolation procedure (e.g. rotor/filter type or pore size). Next, UC-EVs and SEC-EVs were characterized based on size distribution, morphology, and the presence or absence of protein markers. Figure 2B shows a representative size distribution profile of UC-EVs and SEC-EVs based on Nanoparticle Tracking Analysis. SEC-EVs had a smaller size distribution with the highest peak at approximately 90 nm, compared to a broader size range for UC-EVs, peaking at approximately 100 nm. Transmission electron microscopy analysis showed no major morphological differences between UC-EVs and SEC-EVs, as both preparations contained both smaller and larger vesicles (Figure 2C). Western Blot analysis revealed that both UC-EVs and SEC-EVs were enriched for EV marker proteins Alix and CD63, but not TSG101 (Figure 2C). Although the expected band for Alix (96 kDa) was present for both UC-EVs and SEC-EVs, an extra band at 90 kDa was observed in the UC-EV preparation. The presence of double bands for Alix may be explained by differential phosphorylation status, as Alix is known to have multiple phosphorylation sites¹⁷. Why this second band was exclusively found in UC-EVs remains unclear, but might suggest a different vesicle sub-class or activation status. The endoplasmic reticulum protein calnexin was only detected in the cell lysate, confirming the absence of contamination with other membrane compartments in EVs. β -actin was found in similar levels in EVs and cell lysate.

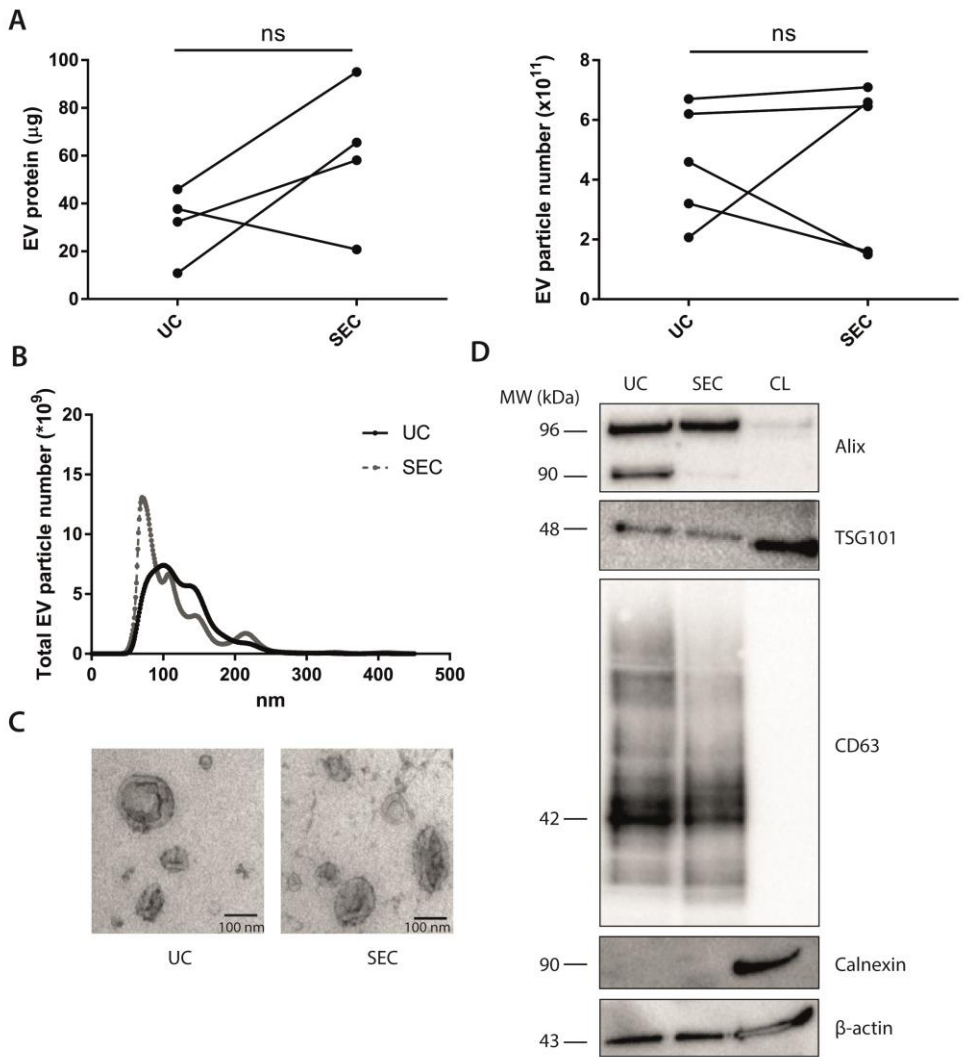


Figure 2 Characterization of UC-EVs and SEC-EVs. A) EV yield as determined by microBCA analysis (EV protein, upper panel) and Nanoparticle Tracking Analysis (NTA) (EV particle number, lower panel). Statistical analysis was performed using an unpaired student's t-test. B) Size distribution profile of UC-EVs and SEC-EVs as determined by NTA. C) Transmission electron microscopy pictures of UC-EVs and SEC-EVs. Scale bar = 100 nm. D) Western Blot of UC-EVs, SEC-EVs and cell lysate (CL). Abbreviations: CL = cell lysate, MW = molecular weight, SEC = size-exclusion chromatography, UC = ultracentrifugation.

CPC-derived EVs have previously been shown to stimulate migration of human microvascular endothelial cells (HMECs) in a scratch wound assay¹⁴. As the mitogen-activated protein kinase1/2 (MAPK1/2) – extracellular signal-regulated kinase1/2 (ERK1/2) pathway is known to play an important role in cell survival, migration and angiogenesis during wound healing^{18–20}, EV-induced ERK1/2 phosphorylation was used as a read-out to evaluate the possible differences in functionality of UC-EVs and SEC-EVs. To investigate the functionality of EV preparations, HMECs were stimulated with UC-EVs and SEC-EVs (Figure 3A).

Due to a lack of consensus in the EV-field on the most accurate method for EV quantification, HMECs were stimulated with both equal amounts of UC-EV and SEC-EV protein (Figure 3B), and equal numbers of EV particles (Figure 3C). Levels of phosphorylated ERK1/2 and total ERK1/2 were determined using western blotting, after which pERK/ERK ratios were calculated. A dose-dependent increase in ERK phosphorylation was observed for SEC-EVs, as treatment with 3 μg SEC-EVs led to a higher pERK/ERK ratio compared to 1 μg SEC-EVs (2.1 ± 0.3 for 3 μg SEC-EVs vs 1.2 ± 0.2 for 1 μg SEC-EVs). Moreover, stimulation with 3 μg SEC-EVs resulted in a higher pERK/ERK ratio compared to stimulation with 3 μg of UC-EVs (2.1 ± 0.3 for SEC-EVs vs 1.0 ± 0.2 for UC-EVs). The same trend was observed after adding equal numbers of EV particles to HMECs (Figure 3C). Stimulation of HMECs with $6 \cdot 10^{10}$ SEC-EVs resulted in higher pERK/ERK ratio compared to $6 \cdot 10^{10}$ UC-EVs (3.56 ± 1.29 for SEC particles vs 1.42 ± 0.24 for UC particles). These results show that CPC-derived SEC-EVs have higher functionality compared to UC-EVs.

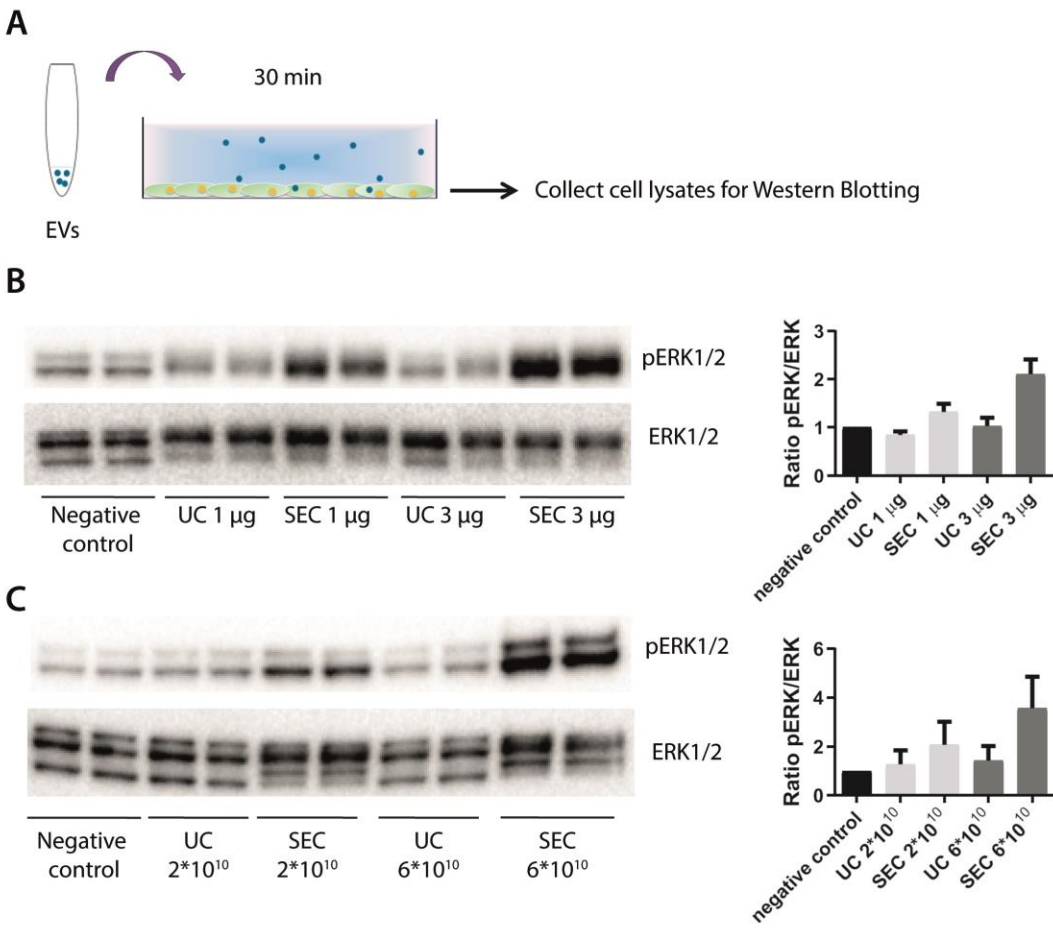


Figure 3 Assessment of UC-EV and SEC-EV functionality. A) HMECs were stimulated with EVs for 30 minutes, after which phosphorylated ERK1/2 and total ERK1/2 protein levels were determined using Western Blotting. B) Stimulation of HMECs with equal amounts of UC-EV and SEC-EV protein. C) Stimulation with equal numbers of UC-EV and SEC-EV particles. Abbreviations: ERK = extracellular signal-regulated kinase, SEC = size-exclusion chromatography, UC = ultracentrifugation.

Discussion

The striking difference in functionality between UC-EVs and SEC-EVs may result from the high shear forces that are applied during high speed centrifugation during UC isolation. These may detrimentally affect signaling molecules on the EV surface, thereby preventing UC-EVs to activate, bind to or be taken up by recipient cells. Indeed, UC-EVs have previously been described to appear ruptured when studied using transmission electron microscopy and fluorescence correlation spectroscopy¹³. Furthermore, the size distribution profile of SEC-EVs also differed from UC-EVs, as SEC-EVs were found to be smaller in size compared to UC-EVs. The apparent larger size may be the result of aggregation or fusion of EVs during UC, as also suggested by others^{9,11,13}. Alternatively, UC isolation may enrich for larger EVs that sediment more efficiently. Whether and how this contributes to EV functionality remains to be investigated. Furthermore, as characteristics of isolated EVs vary between cell types, differences in functionality between SEC-EVs and UC-EVs may be cell type-dependent. This needs to be addressed in future studies.

In this study, we used induction of ERK phosphorylation as an outcome parameter to assess EV functionality, as activation of HMECs via pERK has been shown to be indicative for the angiogenic potential of EVs¹⁵. One could argue that SEC-EVs may be contaminated with other soluble materials that affect ERK phosphorylation. Although we cannot exclude this completely, Western Blot analyses as well as protein and particle number measurements indicate that SEC isolation allows for EV preparations with similar purity as UC (Figure 1A,D). Additionally, CPC-EVs may affect other processes involved in cardiac disease, as treatment with CPC-EVs has been shown to result in increased cardiac function after MI in mice by enhancing angiogenesis, as well as reducing cardiomyocyte apoptosis¹⁶. Whether SEC-EVs display increased functionality for cardiac repair *in vivo*, as well as for other therapeutic strategies, therefore remains to be investigated.

In conclusion, one of the major challenges for developing EV therapeutics is finding a scalable isolation method that yields EVs with high functionality. Although previous reports already suggested that EV function might be affected by the isolation procedure, to our knowledge, we are the first to show that EV isolation technique can actually affect their functionality. SEC

isolation results in more functional EVs compared to UC isolation, which is especially important when developing EVs as therapeutics.

Acknowledgements

The authors thank Sander van de Weg (UMC Utrecht) for excellent assistance with electron microscopy. EAM is supported by the Project SMARTCARE-II of the BioMedicalMaterials institute, co-funded by the ZonMw-TAS program (#116002016), the Dutch Ministry of Economic Affairs, Agriculture and Innovation and the Netherlands CardioVascular Research Initiative (CVON): the Dutch Heart Foundation, Dutch Federations of University Medical Centers, the Netherlands Organization for Health Research and Development, and the Royal Netherlands Academy of Sciences. PV is funded by a VENI fellowship (#13667) from the Netherlands Organisation for Scientific Research (NWO). The authors declare no conflicts of interest.

References

1. Valadi, H. *et al.* Exosome-mediated transfer of mRNAs and microRNAs is a novel mechanism of genetic exchange between cells. *Nat. Cell Biol.* **9**, 654–9 (2007).
2. Ratajczak, J. *et al.* Embryonic stem cell-derived microvesicles reprogram hematopoietic progenitors: evidence for horizontal transfer of mRNA and protein delivery. *Leukemia* **20**, 847–56 (2006).
3. Skog, J. *et al.* Glioblastoma microvesicles transport RNA and proteins that promote tumour growth and provide diagnostic biomarkers. *Nat. Cell Biol.* **10**, 1470–6 (2008).
4. Sluijter, J. P. G., Verhage, V., Deddens, J. C., van den Akker, F. & Doevendans, P. A. Microvesicles and exosomes for intracardiac communication. *Cardiovasc. Res.* **102**, 302–11 (2014).
5. Haney, M. J. *et al.* Exosomes as drug delivery vehicles for Parkinson's disease therapy. *J. Control. Release* **207**, 18–30 (2015).
6. Julich, H., Willms, A., Lukacs-Kornek, V. & Kornek, M. Extracellular vesicle profiling and their use as potential disease specific biomarker. *Front. Immunol.* **5**, 413 (2014).
7. Timmers, L. *et al.* Human mesenchymal stem cell-conditioned medium improves cardiac function following myocardial infarction. *Stem Cell Res.* **6**, 206–14 (2011).
8. Lai, R. C. *et al.* Exosome secreted by MSC reduces myocardial ischemia/reperfusion injury. *Stem Cell Res.* **4**, 214–22 (2010).
9. Linares, R., Tan, S., Gounou, C., Arraud, N. & Brisson, A. R. High-speed centrifugation induces aggregation of extracellular vesicles. *J. Extracell. vesicles* **4**, 29509 (2015).
10. Bobrie, A., Colombo, M., Krumeich, S., Raposo, G. & Théry, C. Diverse subpopulations of vesicles secreted by different intracellular mechanisms are present in exosome preparations obtained by differential ultracentrifugation. *J. Extracell. vesicles* **1**, (2012).
11. Lamparski, H. G. *et al.* Production and characterization of clinical grade exosomes derived from dendritic cells. *J. Immunol. Methods* **270**, 211–226 (2002).
12. Taylor, D. D. & Shah, S. Methods of isolating extracellular vesicles impact down-stream analyses of their cargoes. *Methods* **87**, 3–10 (2015).
13. Nordin, J. Z. *et al.* Ultrafiltration with size-exclusion liquid chromatography for high yield isolation of extracellular vesicles preserving intact biophysical and functional properties. *Nanomedicine* **11**,

- 879–83 (2015).
14. Vrijisen, K. R. *et al.* Cardiomyocyte progenitor cell-derived exosomes stimulate migration of endothelial cells. *J. Cell. Mol. Med.* **14**, 1064–1070 (2010).
 15. Vrijisen, K. R. *et al.* Exosomes from Cardiomyocyte Progenitor Cells and Mesenchymal Stem Cells Stimulate Angiogenesis Via EMMPRIN. *Adv. Healthc. Mater.* **5**, 2555–2565 (2016).
 16. Barile, L. *et al.* Extracellular vesicles from human cardiac progenitor cells inhibit cardiomyocyte apoptosis and improve cardiac function after myocardial infarction. *Cardiovasc. Res.* **103**, 530–541 (2014).
 17. Watson, D. C. *et al.* Efficient production and enhanced tumor delivery of engineered extracellular vesicles. *Biomaterials* **105**, 195–205 (2016).
 18. Ballif, B. A. & Blenis, J. Molecular mechanisms mediating mammalian mitogen-activated protein kinase (MAPK) kinase (MEK)-MAPK cell survival signals. *Cell Growth Differ.* **12**, 397–408 (2001).
 19. Eliceiri, B. P., Klemke, R., Strömblad, S. & Chersesh, D. A. Integrin alphavbeta3 requirement for sustained mitogen-activated protein kinase activity during angiogenesis. *J. Cell Biol.* **140**, 1255–63 (1998).
 20. Alavi, A., Hood, J. D., Frausto, R., Stupack, D. G. & Chersesh, D. A. Role of Raf in vascular protection from distinct apoptotic stimuli. *Science* **301**, 94–6 (2003).
 21. Smits, A. M. *et al.* Human cardiomyocyte progenitor cells differentiate into functional mature cardiomyocytes: an in vitro model for studying human cardiac physiology and pathophysiology. *Nat. Protoc.* **4**, 232–243 (2009).

Supplementary materials

Cell culture

CPCs and HMECs were cultured in the appropriate cell culture medium^{14,21}. For EV isolation, CPCs were cultured for 3 days, after which medium was replaced with serum-free Medium 199 (Gibco, 31150-022). Conditioned medium (CM) from approximately 400 million cells was collected after 24 hours. Cells were passaged at 80-90% confluency using 0.25% trypsin digestion, and all cells were incubated at 37°C (5% CO₂ and 20% O₂).

EV isolation protocol

EVs were isolated using ultracentrifugation (UC) and ultrafiltration combined with size-exclusion chromatography (SEC). Cell culture CM was precleared from debris by centrifugation at 2000 x *g* for 15 min, followed by filtration (0.45 μm). Next, CM was divided for the two isolation techniques. For UC, CM was centrifuged using a type 50.2 Ti fixed-angle rotor for 1 hour at 100.000 x *g* to pellet EVs, and washed with phosphate buffer by centrifugation at 100.000 x *g* subsequently. For SEC, CM was concentrated using 100-kDa molecular weight cut-off (MWCO) Amicon spin filters (Merck Millipore). Subsequently, concentrated CM was loaded onto a S400 highprep column (GE Healthcare, Uppsala, Sweden) using an AKTASart (GE Healthcare) containing a UV 280nm flow cell. The EV-containing fractions were pooled after elution and concentrated using a 100-kDa MWCO Amicon spin filter. Both EV preparations were filtered (0.45 μm) afterwards. The particle amount and size distribution were measured using Nanoparticle Tracking Analysis (Nanosight NS500, Malvern) with the camera level set at 15, and the detection threshold at 5. Protein content was determined using a microBCA protein assay kit™ (Thermo Scientific). Transmission electron microscopy pictures were made with a FEI Tecnai™ transmission electron microscope.

Assessment of EV functionality

First, HMECs were starved in basal MCDB-131 medium for 3 hours. Next, HMECs were either stimulated with equal amounts EV protein (1 or 3 μg) or equal amounts of EV particles (2 x 10¹⁰ or 6 x 10¹⁰ particles) for 30 minutes, after which cells were lysed using lysis buffer (Roche, 04719964000). Cell lysates were centrifuged for 10 minutes at 14.000 x *g*, and phosphorylated ERK1/2 and total ERK1/2 protein levels were determined using Western Blotting.

Western blotting

Proteins were loaded on pre-casted Bis-Tris protein gels (ThermoFischer, NW04125BOX) for 1 hour at 160V, after which proteins were transferred to PVDF membranes (Millipore, IPVH00010). After incubation with antibodies for 42/44 pERK1/2 (Cell Signaling, 43705), 42/44 ERK1/2 (Cell Signaling, 91025), Alix (Abcam, 177840), TSG101 (Abcam, 30871), CD63 (Abcam, 8219), Calnexin (Tebu-bio, GTX101676), or β -actin (Sigma, A5441) a chemiluminescent peroxidase substrate (Sigma, CPS1120) was used to visualize the proteins. Quantification of the images was performed using ImageJ software (1.47V).

Statistical analysis

Data are presented as mean \pm SEM. Student's t-test was used for comparison of two groups. A significance level of $p < 0.05$ was used for the analysis.

Cardiac progenitor-derived extracellular vesicles do not reduce infarct size after myocardial infarction in mice, independently of isolation method

Emma A. Mol MSc^{1,2}, Marieke T. Roefs Msc¹, Hemse Al-Khamisi BSc¹, Maike A.D. Brans BSc¹, Lena Bosch PhD¹, Saskia C.A de Jager PhD¹, Marie-José Goumans PhD², Pieter Vader PhD^{1,3}, Joost P.G. Sluijter PhD^{1,4,5}

In preparation

¹Department of Cardiology, Laboratory of Experimental Cardiology, University Medical Center Utrecht, Utrecht 3584, The Netherlands

²Laboratory of Cardiovascular Cell Biology, Department of Cell and Chemical Biology, Leiden University Medical Center, Leiden 2333ZA, The Netherlands

³Laboratory of Clinical Chemistry and Haematology, University Medical Center Utrecht, Utrecht 3584, The Netherlands

⁴UMC Utrecht Regenerative Medicine Center, University Medical Center, Utrecht 3584CT, The Netherlands

⁵University Utrecht, Utrecht 3508TC, The Netherlands

Abstract

Introduction Local injection of extracellular vesicles (EVs) is a potential cell-free therapeutic approach for cardiac repair after myocardial infarction (MI). The enhanced cardiac function after progenitor cell transplantation is mainly ascribed to EVs released by the injected cells, containing bioactive paracrine factors. Previously, cardiac progenitor derived (CPC)-EVs have been shown to reduce infarct size 2 days after experimentally induced MI in mice. Ultrafiltration combined with size-exclusion chromatography (SEC) is a scalable EV isolation method that could potentially be used for the production of clinical-grade EVs. Recently, we have demonstrated that EVs isolated using size-exclusion chromatography-isolated EVs (SEC-EV) display enhanced functionality *in vitro* as compared to ultracentrifugation-isolated EVs (UC-EV). Here, we aimed to investigate whether SEC-EVs also have improved therapeutic efficacy when compared to UC-EVs *in vivo*, using two different preclinical models of MI.

Methods CPCs were cultured in serum-free medium for 24 hours after which CPC-EVs were isolated using either UC or ultrafiltration, combined with SEC. Severe Combined Immunodeficient (SCID) mice underwent either a permanent ligation of the left anterior descending artery or ligation followed by reperfusion after 1 hour of ischemia and received treatment with UC-EVs or SEC-EVs by intramyocardial injection. After 2 days, a double blinded analysis was performed to assess infarct size (IS) and area at risk (AAR). Levels of plasma Troponin I and global longitudinal and reverse longitudinal strain rates were also measured. To confirm if the injected EVs displayed functionality *in vitro*, EVs were added to human microvascular endothelial cells (HMEC-1) *in vitro* and activation of extracellular signal regulated kinase 1/2 (ERK1/2) pathway was assessed.

Results The isolated EVs were bioactive as shown by their ability to activate the ERK1/2 pathway in HMEC-1 cells *in vitro*. However, upon injection of either UC-EVs or SEC-EVs post MI, IS analysis showed no change in IS/left ventricular area 2 days after treatment in the permanent ligation model and the reperfusion infarct model, in which also IS/AAR did not change compared to PBS injected animals. Furthermore, strain analysis showed no significant differences in global or reverse longitudinal strain values between PBS, UC-EV, or SEC-EV treated groups in the reperfusion model. Plasma levels of Troponin I did not significantly differ between the groups in either infarct model.

Conclusion As no change in infarct size was observed 2 days after treatment with UC-EV or SEC-EV compared to PBS in two different infarct models, we were not able to determine if the choice of EV isolation method influences therapeutic efficacy of EVs *in vivo*. These results are in contrast with previously reported studies using CPC-EVs that demonstrated reduced infarct size at 2 days post MI. Future studies should address if potential differences between CPC clones, culture media, or dosing could explain these different outcomes.

Introduction

Cardiovascular disease (CVD) is one of the most prevalent causes of death worldwide, with myocardial infarction (MI) accounting for one third of all deaths by CVD¹. Although acute mortality decreased due to improved arterial reperfusion strategies, this also induces additional damage, referred to as ischemia-reperfusion (I/R) injury. Approximately 25% of patients that survive a MI are known to develop heart failure (HF)². Currently, there is no curative treatment available for chronic heart failure patients besides heart transplantation. Progenitor cell therapy has been proposed as potential therapy to prevent HF development by reducing I/R injury and reducing infarct size. While cell types of different origins (e.g. mesenchymal stromal cells, bone marrow derived mononuclear cells) have been used, cardiac progenitors have gained attention because of their cardiac origin and the possibility to differentiate in all cardiac cell types^{3,4}. CPC therapy in mice has been shown to increase ejection fraction and inhibit adverse ventricular remodeling post-MI⁵. However, despite functional improvement, a low cell engraftment was observed after intramyocardial injection. This could be due to an immediate wash-out of cells through the venous drainage after intramyocardial injection, which we previously described⁶. Using carriers such as gelatin microspheres reduced this wash-out of cells, but did not translate into increased beneficial effects on cardiac function⁷. Given the low retention despite functional improvement, it has been suggested that paracrine factors secreted by CPCs cause this beneficial effect on cardiac function. Indeed, administration of conditioned medium from progenitor cells also preserved cardiac function post-MI, thus resembling studies injecting the cells themselves⁸. Further studies showed that extracellular vesicles (EVs) are important carriers of bioactive paracrine factors responsible for this beneficial effect⁹⁻¹¹.

EVs are nanosized lipid bi-layered particles that play important roles in intercellular communication in both health and disease. After internalization by recipient cells, EVs are able to transfer their biological cargo (e.g. mRNAs, small RNAs, proteins, and lipids), resulting in phenotypical changes¹²⁻¹⁵. Recently, we demonstrated that EV secretion from CPCs is essential to reduce infarct size¹⁶, since Rab27A knock down-CPCs were not able to reduce infarct size in mice after 2 days as compared to control CPCs. Indeed, direct CPC-EV treatment reduced infarct size 2 days after permanent ligation of the left anterior descending artery (LAD)¹⁶. Thus, CPC-EVs may be a potential off-the-shelf therapy to induce cardiac repair, aiming to treat chronically diseased patients.

Currently, ultracentrifugation, based on high-speed sedimentation, is the most commonly used isolation method for EVs. Although widely used, EV isolation using UC is a labor intensive method, yield is operator dependent, and is limited in its ability to isolate a sufficient numbers of EVs for clinical application^{17,18}. In contrast, ultrafiltration combined with size-exclusion chromatography (SEC) is a scalable method that could potentially be used for clinical-grade

production of EVs¹⁹. Moreover, we have previously shown that isolating EVs using SEC yields EVs with a higher bioactivity compared to UC in a functional assay *in vitro*²⁰. To investigate whether these differences also translate to distinct behavior *in vivo*, we here sought to determine whether UC-EV and SEC-EV have different therapeutic efficacy in two commonly used infarct models in mice.

Material and Methods

Cell culture

Human microvascular endothelial cells (HMEC-1 cells) were cultured in HMEC-1 medium (83,8% MCDB-131 (Invitrogen, 10372019), 0.1% human EGF (PeproTech/Invitrogen, 016100-15-A), 0.1% Hydrocortison (Sigma, H6909-10), 1% Penicillin/Streptomycin (Invitrogen, 15140122), 10% fetal bovine serum (FBS) (Life-Tech, 10270), and 5% L-glutamine (Invitrogen, 25030024). Human fetal heart tissue was obtained by individual permission using standard written informed consent procedures and prior approval of the ethics committee of the Leiden University Medical Center, the Netherlands. This is in accordance with the principles outlined in the Declaration of Helsinki for the use of human tissue or subjects. Cardiac progenitor cells (CPCs) were cultured in SP++ medium (22% EGM-2 (Lonza, CC-4176), 66% Medium 199 (Gibco, 31150-022), 10% FBS (Life-Tech, 10270), 1% Penicillin/Streptomycin (Invitrogen, 15140122), and 1% MEM nonessential amino acids (Gibco, 11140), as described before³. Cells were incubated at 37°C with 5% CO₂ and 20% O₂ and passaged at 80-90% confluency after digestion with 0.25% trypsin-EDTA. Before EV collection, CPCs were cultured for 3 days on SP++ medium until 80-90% confluency, followed by 24 hours of culture on Medium 199 without any additives.

EV isolation

EV isolation was performed as described before²⁰. In brief, conditioned medium (CM) was collected after 24 hours of culture in Medium 199 without any additives, centrifuged for 15 min at 2000 x *g* and passed through a 0.45 µm filter (0.45 µm Nalgene filter bottles) to remove cell debris. Next, the CM was equally divided, and half was used for EV isolation using ultracentrifugation (UC), and the other half for EV isolation using ultrafiltration followed by size-exclusion chromatography (SEC). For UC, EVs were pelleted by a 1 hour centrifugation at 100.000 x *g* using a type 50.2 Ti fixed-angle rotor. EVs were washed with PBS, followed by a second 100.000 x *g* centrifugation step. For SEC, CM was concentrated first using 100-kDa molecular weight cut-off (MWCO) Amicon spin filters (Merck Millipore). Next, the concentrated CM was loaded onto a S400 high-prep column (GE Healthcare, Uppsala, Sweden) using an AKTASart (GE Healthcare) containing an UV 280nm flow cell. The fractions containing the EVs were pooled and again concentrated using a 100-kDa MWCO Amicon spin filter. After isolation, both EV preparations were passed through a 0.45 µm filter. Number of particles was determined

using Nanoparticle Tracking Analysis (Nanosight NS500, Malvern), using a camera level of 15 and a detection threshold of 5.

EV functionality

1.2×10^5 HMEC-1 cells were plated into a 48-wells plate the day before stimulation. HMEC-1 cells were starved using basal MCDB131 medium for 3 hours before stimulation. To stimulate HMEC-1 cells, 6×10^{10} EVs were added for 30 minutes to the starvation medium, unless stated otherwise. Cells were put on ice, lysed using lysis buffer (Roche, 04719964000), and centrifuged at $14.000 \times g$ for 10 minutes to remove cell debris. Protein levels of phosphorylated extracellular signal regulated kinase 1/2 (pERK1/2) and total ERK 1/2 (ERK1/2) were determined using Western Blotting as described below.

Western blotting

Lysates were loaded onto pre-casted 4-12% Bis-Tris protein gels (ThermoFisher, NW04125BOX). The gels were run for 1 hour at 160V, followed by blotting of the proteins on PVDF membranes (Millipore, IPVH00010). Membranes were blocked with 5% BSA in TBS and incubated with antibodies against 42/44 pERK1/2 (1:1000) (Cell Signaling, 43705) or 42/44 ERK1/2 (1:1000) (Cell Signaling, 91025) dissolved in 0.5% BSA in TBS for 1 hour. Membranes were washed 3 times for 5 minutes with TBS-0.1%Tween, followed by incubation with secondary goat anti-rabbit HRP antibody (Dako, P0448) dissolved in 5% milk in TBS-0.1%Tween for 1 hour. Next, membranes were washed with TBS for 30 minutes and the proteins were detected with chemiluminescent peroxidase substrate (Sigma, CPS1120) using a Chemi Doc™ XRS+ system (Bio-Rad) and Image Lab™ software.

Animal experiments

All animal experiments were performed conform the 'Guide for the Care and Use of Laboratory Animals' and carried out after approval by the Animal Ethical Experimentation Committee, Utrecht University, the Netherlands. Healthy male NOD.CB17-Prkdcscid/NCrHsd mice (age 10-14 weeks, weight 20-30g) were obtained from Envigo and received standard chow and water *ad libitum* and were housed under standard conditions with 12-h light/dark cycles until experimental procedures. Animals were randomized to one of the three groups and all operators were blinded during surgery, intramyocardial injections, and subsequent analyses.

Induction of myocardial infarction and EV therapy

Mice were anesthetized by intraperitoneal injection of medetomidine (0.05 mg/kg body weight), midazolam (5 mg/kg) and fentanyl (0.5 mg/kg), followed by intubation and connection to a respirator with a 1:1 oxygen-air ratio (times/min). Body temperature was maintained at 37 °C

during surgery using an automatic heating blanket. Left lateral thoracotomy was performed to access the heart. For permanent ligation, the LAD was ligated using an 8-0 Ethilon suture (Ethicon). For ischemia/reperfusion, the LAD was ligated for 1 hour using an 8-0 Ethilon suture (Ethicon) and a polyethylene-10 tube to ensure easy removal of the suture. Ischemia was confirmed by observing immediate blanching of the cardiac tissue upon LAD ligation. Two times five μl of either PBS, UC-EVs, or SEC-EVs were intramyocardially injected into the border zone using a 30G needle, either 15 min after permanent ligation or at the moment of reperfusion. The injected EV dose was 10×10^{10} particles. All surgeries and injections were performed by blinded operators. Next, the surgical wounds were closed, followed by a subcutaneous injection of antagonist consisting of atipamezole hydrochloride (3.3 mg/kg), flumazenil (0.5 mg/kg), and buprenorphine (0.15 mg/kg) as pain relief.

Termination

2 days post-injection, mice were euthanized after being anesthetized using sodium pentobarbital (60.0 g/kg). For the I/R injury model, blood was collected in EDTA tubes through orbital puncture. Next, the LAD was again ligated at the same place as MI induction. The thoracic aorta was cannulated with a 21-24G catheter (Abbotath) using a 1 ml syringe. 4% of Evans Blue dye was injected until a clear demarcation between area-at-risk and healthy tissue was apparent. The heart was removed and washed with PBS several times to remove excess dye. Heart weight and tibia length were assessed.

For permanent ligation, mice were euthanized after being anesthetized using sodium pentobarbital (60.0 g/kg). Blood was collected through orbital puncture in EDTA tubes to determine plasma levels of Troponin I. The heart was flushed through the right ventricle using 5 mL of PBS. Heart weight and tibia length were assessed.

Infarct size

To determine infarct size, the hearts were cut into 3-4 equal slices using razor blades. Next, slices were incubated with 1% TTC solution at 37°C for 15-20 minutes followed by incubation in formalin for 5-10 minutes. Slices were weighed to be able to correct for differences in slice size. Images were taken using a SZH10 Olympus Zoom Stereo Microscope and IC Capture software, version 2.4. For ischemia-reperfusion injury, the infarct area (white), area-at-risk (red), and healthy area (blue) were assessed to calculate infarct size. Infarct size (IS) was expressed as a percentage of area-at-risk (AAR) and total left ventricle (LV). For permanent ligation, infarct area (white) and healthy area (red) were used to determine infarct size. Infarct size was expressed as percentage of total left ventricle.

Echocardiography

At baseline and 2 days after I/R injury, anesthesia was induced by inhalation of 2.0% isoflurane in a mixture of oxygen/air (1:1). Echocardiography was used to determine global longitudinal strain and reverse strain rate. Heart rate, respiration, and rectal temperature were constantly monitored, and body temperature was maintained at 36-38°C using heat lamps. Images were taken and analyzed using the Vevo 2100 System and VevoLab Software (Fujifilm VisualSonics Inc., Toronto, Canada).

Statistical analysis

Statistical analysis were performed using SPSS and Graphpad Prism. Data are presented as mean \pm SD. Data were tested for normal distribution. One-way ANOVA was used to compare multiple groups and data was corrected for multiple testing using Tukey post-hoc test.

Results

Previously, we have shown that EV isolation technique can affect their functionality *in vitro*, as SEC isolation resulted in more functional EVs compared to UC isolation²⁰. To investigate if the choice of EV isolation method also affects EVs' therapeutic efficacy *in vivo*, mice were subjected to permanent ligation (Figure 1A) and treated with either UC-EVs or SEC-EVs 15 minutes after ischemia induction. After 48 hours, surprisingly, infarct size as determined by IS/LV did not differ between PBS and SEC-EV-treated groups (32.6 ± 12.0 vs $29.1 \pm 11.1\%$, $p = 0.73$; Figure 1B+C) nor between UC-EV and SEC-EV-treated groups (28.7 ± 8.7 vs $29.1 \pm 11.1\%$, $p=0.99$). Next, in order to investigate if EVs potentially affect a different mechanism, mice were subjected to 60 minutes of ischemia, followed by reperfusion and treatment with either UC-EVs or SEC-EVs (Figure 1D). Also in this model, infarct size after I/R injury, as assessed by IS/AAR, did not differ between PBS and SEC-EV treated groups (46.9 ± 13.6 vs $49.4 \pm 8.8\%$, respectively, $p=0.92$; Figure 1E+F) nor between UC-EV and SEC-EV treated groups (50.0 ± 20.2 vs $49.4 \pm 8.8\%$, respectively, $p=0.99$). In addition, IS/LV was comparable between all groups (19.1 ± 7.9 for PBS vs $17.0 \pm 8.8\%$ for SEC-EV, $p=0.88$ and 22.3 ± 7.9 for UC-EV vs $17.0 \pm 8.8\%$ for SEC-EV, $p=0.36$; Figure 1G), as was AAR/LV (42.6 ± 15.5 for PBS vs $36.1 \pm 22.7\%$ for SEC-EV, $p=0.67$ and 45.3 ± 9.7 for UC-EV vs $36.1 \pm 22.7\%$ for SEC-EV, $p=0.48$; Figure 1H).

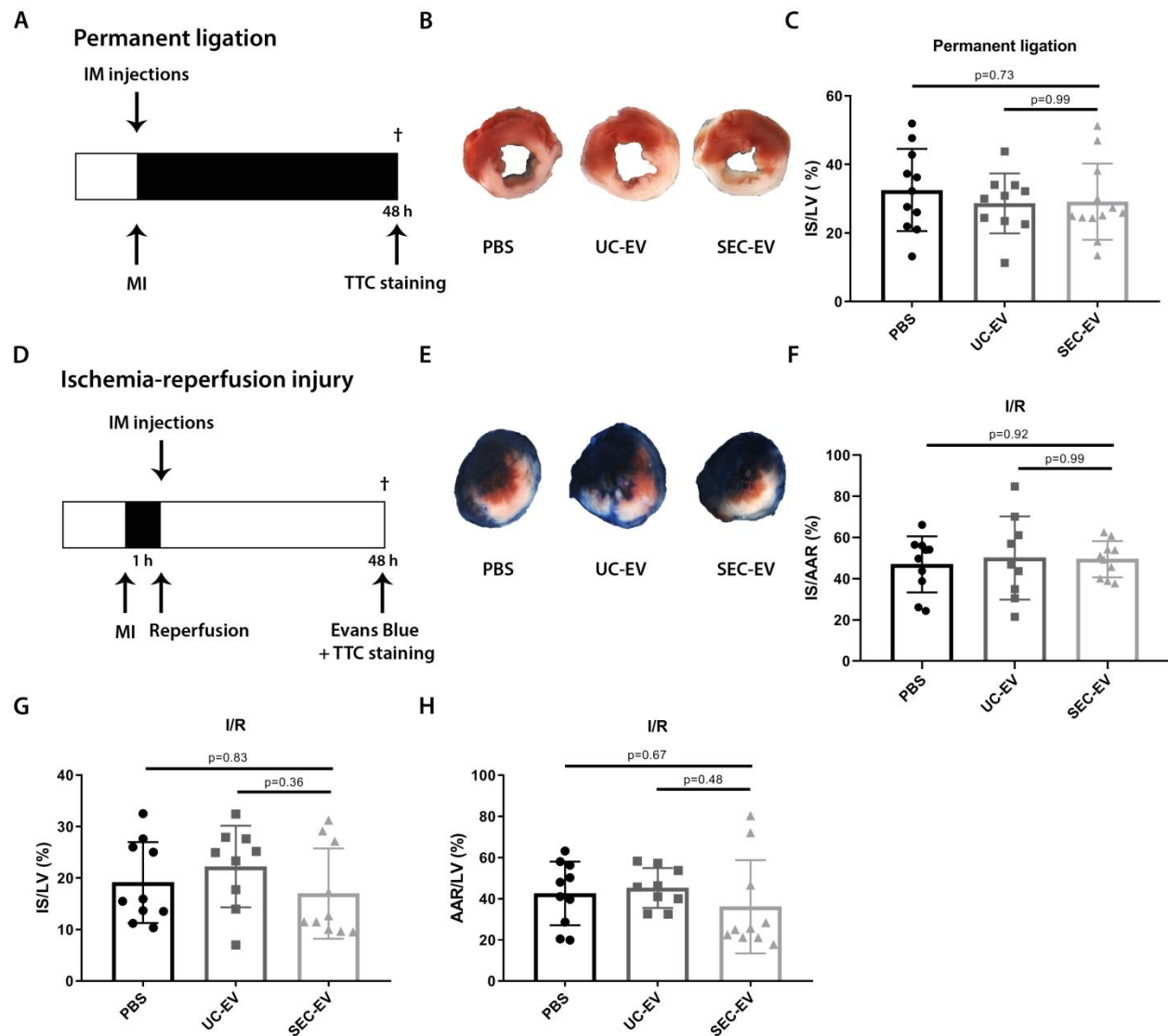


Figure 1 Infarct size is not affected by treatment with UC-EVs or SEC-EVs after experimentally induced ischemia in two mouse infarct models. A) Timeline and experimental set-up of the permanent ligation model. B) Representative images of TTC stained heart sections. C) Infarct size was not different between PBS, UC-EV or SEC-EV treated groups after permanent ligation. D) Timeline and experimental set-up of the ischemia-reperfusion injury model. E) Representative images of Evans Blue and TTC stained heart sections. F) Infarct size expressed as IS/AAR was comparable between all the groups, as was IS/LV (G) and AAR/LV (H).

While volume measurements are used to assess cardiac function at a later stage, speckle tracking analysis is more sensitive to detect early myocardial deformations. Therefore, global longitudinal strain (GLS) and reverse longitudinal strain rates (rLSR) were assessed to evaluate myocardial contractility 2 days post-I/R injury. GLS did not differ between PBS and SEC-EV treated groups (-12.5 ± 5.1 vs -12.1 ± 3.9 , $p=0.99$; Figure 2A) nor between UC-EV and SEC-EV treated groups (-10.7 ± 7.5 vs -12.1 ± 3.9 , $p=0.85$). Furthermore, also rLSR, a measure of

diastolic dysfunction, was comparable between the groups (5.9 ± 3.5 for PBS vs 4.2 ± 2.3 for SEC-EV, $p=0.62$ and 6.0 ± 4.9 for UC-EV vs 4.2 ± 2.3 for SEC-EV, $p=0.57$). In summary, we did not observe early functional improvement after treatment with EVs.

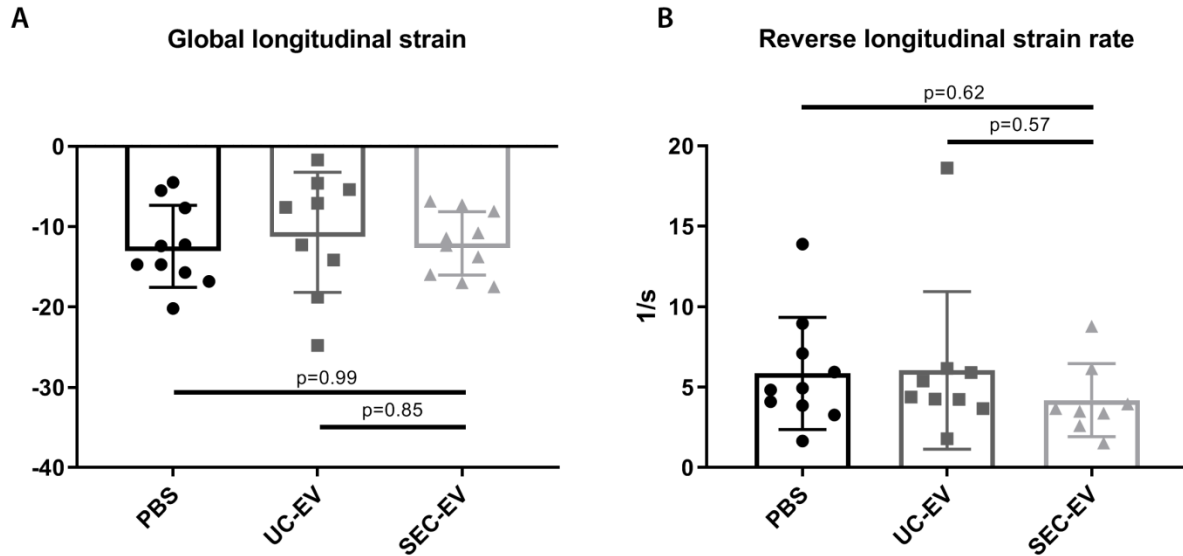


Figure 2 Global longitudinal strain and reverse longitudinal strain rate are unaffected after treatment with UC-EVs or SEC-EVs. Strain analysis was performed 2 days post-I/R injury. No functional improvement was observed after treatment with either UC-EVs or SEC-EVs as assessed by global longitudinal strain (A) and reverse strain rate (B).

Cardiac troponin I is a well-known biomarker used for detection of acute myocardial injury. Therefore, plasma levels of cardiac troponin I were assessed to evaluate the amount of cardiac muscle damage in all three groups 2 days post-MI. Troponin I levels did not differ between PBS and SEC-EV treated groups in the permanent ligation model (41811 ± 18539 vs 34369 ± 16174 ng/L, respectively, $p = 0.67$; Figure 3A) nor between UC-EV and SEC-EV treated groups (44311 ± 27372 vs 34369 ± 16174 ng/L, respectively, $p=0.51$). Similar findings were observed for the I/R injury model (95.3 ± 78.0 for PBS vs 189.9 ± 291.7 ng/L for SEC-EV, $p = 0.90$ and 401.6 ± 824.7 for UC-EV vs 189.9 ± 291.7 ng/L for SEC-EV, $p=0.62$; Figure 3B). Next, the ratio between heart weight/tibia length (HW/TL) was calculated for each group. Interestingly, a significant decrease in HW/TL ratio was observed for the SEC-EV-treated group compared to PBS- and UC-EV-treated groups after permanent ligation (9.6 ± 1.2 for PBS vs 8.6 ± 0.7 for SEC-EV, $p<0.05$ and 9.7 ± 1.0 for UC-EV vs 8.6 ± 0.7 for SEC-EV, $p<0.05$; Figure 4A). Moreover, a similar trend was observed for SEC-EVs after I/R injury (7.2 ± 0.6 for PBS vs 6.8 ± 0.4 for SEC-EVs, $p = 0.25$ and 7.2 ± 0.6 for UC-EV vs 6.8 ± 0.4 for SEC-EV, $p=0.29$; Figure 4B).

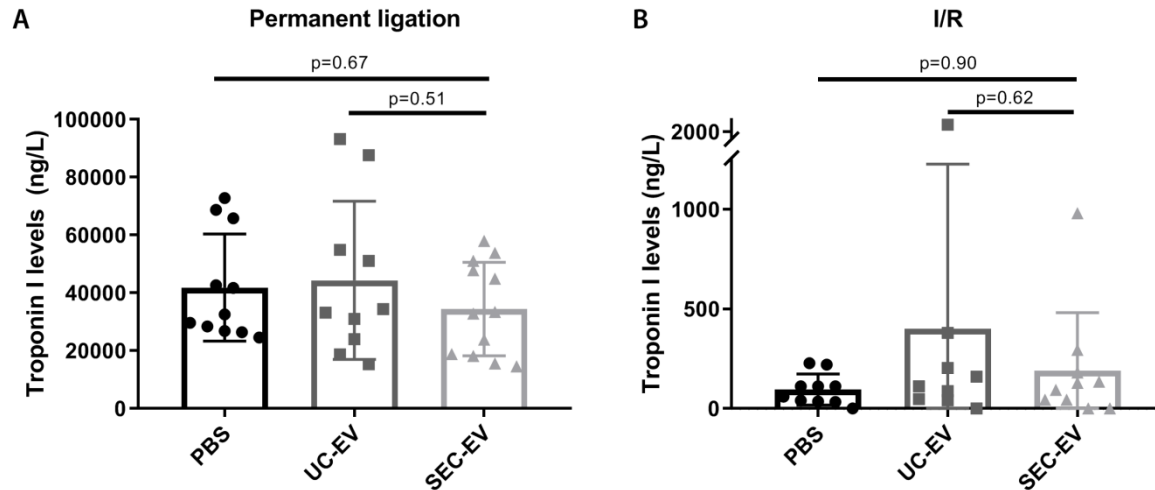


Figure 3 Plasma levels of Troponin I are unaffected by UC-EV or SEC-EV treatment. Plasma levels of troponin I were determined 2 days post-MI. A) Plasma levels of troponin I after UC-EV or SEC-EV treatment are comparable to those after PBS treatment 2 days after permanent ligation. B) Plasma levels of troponin I were not different between groups 2 days post-I/R injury.

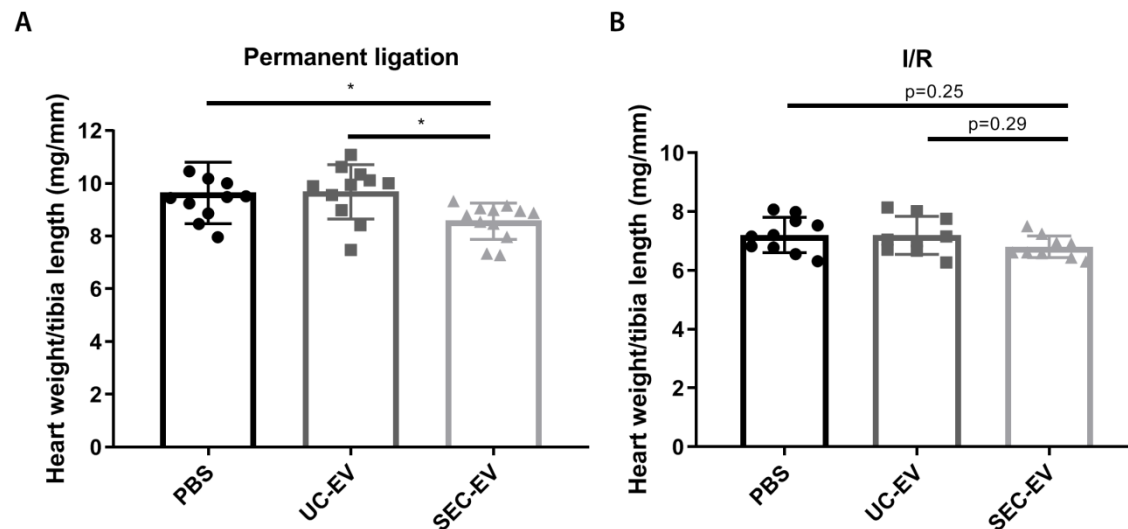


Figure 4 HW/TL ratio is decreased after treatment with SEC-EVs. HW/TL ratio was calculated for all three groups. A) A significant decrease in HW/TL ratio is observed after treatment with SEC-EVs as compared to PBS and UC-EVs. B) A lower HW/TL ratio is observed after treatment with SEC-EVs in I/R injury, although not significant.

Since we observed that infarct size is not affected by SEC-EV or UC-EV treatment, we questioned whether the injected EV batches were indeed functional, also in an *in vitro* setting. HMEC-1 cells were stimulated with 6×10^{10} UC-EVs or SEC-EVs or PBS for 30 min to assess ERK1/2 activation. Comparable to our previous study²⁰, SEC-EV stimulation resulted in higher ERK1/2 phosphorylation, as compared to UC-EVs, thereby confirming their functionality *in vitro* (Figure 5).

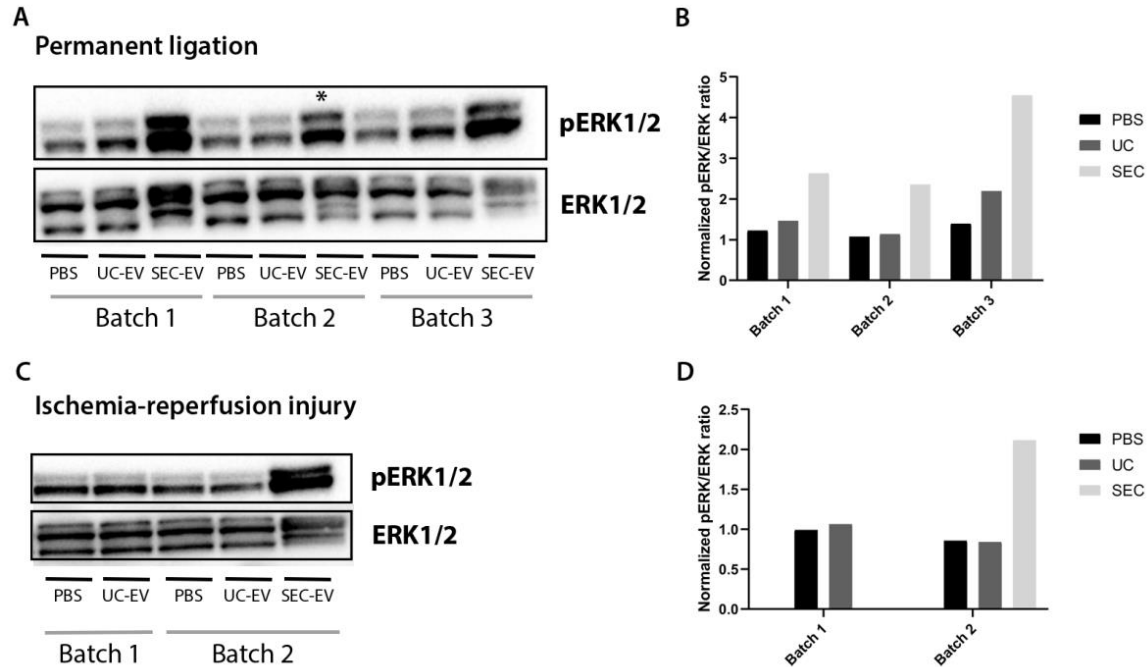


Figure 5 EVs' bioactivity is confirmed *in vitro*. A) Bioactivity of all three EV batches was assessed using an *in vitro* assay. HMEC-1 were stimulated with 6×10^{10} EVs for 30 minutes, after which pERK1/2/ERK1/2 ratio was determined using western blotting. All three SEC-EV batches show increased ERK1/2 activation compared to PBS and UC-EV. * indicates the use of an EV dose of 0.95×10^{10} EVs to stimulate HMEC-1. B) The two batches of EVs used in I/R injury were tested for their ability to activate ERK1/2. Due to a too low amount of SEC-EVs left for *in vitro* studies, this value is missing for SEC-EV in batch 1. SEC-EVs were able to activate ERK to a higher extent compared to PBS and UC-EV.

Discussion

Cellular therapeutics have been developed aiming to replace and/or repair the damaged myocardium after MI. Injection of CPC into the myocardium resulted in beneficial effects on cardiac function despite low cell engraftment, indicating the involvement of paracrine mediators⁵. CPC-EVs have been identified as paracrine secretions from CPC carrying important bioactive factors. Indeed, CPC-EV treatment resulted in significant reduction in infarct size 2 days after permanent ligation of the LAD in mice¹⁶. Hence, moving towards the use of EVs for therapeutic application, large scale production of EVs with maintained functionality is crucial. Therefore, standardized protocols and scalable isolation methods are needed. Previously, we have shown that isolation method can influence EV functionality *in vitro*, as SEC isolation resulted in more functional EVs compared to UC²⁰. With the aim to investigate possible differences in functionality between EVs isolated with UC or SEC *in vivo*, we assessed infarct size after PBS, UC-EV, or SEC-EV treatment 2 days after permanent ligation or I/R injury in mice.

Surprisingly, EV treatments were not successful in exerting therapeutic effects since infarct sizes were comparable between UC-EV, SEC-EV and PBS treated groups after permanent ligation as well as after I/R injury. To investigate if EV treatment led to early functional differences, we measured GLS and rLSR, parameters that are considered to be sensitive measures of early myocardial deformation²¹. Similar to infarct size measurements, no functional improvements were detected upon treatment with EVs based on global longitudinal strain and reverse strain rate. Interestingly, we did observe a significant difference in HW/TL ratio after SEC-EV treatment compared to PBS and UC-EV in the permanent ligation model. Moreover, the same trend was visible after I/R injury. HW/TL ratio is a measure of cardiac hypertrophy, as an increased ratio could indicate that hearts are compensating for volume lost by necrotic cardiomyocytes after MI^{22,23}. Previous studies reported increased HW/TL ratios when measured 1 to 4 weeks post-MI, and in those studies effective treatment was able to reduce HW/TL ratios²⁴⁻²⁷. Although our study used a more acute time point, this may indicate that SEC-EV have effects on edema formation and/or inflammation. Future studies should be performed to investigate the role of SEC-EVs in this process in more detail.

Our data is in contrast with previous reports that did show reduced infarct size upon CPC-EV treatment¹⁶. There are several possible explanations for these different observations. First, we observed high variability in infarct size within the PBS treated group for both MI models. One might argue that detecting a small beneficial effect after EV treatment is difficult when such a high variability is present between initial infarct sizes. However, when comparing troponin levels, infarct sizes, and strain values to other reports, similar variability is generally observed^{11,16,28-31}. Secondly, we employed a different CPC clone compared to our previous study¹⁶. Different Sca1+ CPC subpopulations have been discovered within the human heart that are either more committed to the vascular (N-glycosylated PECAM1+ CPC) or cardiomyocyte lineage (N-glycosylated GRP78+ CPC)^{32,33}. Future studies should reveal if the CPC clone used in our current and previous studies represent different CPC subpopulations and if that could explain the differences in functional efficacy. Thirdly, differences in culture protocol could influence outcome. In order to make our EV preparation suitable for future human application, we isolated EVs from serum-free basal medium, which is different from other studies that mostly use 'EV-depleted' FBS-containing medium. In those studies, EVs are depleted from serum before culturing via an overnight ultracentrifugation step. Doubts have been raised on whether ultracentrifugation leads to efficient removal of serum-derived EVs and extracellular RNA³⁴⁻³⁷. Indeed, although ultracentrifugation highly reduced the amount of RNAs present in FBS, residual serum-derived RNAs could still be detected in EV preparations from EV-depleted FBS-containing medium³⁴. Hence, serum RNA and/or proteins may be co-isolated when associated to other macromolecules that have similar sizes as EVs. Furthermore, it has been reported for neuroblastoma-derived EVs that serum-free culturing alters protein composition of EVs³⁸. Whether CPCs produce EVs with different cargo in response to serum-free medium compared to

EV-depleted medium remains unclear to date. Future research should reveal if this change to serum-free culture media in our study is responsible for the observed differences in functional outcome compared to other studies.

Alternatively, differences in EV dose could explain our findings, despite the fact that our EV dose correlates to the amount of EV protein used in previous studies and that therapeutic effects have been obtained using similar numbers of EVs^{10,11,16}. The optimal EV dose needed for therapeutic efficacy post-MI has not been adequately covered by previous studies. Thus, in our study we may administer either too low or too high doses in order to achieve therapeutic benefits post-MI. Future studies should therefore focus on determining dose-response curves for EV therapeutics.

When assessing the functionality of the used EV batches *in vitro*, we found that SEC-EV were still able to activate ERK1/2 to a higher extent than PBS and UC-EV, which is in agreement with our previously reported study²⁰, thereby indicating some level of functionality before injection *in vivo*. Yet, one could question the predictive value of this *in vitro* assay for EV functionality *in vivo*, since our *in vitro* results do not correspond to our *in vivo* data. To date, we are not aware of an *in vitro* assay that is able to assess and predict EV functionality *in vivo*. The development of such an assay would be a valuable contribution when exploring the use of EV therapeutics after MI.

In conclusion, we observed no difference in infarct size between PBS, UC-EV and SEC-EV treated groups after permanent ligation nor after I/R injury, which is in contrast to previously reported studies. Future studies should address whether high variability within the MI models, or differences in CPC clones, serum-free culture media, or dosing could explain these differences.

Acknowledgements

This work is supported by the Project EVICARE (#725229) of the European Research Council (ERC) to JS, co-funded by the Project SMARTCARE-II of the BioMedicalMaterials institute to JS/MJG, the ZonMw-TAS program (#116002016) to JS/MJG, the Dutch Ministry of Economic Affairs, Agriculture and Innovation and the Netherlands CardioVascular Research Initiative (CVON): the Dutch Heart Foundation to JS/MJG, Dutch Federations of University Medical Centers, the Netherlands Organization for Health Research and Development, and the Royal Netherlands Academy of Sciences.

References

1. WHO. *Global Health Observatory data*. (2019).
2. Hellermann, J. P. *et al*. Heart failure after myocardial infarction: a review. *Am. J. Med.* **113**, 324–30 (2002).
3. Smits, A. M. *et al*. Human cardiomyocyte progenitor cells differentiate into functional mature cardiomyocytes: an in vitro model for studying human cardiac physiology and pathophysiology. *Nat. Protoc.* **4**, 232–243 (2009).
4. van Vliet, P. *et al*. Progenitor cells isolated from the human heart: a potential cell source for regenerative therapy. *Neth. Heart J.* **16**, 163–9 (2008).
5. Smits, A. M. *et al*. Human cardiomyocyte progenitor cell transplantation preserves long-term function of the infarcted mouse myocardium. *Cardiovasc. Res.* **83**, 527–35 (2009).
6. van den Akker, F. *et al*. Intramyocardial stem cell injection: go(ne) with the flow. *Eur. Heart J.* **38**, 184–186 (2017).
7. Feyen, D. A. M. *et al*. Gelatin Microspheres as Vehicle for Cardiac Progenitor Cells Delivery to the Myocardium. *Adv. Healthc. Mater.* **5**, 1071–9 (2016).
8. Timmers, L. *et al*. Human mesenchymal stem cell-conditioned medium improves cardiac function following myocardial infarction. *Stem Cell Res.* **6**, 206–14 (2011).
9. Arslan, F. *et al*. Mesenchymal stem cell-derived exosomes increase ATP levels, decrease oxidative stress and activate PI3K/Akt pathway to enhance myocardial viability and prevent adverse remodeling after myocardial ischemia/reperfusion injury. *Stem Cell Res.* **10**, 301–312 (2013).
10. Chen, L. *et al*. Cardiac progenitor-derived exosomes protect ischemic myocardium from acute ischemia/reperfusion injury. *Biochem. Biophys. Res. Commun.* **431**, 566–71 (2013).
11. Barile, L. *et al*. Extracellular vesicles from human cardiac progenitor cells inhibit cardiomyocyte apoptosis and improve cardiac function after myocardial infarction. *Cardiovasc. Res.* **103**, 530–541 (2014).
12. Pegtel, D. M. *et al*. Functional delivery of viral miRNAs via exosomes. *Proc. Natl. Acad. Sci. U. S. A.* **107**, 6328–33 (2010).
13. Ratajczak, M. Z. & Ratajczak, J. Horizontal transfer of RNA and proteins between cells by extracellular microvesicles: 14 years later. *Clin. Transl. Med.* (2016).
14. Ratajczak, J. *et al*. Embryonic stem cell-derived microvesicles reprogram hematopoietic progenitors: evidence for horizontal transfer of mRNA and protein delivery. *Leukemia* **20**, 847–56 (2006).
15. Valadi, H. *et al*. Exosome-mediated transfer of mRNAs and microRNAs is a novel mechanism of genetic exchange between cells. *Nat. Cell Biol.* **9**, 654–9 (2007).
16. Maring, J. A. *et al*. Cardiac progenitor cell-derived extracellular vesicles reduce infarct size and associate with increased cardiovascular cell proliferation. *J. Cardiovasc. Transl. Res.* **12**, 5–17 (2019).
17. Linares, R., Tan, S., Gounou, C., Arraud, N. & Brisson, A. R. High-speed centrifugation induces aggregation of extracellular vesicles. *J. Extracell. vesicles* **4**, 29509 (2015).
18. Taylor, D. D. & Shah, S. Methods of isolating extracellular vesicles impact down-stream analyses of their cargoes. *Methods* **87**, 3–10 (2015).
19. Nordin, J. Z. *et al*. Ultrafiltration with size-exclusion liquid chromatography for high yield isolation of extracellular vesicles preserving intact biophysical and functional properties. *Nanomedicine* **11**, 879–83 (2015).
20. Mol, E. A., Goumans, M. J., Doevendans, P. A., Sluijter, J. P. G. & Vader, P. Higher functionality of extracellular vesicles isolated using size-exclusion chromatography compared to ultracentrifugation. *Nanomedicine Nanotechnology, Biol. Med.* **13**, 2061–2065 (2017).

21. Schnelle, M. *et al.* Journal of Molecular and Cellular Cardiology Echocardiographic evaluation of diastolic function in mouse models of heart disease. *J. Mol. Cell. Cardiol.* **114**, 20–28 (2018).
22. Rubin, S. A., Fishbein, M. C. & Swan, H. J. C. Compensatory hypertrophy in the heart after myocardial infarction in the rat. *J. Am. Coll. Cardiol.* **1**, 1435–1441 (1983).
23. Muhlestein, J. B. Adverse left ventricular remodelling after acute myocardial infarction: is there a simple treatment that really works? *Eur. Heart J.* **35**, 144–6 (2014).
24. Chang, W., Wu, Q., Xiao, Y. & Jiang, X. Acacetin protects against cardiac remodeling after myocardial infarction by mediating MAPK and PI3K / Akt signal pathway. *J. Pharmacol. Sci.* **135**, 156–163 (2017).
25. Fan, J. *et al.* Recombinant frizzled1 protein attenuated cardiac hypertrophy after myocardial infarction via the canonical Wnt signaling pathway. 3069–3080 (2018).
26. Liu, Z. *et al.* A CRM1 inhibitor alleviates cardiac hypertrophy and increases the nuclear distribution of NT-PGC-1 α in NRVMs. (2019).
27. McDonald, H. *et al.* Hexarelin treatment preserves myocardial function and reduces cardiac fibrosis in a mouse model of acute myocardial infarction. **6**, (2018).
28. Ellenbroek, G. H. J. M. *et al.* Leukocyte-Associated Immunoglobulin-like Receptor-1 is regulated in human myocardial infarction but its absence does not affect infarct size in mice. *Sci. Rep.* **7**, 18039 (2017).
29. Deddens, J. C. *et al.* Targeting chronic cardiac remodeling with cardiac progenitor cells in a murine model of ischemia/reperfusion injury. *PLoS One* **12**, e0173657 (2017).
30. Webber, M. J. & Dankers, P. Y. W. Supramolecular hydrogels for biomedical applications. *Macromol. Biosci.* **19**, 1800452 (2019).
31. Frobert, A., Valentin, J., Magnin, J., Riedo, E. & Cook, S. Prognostic value of Troponin I for infarct size to improve preclinical myocardial infarction small animal models. **6**, 1–10 (2015).
32. Moerkamp, A. T. *et al.* Glycosylated cell surface markers for the isolation of human cardiac progenitors. **26**, 1552–1565 (2017).
33. Leung, H. W. *et al.* mAb C19 targets a novel surface marker for the isolation of human cardiac progenitor cells from human heart tissue and differentiated hESCs. *J. Mol. Cell. Cardiol.* **82**, 228–237 (2015).
34. Wei, Z., Batagov, A. O., Carter, D. R. F. & Krichevsky, A. M. Fetal Bovine Serum RNA Interferes with the Cell Culture derived Extracellular RNA. *Sci. Rep.* **6**, 31175 (2016).
35. Driedonks, T. A. P., Twilhaar, M. K. N. & Nolte-'t Hoen, E. N. M. N.-. Technical approaches to reduce interference of Fetal calf serum derived RNA in the analysis of extracellular vesicle RNA from cultured cells. *J. Extracell. Vesicles* **8**, (2019).
36. Shelke, G. V., Lässer, C., Ghossein, Y. S. & Lötvall, J. Importance of exosome depletion protocols to eliminate functional and RNA-containing extracellular vesicles from fetal bovine serum. *J. Extracell. vesicles* **3**, (2014).
37. Kornilov, R. *et al.* Efficient ultrafiltration-based protocol to deplete extracellular vesicles from fetal bovine serum. *J. Extracell. Vesicles* **7**, (2018).
38. Li, J. *et al.* Serum-free culture alters the quantity and protein composition of neuroblastoma-derived extracellular vesicles. *J. Extracell. vesicles* **4**, 26883 (2015).

Injectable supramolecular ureidopyrimidinone hydrogels provide sustained release of extracellular vesicle therapeutics

Emma A. Mol MSc^{1,2}, Zhiyong Lei PhD¹, Marieke T. Roefs MSc¹, Maarten H. Bakker PhD³, Marie-José Goumans PhD², Pieter A. Doevendans PhD^{1,4,5}, Patricia Y.W. Dankers PhD³, Pieter Vader PhD⁶, Joost P.G. Sluijter PhD^{1,4,7}

Advanced Healthcare Materials 2019; 8: 1900847

¹Department of Cardiology, Laboratory of Experimental Cardiology, University Medical Center Utrecht, Utrecht 3584, The Netherlands

²Laboratory of Cardiovascular Cell Biology, Department of Cell and Chemical Biology, Leiden University Medical Center, Leiden 2333ZA, The Netherlands

³Institute for Complex Molecular Systems, Department of Biomedical Engineering, Laboratory of Chemical Biology, Eindhoven University of Technology, 5600 MB Eindhoven, The Netherlands

⁴UMC Utrecht Regenerative Medicine Center, University Medical Center, Utrecht 3584CT, The Netherlands

⁵CMH NL-HI, Utrecht 3584CX, The Netherlands

⁶Laboratory of Clinical Chemistry and Haematology, University Medical Center Utrecht, Utrecht 3584, The Netherlands

⁷University Utrecht, Utrecht 3508TC, The Netherlands

Abstract

Extracellular vesicles (EVs) are small vesicles secreted by cells and have gained increasing interest as both drug delivery vehicles or as cell-free therapeutics for regenerative medicine. To achieve optimal therapeutic effects, strategies are being developed to prolong EV exposure to target organs. One promising approach to achieve this is through EV-loaded injectable hydrogels. In this study, the use of a hydrogel based on ureido-pyrimidinone (UPy) units coupled to poly(ethylene glycol) chains (UPy-hydrogel) is examined as potential delivery platform for EVs. UPy-hydrogel undergoes a solution-to-gel transition upon switching from a high to neutral pH, allowing immediate gelation upon administration into physiological systems. Here, we show sustained EV release from UPy-hydrogel measured over a period of 4 days. Importantly, EVs retained their functional capacity after release. Upon local administration of fluorescently labeled EVs incorporated in a UPy-hydrogel *in vivo*, EVs were still detected in the UPy-hydrogel after 3 days, whereas in the absence of a hydrogel, EVs were internalized by fat and skin tissue near the injection site. Together, these data demonstrate that UPy-hydrogels provide sustained EV release over time and enhance local EV retention *in vivo*, which could contribute to improved therapeutic efficacy upon local delivery and translation towards new applications.

Main text

Extracellular vesicles (EVs) are nano-sized lipid bilayer-enclosed particles that play major roles in cell to cell communication and tissue homeostasis¹⁻³. EVs contain specific cargo including genetic material (mRNA, miRNA, lncRNA), proteins, and lipids⁴. They are released by every cell type of the human body studied to date. The ability of EVs to naturally target and cross membrane barriers and deliver their biological cargo intracellularly makes them potentially useful as drug delivery vehicles^{5,6}. Moreover, EVs have also gained interest as potential off-the-shelf therapeutics for regenerative medicine applications, since the beneficial effect of progenitor cell therapy has been ascribed to paracrine factors including EVs, mainly due to their anti-inflammatory, anti-fibrotic, pro-proliferative and pro-angiogenic characteristics⁷⁻⁹. For regenerative medicine applications, EVs may be derived from various cell sources, including mesenchymal stromal cells (MSC), tissue-specific progenitor cells, or induced pluripotent stem cells (iPSC)¹⁰⁻¹⁴. Furthermore, EVs have been considered for application in different patient categories, including peripheral artery disease, cardiomyopathies, chronic kidney disease and osteoporosis/cartilage degradation¹⁵⁻²¹.

Often, injection of cellular therapeutics demonstrated only modest beneficial outcomes in different patients groups, as a result of retention problems²²⁻²⁵. One example is the randomized, controlled BOne marrOw transfer to enhance ST-elevation infarct regeneration (BOOST) trial, where an intracoronary infusion of a single dose of bone marrow cells (BMCs) was performed in patients with acute myocardial infarction²⁴. They found an improved cardiac function after 6 months, however, this beneficial effect was lost after 18 months. Further studies showed that only 5% of the BMCs were retained in the heart after intracoronary infusion, indicating potential retention problems with cellular therapeutics²⁶. Similarly, strategies to enhance EV delivery in chronically diseased patients and prolong exposure of EV therapeutics have yet to be optimized to achieve their full potential for true therapeutic efficacy.

Several EV administration routes have been investigated to date, of which intravenous injection is the most widely studied. Unfortunately, intravenously injected EVs are rapidly taken up by the liver and spleen, thereby hampering delivery to other tissues²⁷⁻²⁹. On the other hand, local administration into the diseased organs could be a valuable approach to enhance tissue-specific EV delivery, thereby improving their efficiency and safety profile. However, when investigating cell retention after local injection into porcine hearts³⁰, we previously observed an immediate wash-out of almost all cells via the venous drainage system, resulting in a substantial cell loss. Furthermore, Beegle et al. investigated the retention of VEGF-overexpressing MSC after local intramuscular injection into the hindlimb using bioluminescent imaging³¹, and found that the cell numbers after injection rapidly declined over time, and only less than 0.1% of the total number of injected MSC could be detected after a period of 28 days.

Given this immediate wash-out of cells, which may also be expected for EVs and will lead to decreased therapeutic exposure, the usage of patches, injectable microcarriers or hydrogels is intensively studied, aiming for increased retention of therapeutics³²⁻³⁵. A recent example is the study from Nikraves et al., showing controlled release of osteoblast-derived EVs using two alginate-based microgels³⁴. In addition, the EV release profile was tunable based on physical structuring of the alginate polymers. Incorporation of EVs in a hydrogel could allow for controlled EV release over longer periods, which could even further enhance therapeutic exposure, maximizing their efficacy.

Injectable hydrogels are among the most promising candidate systems to increase EV local retention. These systems are either based on natural (*e.g.* extracellular matrix-derived, or collagen/fibrin-based) materials, that closely mimic the host tissue, or synthetic materials (*e.g.* poly(ethylene glycol) (PEG) or poly(N-isopropylacrylamide)-based), that are easily tunable, have controllable biochemical properties, and might be less vulnerable to batch-to-batch variation^{36,37}. Moreover, various injectable hydrogels are available that differ in composition and mechanical and gelation properties induced by changes in physiological conditions such as temperature, ionic strength, and pH³⁷.

One highly potential injectable material is the ureido-pyrimidinone (UPy) supramolecular hydrogelator (UPy-hydrogel)³⁸. This gel consists of polymers comprising a poly(ethylene glycol) (PEG) backbone telechelically coupled to two UPy-units that can form transient supramolecular networks by dimerization of the UPy-moieties by four-fold hydrogen-bonding and concomitant stacking into nanofibrous structures. This nanofiber formation is facilitated by additional urea groups introducing lateral hydrogen bonding in a hydrophobic pocket provided by additional alkyl spacers. The nanofibrous structures form the transient network by entanglements and supramolecular crosslinking between the nanofibers³⁸. The UPy-hydrogel undergoes a solution-to-gel transition when the pH is switched from high to neutral, *i.e.* from basic to neutral environment, with a threshold at \sim pH 8.5, dependent on the concentration of UPy-polymers. This unique property allows gelation upon injection into physiological systems. The molecular weight of the PEG polymer can also be tuned, resulting in UPy-hydrogels with different functional properties³⁹, of which the characteristics have been reported extensively before³⁸⁻⁴².

Over the past years, UPy-hydrogels have also been investigated as controlled release system for different applications, including for growth factor and miRNA delivery^{40,42}. Here, we investigated the use of UPy-hydrogel as a platform for EV delivery, aiming to prolong local delivery of EVs to targeted organs.

To investigate if EV delivery can be prolonged when EVs are incorporated into UPy-hydrogels, we used EVs released from cardiac-derived progenitor cells as they have well-known functionalities^{21,43-45}. EV preparations were characterized based on size distribution profile,

measured by Nanoparticle Tracking Analysis (NTA) before encapsulation as well as after release from UPy-hydrogel, and by expression of EV markers (Figure 1A+B). According to NTA, EVs displayed a classical size distribution profile peaking at 100 nm, as we have seen before⁴³. Moreover, encapsulation and release of EVs from UPy-hydrogels did not affect their size distribution profile. Western blot analysis showed an enrichment of typical EV markers such as Alix, CD81, and CD63 as compared to cell lysates. In contrast, calnexin, an endoplasmatic reticulum marker, was undetectable in EVs, confirming a lack of contamination with other membrane compartments.

To study the use of UPy-hydrogels for sustained EV delivery, EVs were loaded into UPy-hydrogels and transferred to an insert of a transwell system containing medium in the bottom compartment. In order to determine the kinetics of EV release from UPy-hydrogels, conditioned medium was sampled at several time points. Subsequently, a bead capture assay was performed to measure EV release in the conditioned medium. When using magnetic beads coated with antibodies directed against the EV markers CD9, CD81, or CD63 and their corresponding fluorescent detection antibodies, we were able to detect different EV marker proteins being released from CPC (Supplemental Figure 1). To assess EV release from UPy-hydrogels, EVs were captured using CD63 antibody-coated magnetic beads and fluorescently labeled with antibodies directed against CD63 (Figure 1C).

The molecular weight of the PEG block within UPy-hydrogels can be varied which may result in different kinetics of release. Therefore, first, EV release patterns from UPy-hydrogels with a PEG block of 10 kg mol⁻¹ (UPy10k) or 20 kg mol⁻¹ (UPy20k) were compared, which revealed a delayed EV release from the UPy10k-hydrogels as compared to UPy20k-hydrogels (Supplemental Figure 2)³⁸. Moreover, the release pattern of the UPy10k-hydrogels showed less variation. Therefore, we decided to continue with the UPy10k-hydrogels for future experiments. Next, EV signals in conditioned medium were assessed for UPy-hydrogels with and without EVs at different time points (Figure 1D). The percentage of EVs that was released from the gel after 4 days was estimated to be approximately 10%, as assessed using a standard curve of known EV concentrations. A gradual and sustained release of EVs from UPy-hydrogel was observed over a period of several days rather than an immediate burst of EVs, indicating its potential to prolong EV delivery. When measuring long-term release of EVs from UPy-hydrogels, we found that EVs are continuously released from the hydrogel for up to 2.5 weeks (Supplemental Figure 3). In contrast, Hernandez et al. investigated EV release from extracellular matrix-derived (ECM) hydrogels and found that the majority of released EVs were already detected 1 day after encapsulation, thus the release profile of EVs from our UPy-hydrogel seems favourable as compared to EV release from ECM hydrogels³⁵. EV release from ECM hydrogels varied from 25-45% after 3 days, depending on hydrogel tissue source. Furthermore, when incorporating miRNA or anti-miR molecules in UPy-hydrogels, Bakker et al. observed near complete release

from UPy-hydrogels within 2 days⁴². This release could be delayed by using cholesterol-conjugated molecules, suggesting an affinity of cholesterol to the UPy-hydrogel network. EVs are much larger in size and also contain high levels of cholesterol, which could possibly explain the more gradual release of EVs compared to miRNA or anti-miR molecules. Since our method of EV detection is based on the expression of CD63, we cannot exclude a bias for a specific EV population. However, since we were able to detect multiple EV markers using this method (Supplemental Figure 1), and as we are mainly interested in release of EVs from UPy-hydrogels and its application *in vivo* in general, we assume the release profile is similar for other EV populations of the same size and composition.

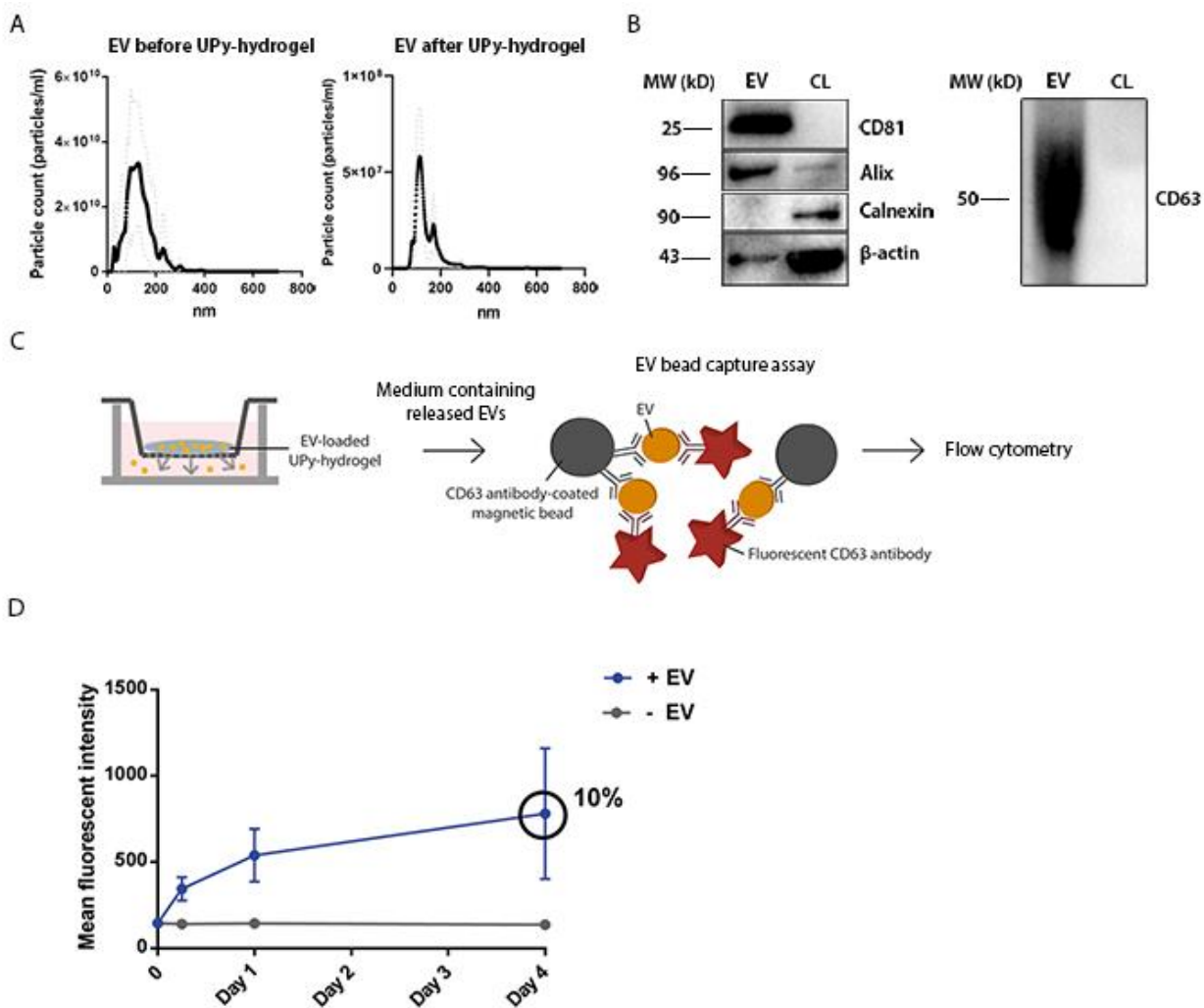


Figure 1 Sustained release of EVs from UPy-hydrogel *in vitro*. CPC-derived EVs were isolated using ultrafiltration followed by size-exclusion chromatography. A) Nanoparticle Tracking Analysis (NTA) was performed to show EVs' size distribution before encapsulation and after release from UPy-hydrogel. NTA revealed an average EV size of 100 nm, which was not affected by incorporation into and release from UPy-hydrogels. Results are presented as mean \pm SD (black line and dotted line, respectively). B) The presence of typical EV markers CD81, Alix, CD63, in our EV preparation was confirmed using Western Blot analysis. The endoplasmic reticulum membrane protein calnexin was not present in

our EVs. C) To evaluate EV release from UPy-hydrogel, conditioned medium containing the released EVs were collected at several time points up to 4 days. An EV bead capture assay was performed to assess EV release based on CD63+fluorescent intensity. D) Approximately 10% of the initial EVs were released from UPy-hydrogel after 4 days, calculated by using a standard curve of multiple known EV concentrations. Data are displayed as mean \pm SD of three replicate experiments. Abbreviations: CL = cell lysate, CPC = cardiac progenitor cell, MW = molecular weight.

Importantly, to achieve EVs' full therapeutic potential, they should remain biologically active after release from hydrogels. EVs have the ability to transfer their biological cargo, including proteins and RNA, between cells after EV uptake by the recipient cell⁴⁶. Therefore, to ensure that EVs maintain their integrity after release from UPy-hydrogels, we assessed EV uptake by HMEC-1 cells. Moreover, since CPC-EVs that were used in this study, have been shown to induce phosphorylation of ERK1/2, we used ERK1/2 activation in HMEC-1 as a second outcome parameter to determine EV functionality⁴³. PKH26-labeled EVs were loaded into UPy-hydrogels, placed in a transwell insert and co-cultured with HMEC-1 in the bottom well (Figure 2A). After 4 days, PKH26-labeled EVs were visible in the HMEC-1 co-cultured with EV-loaded UPy-hydrogels, whereas UPy-hydrogels without EVs did not show any positive PKH26-staining (Figure 2B). In addition, we evaluated if EVs maintained their functional ability to activate signaling pathways in targeted HMEC-1 after being released from UPy-hydrogel. Medium containing EVs released from UPy-hydrogels, collected after 1 week but also after 2 weeks, retained the ability to activate ERK signaling as evidenced by an increased pERK/ERK ratio in HMEC-1 upon exposure (Figure 2C). When compared to fresh EVs, EVs released after 1 week can activate ERK1/2 to the same extent as fresh EVs (Supplemental Figure 4). When released after 2 weeks, EVs still retain the ability to activate ERK signaling, although to a lower extent than fresh EVs, which should be further investigated in future studies. Together, these data indicate that EV function is preserved after release from UPy-hydrogels. We showed that after release from UPy-hydrogels EVs retain the ability to be taken up by recipient cells and activate internal signaling pathways, indicating a preserved biological function of EVs.

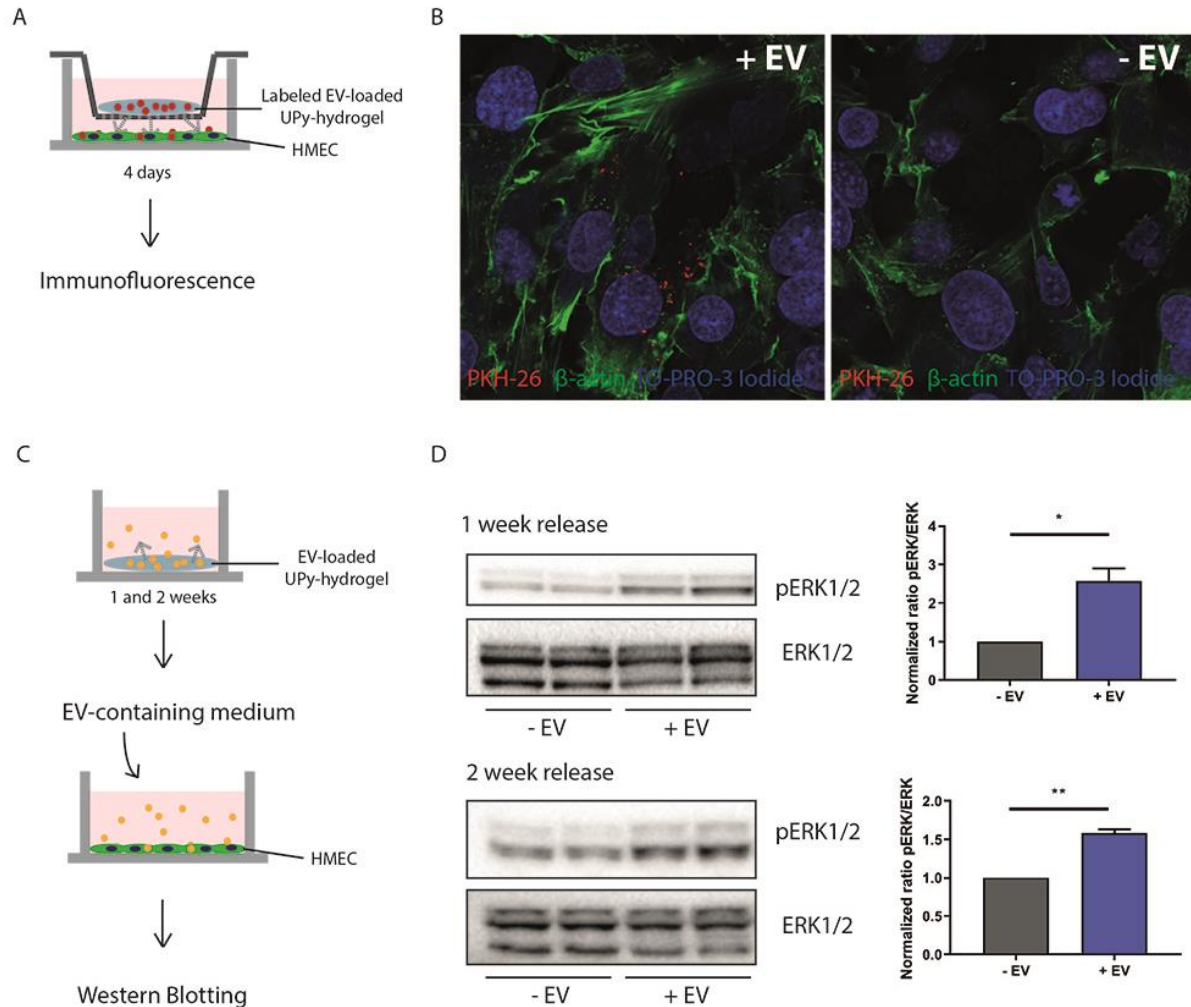


Figure 2 EVs retain their functionality after release from UPy-hydrogel. A) *In vitro* set-up to determine uptake of PKH26-labeled EVs by HMEC-1 after release from UPy-hydrogels. B) Fluorescent image of HMEC-1 co-cultured with either empty or EV-loaded UPy-hydrogels showing that EVs can be taken up by HMEC-1 after release from UPy-hydrogel. C) *In vitro* set-up to determine if EVs maintain their ability to activate ERK signaling. D) EVs collected after 1 or 2 weeks after release retain the ability to induce phosphorylation of ERK1/2. Data are displayed as mean \pm SD. * represents $p < 0.05$ and ** $p < 0.01$ using an unpaired Student's *t* test. Abbreviations: ERK1/2 = extracellular signal-regulated kinase 1/2, HMEC-1 = human microvascular endothelial cells.

The abovementioned results confirmed a sustained EV release from UPy-hydrogels *in vitro*. To achieve increased therapeutic exposure *in vivo* however, improving local EV retention would also be of great importance. Therefore, we evaluated the feasibility of UPy-hydrogel to improve local retention of EVs in an *in vivo* model. UPy-hydrogel loaded with fluorescently-labeled EVs (UPy + EV) or fluorescently-labeled EVs alone (EV) were injected subcutaneously in mice. Solid-like UPy-hydrogels could be detected in all mice 3 days after subcutaneous injection (Figure 3A + Figure S5). UPy-hydrogels, skin, and fat tissue near the injection site were excised and fluorescent signals (800 nm) were visualized using a Pearl Imager (Li-cor). In the UPy + EV group, most of

the fluorescent signal could be detected within the UPy-hydrogel, whereas in the EV group highest fluorescent signals were present in surrounding tissues including skin and subcutaneous fat tissue (Figure 3B). These data clearly show that EV retention *in vivo* can be improved by encapsulating EVs in UPy-hydrogels compared to EV treatment alone.

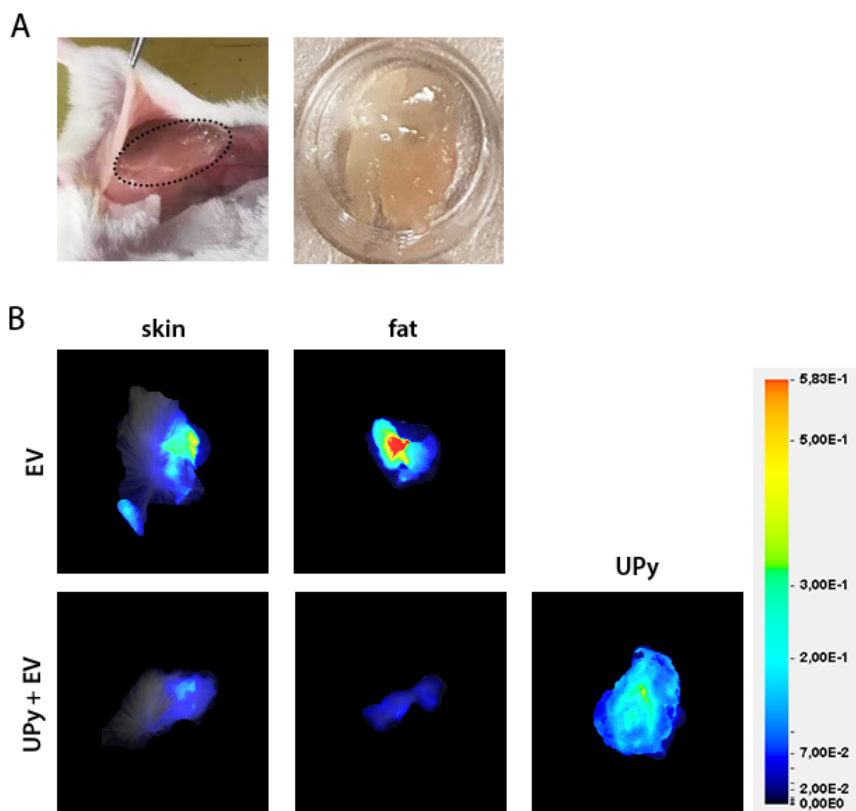


Figure 3 *In vivo* retention of EVs in UPy-hydrogels. A) Subcutaneously injected UPy-hydrogel can be detected as a solid-like gel 3 days after administration. B) Fluorescent images of skin, fat or UPy-hydrogel from mice treated with either EV alone or UPy + EV. In the EV group, most of the fluorescent signal was present in surrounding skin and fat, whereas in the UPy + EV group EVs were retained in the UPy-hydrogel.

Our study may also potentially be extended to other biomedical applications, such as therapeutic drug delivery, where EVs are regularly being used as drug carriers^{47,48}. The injectable nature of UPy-hydrogels makes them an attractive candidate for local clinical applications. For example, Bastings et al. showed that growth factor-loaded UPy-hydrogels could be delivered into the infarcted myocardium by catheter-guided injections⁴⁰. Furthermore, the ability to visualize a Gadolinium(III)-DOTA labeled UPy-hydrogel with contrast enhanced MRI could enhance injection accuracy when applying this to patients, emphasizing feasibility of UPy-hydrogels for translational purposes⁴¹.

Near-infrared fluorescently labeled-EVs were used in this study, which allows for studying their biodistribution in different tissues *in vivo*, but does not allow true quantification. A study by Royo et al. used radioactive labeling of EVs with Na[124I]I and detection with PET to quantify EV biodistribution *in vivo*⁴⁹. The use of radioactive labeled EVs to investigate *in vivo* biodistribution will make quantification possible, however, this method requires specific technologies to be available. EV release kinetics from UPy-hydrogel *in vivo* therefore remains to be investigated.

Interestingly, Gangadaran et al. observed an additional beneficial effect on blood perfusion and formation of new blood vessels in a hind-limb ischemia model when treated with mesenchymal stromal cell derived-EVs (MSC-EV) in Matrigel compared to MSC-EV alone¹⁷. In addition, when combining endothelial progenitor-derived EVs with a shear-thinning hydrogel, Chen et al. showed increased therapeutic efficacy after myocardial infarction compared to EV treatment alone¹⁰. These studies indicate the potential additional value of sustained EV release on tissue repair. Whether sustained EV release from UPy-hydrogels increases therapeutic efficacy *in vivo* compared to a single EV dose remains to be investigated.

In conclusion, this study shows that EVs are gradually released from UPy-hydrogels and remain associated with hydrogels upon injection *in vivo*. Furthermore, EVs keep their functionality after release *in vitro*. Therefore, EV delivery to specific sites may be prolonged using UPy-hydrogel, which could contribute to higher therapeutic effects upon local delivery and translation towards new applications.

Materials and Methods

Cell culture

Cardiac progenitor cells (CPC) and human microvascular endothelial cells (HMEC-1) were cultured as described before^{44,50}. Cells were incubated at 37°C (5% CO₂ and 20% O₂) and passaged at 80-90% confluency using 0.25% trypsin digestion. For EV isolation, CPCs were cultured for 3 days, after which medium was replaced with serum-free Medium 199 (Gibco, 31150-022). After 24 hours, conditioned medium (CM) was collected.

EV isolation protocol

EVs were isolated using ultrafiltration combined with size-exclusion chromatography (SEC)⁴³. First, cell culture CM was centrifuged at 2000 x *g* for 15 min, followed by 0.45 µm filtration to remove residual cell debris. Subsequently, CM was concentrated using 100 kDa molecular weight cut-off Amicon spin filters (Merck Millipore), after which it was loaded onto a S400 highprep column (GE Healthcare, Uppsala, Sweden) and fractionated using an AKTASart (GE Healthcare) system equipped with an UV 280nm flow cell. After elution from the column, EV-containing fractions were pooled, 0.45 µm filtered, and concentrated using a 100-kDa Amicon

spin filter. EV particle number and size distribution were determined using Nanoparticle Tracking Analysis (Nanosight NS500, Malvern). The camera level was set at 15 and the detection threshold at 5.

EV labeling

For *in vitro* experiments, EVs were labeled with PKH-26 using a red fluorescent cell linker kit (Sigma, PKH26GL) according to the manufacturer's protocol. In short, EVs were diluted with Diluent C, followed by incubation with 5 μM dye for 15 minutes at room temperature in the dark. Next, free dye was removed using a Sepharose CL-4B column coupled to an AKTASart, followed by concentration of EV-containing fractions with a 100-kDa Amicon spin filter. For *in vivo* studies, EVs were labeled with Alexa Fluor 790 NHS Ester dyes (ThermoFisher, A37569). EVs were incubated with 30 μM reactive dye in 0.1 M NaHCO_3 in PBS and incubated for 45 min at 37°C while shaking at 450 rpm. After labeling, dye was quenched using a final concentration of 50 mM Tris-HCl for 30 min and free dye was removed using a Sepharose CL-4B column coupled to an AKTASart. EV-containing fractions were concentrated using a 100-kDa Amicon spin filter.

UPy-PEG hydrogel preparation and EV loading

The UPy-PEG polymers with a 10k and 20k PEG-spacer were synthesized as described before (SyMO-Chem BV, Eindhoven, The Netherlands)³⁸. The hydrogelator powder was dissolved at a high pH (11.7) in PBS to the appropriate concentration. The mixture was vigorously shaken for 1 hour at 70 °C until a homogenous mixture was obtained. Subsequently, the mixture was cooled down to RT and pH was confirmed to be approximately 9.

EV release studies

UPy-hydrogels (10% w/w) of 100 μl were mixed with 10×10^{10} EVs in PBS of pH 9 to prevent pre-solidification. Liquid UPy-hydrogels were transferred to transwell inserts with 8 μm pore size (Greiner, 662638) and solidified by raising pH to 7.4. Release of EVs from UPy-hydrogels was examined by placing the transwell inserts in wells containing 1 mL of medium. Next, 200 μL of conditioned medium was collected at 6h, 24h, and 4 days and replaced with new medium after each time point. Release kinetics were assessed using flow cytometry after capturing EVs with antibody-coated magnetic beads, as described before³⁵. In short, EV-containing medium was incubated O/N with either, CD9-, CD81-, or CD63-antibody coated magnetic beads (ExoCap, JSR Life Sciences) and washed with 2% BSA in PBS. Subsequently, CD9-, CD81-, or CD63-Alexa647 antibody (CD9, BD Bioscience, 341648, clone M-L13; CD81, BD Biosciences, 551112, clone JS-81; CD63, BD Biosciences, 561983, clone H5C6) in PBS was added and incubated for 2 hours at RT while shaking. After washing with 2% BSA in PBS, samples were resuspended in 0.25% BSA in PBS for analysis. Mean fluorescence intensity (MFI) of bead-captured EVs was measured using flow cytometry (BD FACSCanto II).

EV functionality

For EV uptake experiments, PKH26-labeled EVs (22×10^{10}) were loaded into an UPy-hydrogel and placed into transwell inserts as described above. 1.2×10^5 HMEC-1 cells were plated in the lower compartment. After 4 days, EV uptake by HMEC-1 cells was determined using fluorescent microscopy. Cells were fixed using 4% PFA and incubated with a primary antibody for β -actin (1:1000) (Sigma, A5441) at RT for 1 hour, followed by incubation with Alexa Fluor 488 goat anti-mouse secondary antibody (1:2000) (Invitrogen, A11001). Nuclei were stained using TO-PRO-3 Iodide (ThermoFischer, T3605). Fluorescent images were taken using a confocal microscope (Zeiss, LSM 700).

EV functionality was also assessed by determining their effect on ERK1/2 phosphorylation as described before^{4321,43-45}. In short, 1.2×10^5 HMEC-1 cells were starved for 3 hours using basal MCDB131-medium, after which conditioned medium from EV-loaded UPy-hydrogels was added and incubated for 30 minutes. Cells were lysed using lysis buffer (Roche, 04719964000), followed by centrifugation at $14,000 \times g$ for 10 minutes. Protein levels of phosphorylated ERK1/2 and total ERK1/2 were assessed using Western Blotting.

Western blotting

Protein lysates were loaded on pre-casted Bis-Tris protein gels (ThermoFischer, NW04125BOX) and run for 1 hour at 160V. Next, proteins were transferred to PVDF membranes (Millipore, IPVH00010), followed by incubation with antibodies for 42/44 pERK1/2 (1:1000) (Cell Signaling, 43705), 42/44 ERK1/2 (1:1000) (Cell Signaling, 91025), Alix (1:1000) (Abcam, 177840), CD81 (1:1000) (Santa Cruz, sc-166029), CD63 (1:1000) (Abcam, 8219), Calnexin (1:1000) (Tebu-bio, GTX101676), or β -actin (1:7500) (Sigma, A5441). To visualize proteins a chemiluminescent peroxidase substrate (Sigma, CPS1120) was used. Quantification of the images was performed using ImageJ software (1.47V).

In vivo studies

Female Balb/CAnnCrl mice (age 10-12 weeks, weight 20-30 g), originally obtained from the Jackson Laboratory and kept in our own breeding facility, were housed under standard conditions with 12-h light/dark cycles and received standard chow and water ad libitum. All experiments were carried out according to the 'Guide for the Care and Use of Laboratory Animals', with prior approval by the Animal Ethical Experimentation Committee, Utrecht University, the Netherlands.

Mice were anesthetized by inhalation of 2.0% isoflurane in a mixture of oxygen/air (1:1). Subsequently, 350 μ L of 4×10^9 EVs (N=2) or 4×10^9 EV-loaded UPy-hydrogels (N=4) were injected subcutaneously in the right flank using a 25 Gy needle. The amount of EVs that were

injected was 4×10^9 . The needle was slowly retracted 30 seconds after injection to prevent any leakage from the injection site. Mice were euthanized three days after subcutaneous injection using sodium pentobarbital (60.0 g/kg). Skin and fat tissue around the injection site and UPy-hydrogels were excised and fluorescent images were acquired using a Pearl Impulse Imager (Licor), as described before⁵¹.

Statistical analysis

Data are presented as mean \pm SD. Unpaired student's *t* test was used for comparison of two groups. Significance levels were set as $p < 0.05$ or $p < 0.01$ as indicated.

Acknowledgements

The authors thank Maïke Brans (UMC Utrecht), Hemse Al-Khamisi (UMC Utrecht), and Maaïke Schotman (TU Eindhoven) for their excellent technical assistance and useful discussions.

This work is supported by the Project EVICARE (#725229) of the European Research Council (ERC) to JS and PYWD, co-funded by the Project SMARTCARE-II of the BioMedicalMaterials institute to JS/MJG, the ZonMw-TAS program (#116002016) to JS/ZL, the Dutch Ministry of Economic Affairs, Agriculture and Innovation and the Netherlands CardioVascular Research Initiative (CVON): the Dutch Heart Foundation to JS/MJG, Dutch Federations of University Medical Centers, the Netherlands Organization for Health Research and Development, and the Royal Netherlands Academy of Sciences. PV is funded by a VENI fellowship (#13667) from the Netherlands Organisation for Scientific Research (NWO).

The authors declare no conflicts of interest.

References

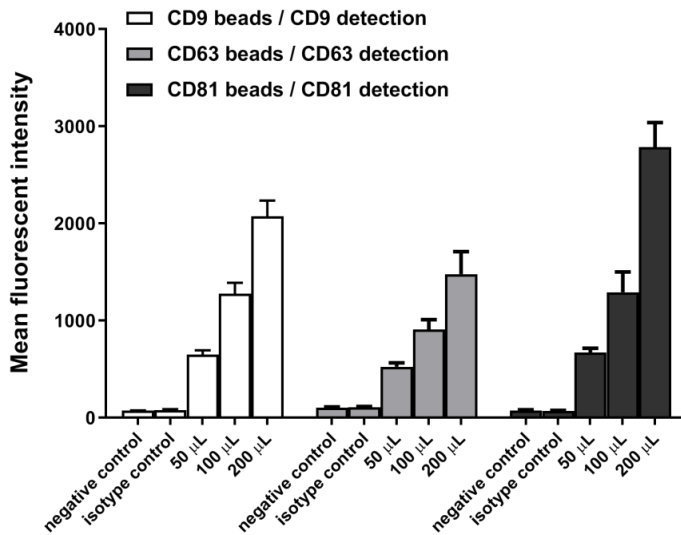
1. Maas, S. L. N., Breakefield, X. O. & Weaver, A. M. Extracellular Vesicles: Unique Intercellular Delivery Vehicles. *Trends Cell Biol.* **27**, 172–188 (2017).
2. Sluijter, J. P. G., Verhage, V., Deddens, J. C., van den Akker, F. & Doevendans, P. A. Microvesicles and exosomes for intracardiac communication. *Cardiovasc. Res.* **102**, 302–11 (2014).
3. György, B. *et al.* Membrane vesicles, current state-of-the-art: emerging role of extracellular vesicles. *Cell. Mol. Life Sci.* **68**, 2667–88 (2011).
4. Raposo, G. & Stoorvogel, W. Extracellular vesicles: Exosomes, microvesicles, and friends. *J. Cell Biol.* **200**, 373–383 (2013).
5. Haney, M. J. *et al.* Exosomes as drug delivery vehicles for Parkinson's disease therapy. *J. Control. Release* **207**, 18–30 (2015).
6. Tang, K. *et al.* Delivery of chemotherapeutic drugs in tumour cell-derived microparticles. *Nat. Commun.* **3**, 1282 (2012).
7. Li, J. J., Hosseini-Beheshti, E., Grau, G. E., Zreiqat, H. & Little, C. B. Stem Cell-Derived Extracellular Vesicles for Treating Joint Injury and Osteoarthritis. *Nanomater. (Basel, Switzerland)* **9**, 261 (2019).

8. Aghajani Nargesi, A., Lerman, L. O. & Eirin, A. Mesenchymal stem cell-derived extracellular vesicles for kidney repair: current status and looming challenges. *Stem Cell Res. Ther.* **8**, 273 (2017).
9. Mol, E. A., Goumans, M.-J. & Sluijter, J. P. G. Cardiac progenitor-cell derived exosomes as cell-free therapeutic for cardiac repair. *Exosomes Cardiovasc. Dis.* **998**, 207–219 (2017).
10. Chen, C. W. *et al.* Sustained release of endothelial progenitor cell-derived extracellular vesicles from shear-thinning hydrogels improves angiogenesis and promotes function after myocardial infarction. *Cardiovasc. Res.* **114**, 1029–1040 (2018).
11. Rohde, E., Pachler, K. & Gimona, M. Manufacturing and characterization of extracellular vesicles from umbilical cord-derived mesenchymal stromal cells for clinical testing. *Cytotherapy* **21**, 581–592 (2019).
12. Sisa, C. *et al.* Mesenchymal Stromal Cell Derived Extracellular Vesicles Reduce Hypoxia-Ischaemia Induced Perinatal Brain Injury. *Front. Physiol.* **10**, 282 (2019).
13. Piryani, S. O. *et al.* Endothelial Cell-Derived Extracellular Vesicles Mitigate Radiation-Induced Hematopoietic Injury. *Int. J. Radiat. Oncol. Biol. Phys.* **104**, 291–301 (2019).
14. Taheri, B. *et al.* Induced pluripotent stem cell-derived extracellular vesicles: A novel approach for cell-free regenerative medicine. *J. Cell. Physiol.* **234**, 8455–8464 (2019).
15. Burger, D. *et al.* Human endothelial colony-forming cells protect against acute kidney injury role of exosomes. *Am. J. Pathol.* **185**, 2309–2323 (2015).
16. Viñas, J. L. *et al.* Transfer of microRNA-486-5p from human endothelial colony forming cell-derived exosomes reduces ischemic kidney injury. *Kidney Int.* **90**, 1238–1250 (2016).
17. Gangadaran, P. *et al.* Extracellular vesicles from mesenchymal stem cells activates VEGF receptors and accelerates recovery of hindlimb ischemia. *J. Control. Release* **264**, 112–126 (2017).
18. Lopatina, T. *et al.* PDGF enhances the protective effect of adipose stem cell-derived extracellular vesicles in a model of acute hindlimb ischemia. *Sci. Rep.* **8**, 1–12 (2018).
19. Qin, Y., Sun, R., Wu, C., Wang, L. & Zhang, C. Exosome: A Novel Approach to Stimulate Bone Regeneration through Regulation of Osteogenesis and Angiogenesis. *Int. J. Mol. Sci.* **17**, (2016).
20. Barile, L. *et al.* Extracellular vesicles from human cardiac progenitor cells inhibit cardiomyocyte apoptosis and improve cardiac function after myocardial infarction. *Cardiovasc. Res.* **103**, 530–541 (2014).
21. Maring, J. A. *et al.* Cardiac Progenitor Cell-Derived Extracellular Vesicles Reduce Infarct Size and Associate with Increased Cardiovascular Cell Proliferation. *J. Cardiovasc. Transl. Res.* **12**, 5–17 (2019).
22. Perin, E. C. *et al.* Evaluation of Cell Therapy on Exercise Performance and Limb Perfusion in Peripheral Artery Disease: The CCTRN PACE Trial (Patients With Intermittent Claudication Injected With ALDH Bright Cells). *Circulation* **135**, 1417–1428 (2017).
23. Rigato, M., Monami, M. & Fadini, G. P. Autologous Cell Therapy for Peripheral Arterial Disease: Systematic Review and Meta-Analysis of Randomized, Nonrandomized, and Noncontrolled Studies. *Circ. Res.* **120**, 1326–1340 (2017).
24. Meyer, G. P. *et al.* Intracoronary bone marrow cell transfer after myocardial infarction: eighteen months' follow-up data from the randomized, controlled BOOST (BOne marrOW transfer to enhance ST-elevation infarct regeneration) trial. *Circulation* **113**, 1287–94 (2006).
25. Schächinger, V. *et al.* Improved clinical outcome after intracoronary administration of bone-marrow-derived progenitor cells in acute myocardial infarction: final 1-year results of the REPAIR-AMI trial. *Eur. Heart J.* **27**, 2775–83 (2006).
26. Hofmann, M. *et al.* Monitoring of bone marrow cell homing into the infarcted human myocardium. *Circulation* **111**, 2198–202 (2005).
27. Wiklander, O. P. B. *et al.* Extracellular vesicle in vivo biodistribution is determined by cell source, route of administration and targeting. *J. Extracell. Vesicles* **4**, 26316 (2015).

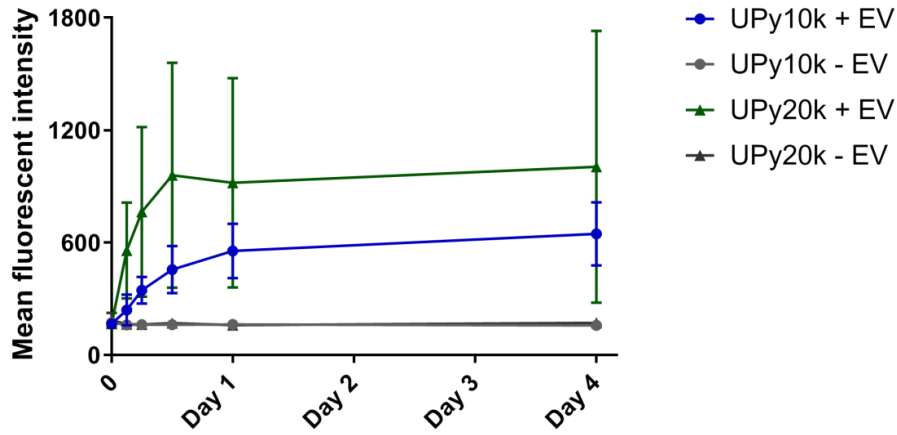
28. Lai, C. P. *et al.* Dynamic biodistribution of extracellular vesicles in vivo using a multimodal imaging reporter. *ACS Nano* **8**, 483–494 (2014).
29. Vader, P., Mol, E. A., Pasterkamp, G. & Schiffelers, R. M. Extracellular vesicles for drug delivery. *Adv. Drug Deliv. Rev.* **106**, 148–156 (2016).
30. van den Akker, F. *et al.* Intramyocardial stem cell injection: go(ne) with the flow. *Eur. Heart J.* **38**, 184–186 (2017).
31. Beegle, J. R. *et al.* Preclinical evaluation of mesenchymal stem cells overexpressing VEGF to treat critical limb ischemia. *Mol. Ther. Methods Clin. Dev.* **3**, 16053 (2016).
32. Silva, A. K. A. *et al.* Thermo-responsive Gel Embedded with Adipose Stem-Cell-Derived Extracellular Vesicles Promotes Esophageal Fistula Healing in a Thermo-Actuated Delivery Strategy. *ACS Nano* **12**, 9800–9814 (2018).
33. Fuhrmann, G. *et al.* Engineering extracellular vesicles with the tools of enzyme prodrug therapy. *Adv. Mater.* **30**, 1–7 (2018).
34. Nikraves, N. *et al.* Physical Structuring of Injectable Polymeric Systems to Controllably Deliver Nanosized Extracellular Vesicles. *Adv. Healthc. Mater.* **8**, e1801604 (2019).
35. Hernandez, M. J. *et al.* Decellularized Extracellular Matrix Hydrogels as a Delivery Platform for MicroRNA and Extracellular Vesicle Therapeutics. *Adv. Ther.* **1**, 1800032 (2018).
36. Spang, M. T. & Christman, K. L. Extracellular matrix hydrogel therapies: In vivo applications and development. *Acta Biomater.* **68**, 1–14 (2018).
37. Peña, B. *et al.* Injectable Hydrogels for Cardiac Tissue Engineering. *Macromol. Biosci.* **18**, e1800079 (2018).
38. Dankers, P. Y. W. *et al.* Hierarchical formation of supramolecular transient networks in water: a modular injectable delivery system. *Adv. Mater.* **24**, 2703–9 (2012).
39. Bastings, M. M. C. *et al.* Quantifying Guest-Host Dynamics in Supramolecular Assemblies to Analyze Their Robustness. *Macromol. Biosci.* **19**, e1800296 (2019).
40. Bastings, M. M. C. *et al.* A fast pH-switchable and self-healing supramolecular hydrogel carrier for guided, local catheter injection in the infarcted myocardium. *Adv. Healthc. Mater.* **3**, 70–78 (2014).
41. Bakker, M. H. *et al.* MRI Visualization of Injectable Ureidopyrimidinone Hydrogelators by Supramolecular Contrast Agent Labeling. *Adv. Healthc. Mater.* **7**, e1701139 (2018).
42. Bakker, M. H., van Rooij, E. & Dankers, P. Y. W. Controlled Release of RNAi Molecules by Tunable Supramolecular Hydrogel Carriers. *Chem. Asian J.* **13**, 3501–3508 (2018).
43. Mol, E. A., Goumans, M. J., Doevendans, P. A., Sluijter, J. P. G. & Vader, P. Higher functionality of extracellular vesicles isolated using size-exclusion chromatography compared to ultracentrifugation. *Nanomedicine Nanotechnology, Biol. Med.* **13**, 2061–2065 (2017).
44. Vrijssen, K. R. *et al.* Cardiomyocyte progenitor cell-derived exosomes stimulate migration of endothelial cells. *J. Cell. Mol. Med.* **14**, 1064–1070 (2010).
45. Vrijssen, K. R. *et al.* Exosomes from Cardiomyocyte Progenitor Cells and Mesenchymal Stem Cells Stimulate Angiogenesis Via EMMPRIN. *Adv. Healthc. Mater.* **5**, 2555–2565 (2016).
46. Mulcahy, L. A., Pink, R. C. & Carter, D. R. F. Routes and mechanisms of extracellular vesicle uptake. *J. Extracell. Vesicles* **3**, 1–14 (2014).
47. Millard, M. *et al.* mTHPC-loaded extracellular vesicles outperform liposomal and free mTHPC formulations by an increased stability, drug delivery efficiency and cytotoxic effect in tridimensional model of tumors. *Drug Deliv.* **25**, 1790–1801 (2018).
48. Qu, M. *et al.* Dopamine-loaded blood exosomes targeted to brain for better treatment of Parkinson's disease. *J. Control. Release* **287**, 156–166 (2018).
49. Royo, F., Cossío, U., Ruiz de Angulo, A., Llop, J. & Falcon-Perez, J. M. Modification of the glycosylation of extracellular vesicles alters their biodistribution in mice. *Nanoscale* **11**, 1531–1537 (2019).

50. Smits, A. M. *et al.* Human cardiomyocyte progenitor cells differentiate into functional mature cardiomyocytes: an in vitro model for studying human cardiac physiology and pathophysiology. *Nat. Protoc.* **4**, 232–43 (2009).
51. Kooijmans, S. A. A. *et al.* PEGylated and targeted extracellular vesicles display enhanced cell specificity and circulation time. *J. Control. Release* **224**, 77–85 (2016).

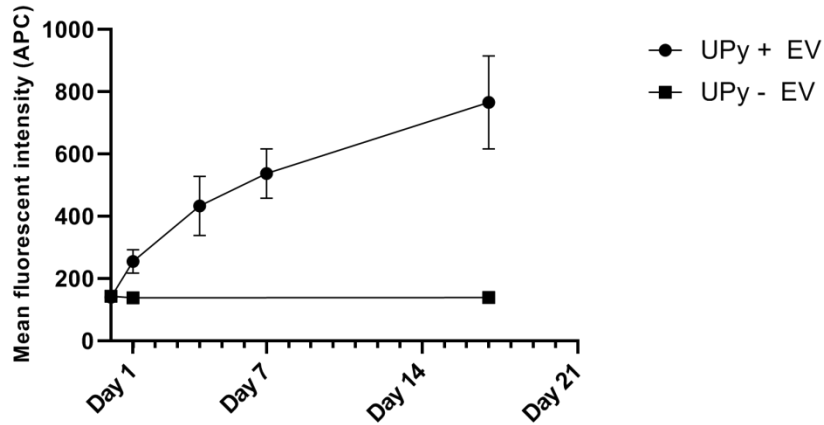
Supplemental material



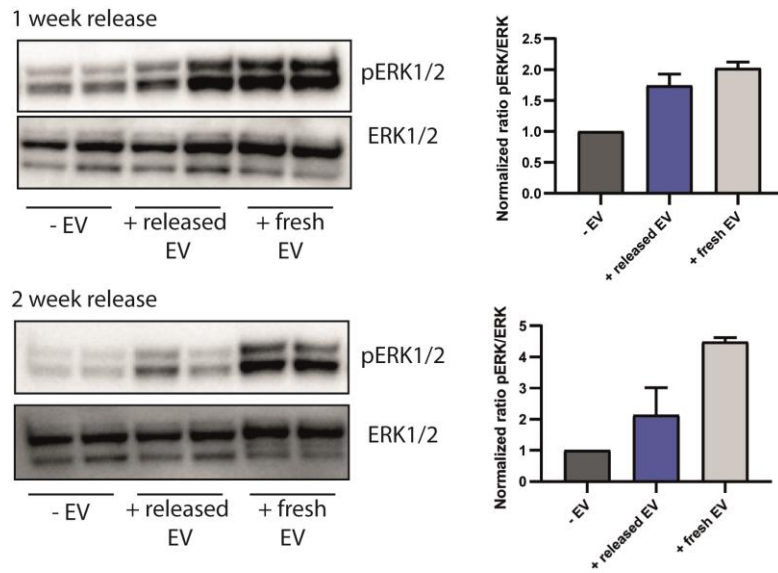
Supplemental Figure 1 EV derived from CPC can be captured using different markers. Conditioned medium (50, 100, and 200 µl) was collected from CPC and a bead capture assay was performed using magnetic beads coated with EV markers CD9, CD81, or CD63 and detected with its corresponding fluorescent antibody. Moreover, increasing volumes of conditioned medium results in higher fluorescent signals, indicating this assay may be used for semi-quantitation of EV release. Mean fluorescence intensity of negative- and isotype control are both at background level.



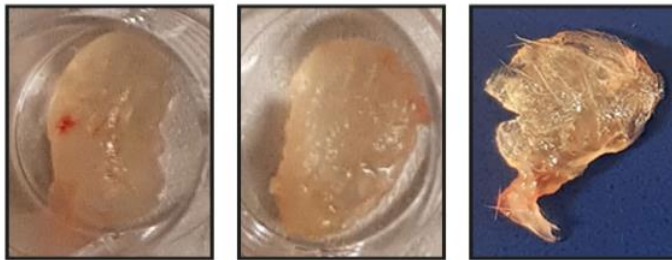
Supplemental Figure 2 Prolonged EV release using UPy10k-hydrogels compared to UPy20k. EV release patterns from UPy-hydrogels with a PEG block of 10 kg mol⁻¹ (UPy10k) or 20 kg mol⁻¹ (UPy20k) were compared. A prolonged and less variable EV release was observed when using UPy10k-hydrogels.



Supplemental Figure 3 Representative image of EV release from UPy-hydrogels measured for up to 2.5 weeks. EVs are continuously released from UPy-hydrogels when measured over a period of 2.5 weeks.



Supplemental Figure 4 Functionality of released EVs compared to fresh EVs. EVs released after 1 week still retain the ability to activate ERK to the same extent as fresh EVs. When released after 2 weeks, EVs still activate ERK signaling, although to a lower extent than fresh EVs.



Supplemental Figure 5 Solid-like gels could be detected in all mice after subcutaneous injection. EV-loaded UPy-hydrogels were subcutaneously injected in mice. 3 days after subcutaneous injection, UPy-hydrogels containing EVs were excised. In all mice we could detect the UPy-hydrogels (N=4 in total).

Effect of storage conditions on extracellular vesicle functionality *in vitro* and *in vivo*

Emma A. Mol MSc^{1,2}, Olivia de Cuba¹, Hemse Al-Khamisi BSc¹, Pieter Vader PhD^{1,3}, J.P.G. Sluiter PhD^{1,4,5}, Marie-José Goumans PhD²

In preparation

¹Department of Cardiology, Laboratory of Experimental Cardiology, University Medical Center Utrecht, Utrecht 3584, The Netherlands

²Laboratory of Cardiovascular Cell Biology, Department of Cell and Chemical Biology, Leiden University Medical Center, Leiden 2333ZA, The Netherlands

³Laboratory of Clinical Chemistry and Haematology, University Medical Center Utrecht, Utrecht 3584, The Netherlands

⁴UMC Utrecht Regenerative Medicine Center, University Medical Center, Utrecht 3584CT, The Netherlands

⁵University Utrecht, Utrecht 3508TC, The Netherlands

Abstract

Extracellular vesicles (EVs) are double-layered membrane particles secreted by cells that have attained increasing interest as disease biomarkers and therapeutic agents. Currently, we lack consensus on how to properly store EVs for different applications. While most studies investigated the effect of storage conditions on physiochemical properties of EVs, fewer studies have assessed if storage conditions affect EV functionality. In this study, we investigated physiochemical properties of cardiac progenitor (CPC)-derived EVs 1 day after storage at -80°C or 4°C , and assessed the effect on EV functionality in both *in vitro* and *in vivo* angiogenesis assays. Here, we show maintained EV size and protein marker expression after -80°C and 4°C storage when compared to freshly isolated EVs, while particle concentration slightly decreased after -80°C storage. Furthermore, we found no apparent difference between -80°C and 4°C -stored EVs *in vitro*, as assessed by ERK1/2 activation in human microvascular endothelial (HMEC-1) cells and wound closure capacity in a scratch migration assay. In addition, we assessed EV functionality in a subcutaneous Matrigel plug assay *in vivo* by quantification of the number of infiltrating CD31+ cells and total cell counts. We found similar numbers of infiltrating CD31+ cells between EV-loaded plugs when compared to PBS-loaded Matrigel plugs, although some plugs had increased numbers of CD31+ cells. In addition, total cell infiltration was non-homogeneously increased upon loading with -80°C and 4°C stored EVs when compared to PBS. No apparent difference was observed between -80°C and 4°C storage. Together, our results indicate preserved physiochemical properties and functionality after short-term CPC-EV storage, which could enable faster translation of EV-based therapeutics towards clinical application.

Introduction

Extracellular vesicles (EVs) are nano-sized, phospholipid bilayer enclosed endogenous messengers, containing a range of biological cargo including proteins, lipids, and RNA. The exact makeup and effects of EVs highly depend on the secreting cell type and external stimuli. Being part of the intercellular communication machinery, EVs can influence the cellular microenvironment and mediate both physiological and pathological processes. These combined properties make EVs an interesting source for both diagnostic and therapeutic applications^{1,2}.

To date, many reports have described EVs' therapeutic functionality both in *in vitro* and *in vivo* studies. At the same time, there is little information or consensus on how to best store them for different applications³⁻⁸. Recent studies have suggested that storage temperature affects EVs' physicochemical characteristics, such as size, morphological features, and protein content⁹⁻¹¹. While most studies have focused on the effect of storage conditions on physiochemical properties, little is known about the effect on EV functionality *in vitro* and *in vivo*.

To study the effect of storage temperatures on EVs' functionality, read-outs to assess EVs' biological effects are required. Previously, we have shown that cardiac progenitor cell (CPC)-derived EVs have a pro-angiogenic effect on endothelial cells *in vitro*, as determined by increased wound closure in a scratch migration assay and higher extracellular signal regulated kinase (ERK) activation in human microvascular endothelial cells (HMEC-1)^{4,6,12,13}. In addition, CPC-EVs stimulate angiogenesis in Matrigel plug assays *in vivo*⁶. To date, no direct comparative studies of different storage conditions on EV functionality have been performed *in vivo*. As we move towards employment of EVs for therapeutic use, the appropriate storage conditions to maintain EV functionality have to be established. Here, we evaluated potential storage mediated effects on CPC-EV functionality. EVs were characterized after overnight storage at -80°C or 4°C after which EV functionality was investigated in both *in vitro* and *in vivo* angiogenesis assays.

Materials and methods

Cell culture

Human fetal heart tissue was obtained by individual permission using standard procedures for written informed consent and prior approval of the ethics committee of the Leiden University Medical Center, the Netherlands. This is in accordance with the principles outlined in the Declaration of Helsinki for the use of human tissue. Cells were cultured on 0.1% gelatin-coated culture flasks. Human cardiac progenitor cells (CPCs) were cultured using SP++ medium (EGM-2 (Lonza, CC-3162) with 66% M199 (Gibco, 31150-030)) supplemented with 10% fetal bovine serum (Biowest, S1810-500), 1% Penicillin-Streptomycin (Gibco, 15140-122), and 1x MEM Non-

Essential Amino Acids Solution (Gibco, 11140-035), as described before¹⁴. Human microvascular endothelial cells (HMEC-1) were cultured in MCDB-131 (Gibco, 10372-019) with 10 ng/mL human Epidermal Growth Factor (EGF) (Peprotech/Invitrogen 016100-15-A), 1 µg/mL Hydrocortisone (Sigma H6909-10), supplemented with 10% fetal bovine serum (Biowest, S1810-500), and 10 mM L-Glutamine (Gibco, 25030-024) freshly added. All cell lines were maintained at 37°C and 5% CO₂ in a humidified incubator.

EV isolation and characterization

CPCs were grown until 80-90% confluency in SP++ culture medium, after which cells were washed with PBS and Medium 199 (M199) was added to collect cell secretions. After 24 hours, conditioned medium (CM) was collected and cleared from large debris by centrifugation at 2000 x *g* for 15 min, followed by filtration (0.45 µm). Next, CM was concentrated using 100 kDa molecular weight cut-off (MWCO) Amicon spin filters (Merck Millipore) and loaded onto a S400 highprep column (GE Healthcare, Uppsala, Sweden) using an AKTASStart (GE Healthcare) containing a UV 280nm flow cell. After elution, the EV-containing fractions were pooled, 0.45 µm filtered, and concentrated using a 100-kDa MWCO Amicon spin filter. Particle concentration and size distribution were analyzed fresh or after storage using Nanoparticle Tracking Analysis (Nanosight NS500, Malvern). Measurements were performed using a camera level of 15, and a detection threshold of 5. To assess protein marker expression, EVs were lysed using RIPA Lysis buffer (Sigma, 20-188). EV protein concentration was determined after storage using a microBCA protein assay kit (Thermo Scientific, 23235).

HMEC-1 stimulation

1.2 x 10⁵ HMEC-1 were starved in basal MCDB-131 medium for 3 hours. Next, HMECs were stimulated with 2 x 10¹⁰ EV particles for 30 minutes, after which cells were lysed using lysis buffer (Roche, 04719964000). Cell lysates were centrifuged for 10 minutes at 14.000 x *g*, and phosphorylated ERK1/2 and Akt, as well as total ERK1/2 and Akt protein levels were determined using Western Blotting.

Western blotting

Proteins were loaded on pre-casted Bis-Tris protein gels (ThermoFischer, NW04125BOX) and run for 1 hour at 160V, after which proteins were transferred to PVDF membranes (Invitrogen, IB401031). After incubation with antibodies for pERK1/2 (Cell Signaling, 43705), ERK1/2 (Cell Signaling, 91025), pAkt (Ser473) (Cell Signaling, 4060S), Akt (Cell Signaling, 9272S), Alix (1:1000) (Abcam, 177840), CD81 (1:1000) (Santa Cruz, sc-166029), CD63 (1:1000) (Abcam, 8219), CD9

(1:1000) (Abcam, ab92726), Calnexin (1:1000) (Tebu-bio, GTX101676), or β -actin (1:7500) (Sigma, A5441) a chemiluminescent peroxidase substrate (Sigma, CPS1120) was used to visualize the proteins. Quantification of the images was performed using ImageJ software (1.47V).

Scratch Assay

HMEC-1 were seeded in 48 well plates and grown overnight to 90-100% confluency. Cell monolayer was scratched in a straight line using a sterile 200 μ l pipet tip. Cells were washed with MCDB-131 and treated with: 1) 20% FBS in MCDB-131 (positive control), 2) MCDB-131 (negative control), 3) EVs in MCDB-131. Two distinct images per well were taken immediately and after 6 hours at 4x magnification (n=4). To quantify the scratch closure over time, images acquired from each sample were further analyzed using Adobe Photoshop CS6. All analyses were performed blinded for treatment.

In vivo Matrigel plug assay

Male Balb/CAnnCrl mice (age 10-14 weeks, weight 20-30 g), originally obtained from the Jackson Laboratory and kept in our own breeding facility, were housed under standard conditions with 12-h light/dark cycles and received standard chow and water ad libitum. All experiments were carried out according to the 'Guide for the Care and Use of Laboratory Animals', with prior approval by the Animal Ethical Experimentation Committee, Utrecht University, the Netherlands. Mice were anesthetized by inhalation of 2.0% isoflurane in a mixture of oxygen/air (1:1). Subsequently, 350 μ L of Matrigel was injected subcutaneously in the left flank using a 25 Gy needle. The Matrigel plugs were loaded with 1.5×10^{11} EVs stored at either 4°C (N=6) or -80°C (N=6), or with PBS (N=4). The needle was slowly retracted 30 seconds after injection to prevent any leakage from the injection site. Mice were euthanized 14 days after subcutaneous injection using sodium pentobarbital (60.0 g/kg). Matrigel plugs were excised and divided in two halves. One half was used for hemoglobin measurements and the other half for immunohistochemistry.

Hemoglobin measurements

Hemoglobin (Hb) levels in the plugs were assessed using QuantiChrom Hemoglobin Assay Kit (DIHB-250, BioAssay Systems). In short, plugs were incubated in RIPA buffer for 10 minutes at 4°C, followed by centrifugation at 9280 x g for 6 minutes at 4°C. Supernatant was collected and 200 μ L of QuantiChrom Reagent was added. OD values were measured at 390-405 nm and hemoglobin levels were calculated using blanks and calibrators (100 mg/dL). Hb levels were corrected for plug weight and expressed as mg/dL per mg Matrigel.

Immunohistochemistry

Matrigel plugs were fixed with formalin and embedded in paraffin. Plugs were sectioned and three sections at different tissue depths were selected for further staining and analysis. Slides were stained by haematoxylin and eosin (H&E). For detection of CD31+ cells, adjacent slides were stained using antibodies for CD31 (Santa Cruz Biotechnology, sc-1506-R), Goat α Rabbit Biotin (Vector, Ba1000), Streptavidin Alexa Fluor 555 Conjugate (Invitrogen, S21381), and counterstained with Hoechst 33342 dye (Invitrogen) for detection of total cell infiltration. Total cell infiltration was assessed by whole section scanning at a 4x magnification using CellSens software. Total cell infiltration was normalized to the PBS-loaded plugs, corrected for plug size, and expressed as total cell infiltration/mm². To assess the number of CD31 positive cells, three representative images were taken at a 20x magnification for each plug depth and manually counted by two independent and blinded observers. CD31+ cell numbers were normalized to the PBS-loaded plugs and expressed as CD31+ cells per hpf.

Statistical Analysis

All data are presented as mean \pm SD. Statistical analysis was performed using SPSS and Graphpad Prism. Samples were tested for normal distribution. Comparison between multiple groups was analyzed using one-way ANOVA and corrected for multiple comparisons by Tukey post-hoc testing.

Results

The aim of this study was to evaluate storage-mediated effects on EV characteristics and functionality. For this purpose, CPC-derived EVs were isolated and stored overnight at -80°C or 4°C. Mode size (Figure 1A) and mean size (Figure 1B) of freshly isolated EVs were approximately 90 nm, matching the classical size for EVs. This was not affected by overnight storage at either temperature. Particle numbers, however, decreased slightly following overnight storage at -80°C compared to freshly isolated EVs (Figure 1C), although the degree of particle loss varied between individual isolations (Supplemental Figure 1). Western blot analysis confirmed enrichment of EV markers CD63, CD81, CD9, and Alix in the EV isolates compared to cell lysate (Figure 1D). Expression of all EV markers was comparable between freshly isolated EVs, -80°C and 4°C stored EVs. β -actin was similarly expressed among all EV storage conditions and also present in cell lysate. ER marker protein calnexin was, as expected, only evident in cell lysate.

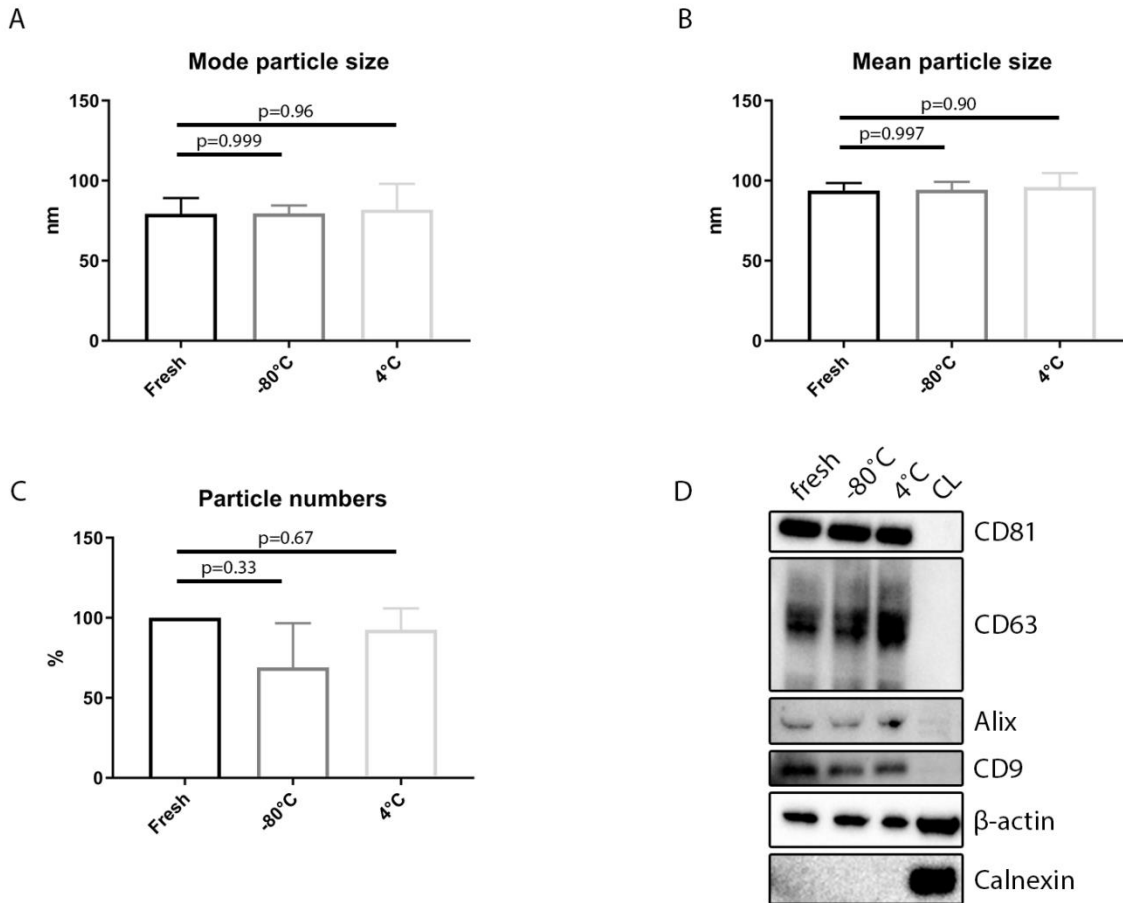


Figure 1 Characterization of freshly isolated EVs and EVs after storage at -80°C and 4°C. Mode size (A) and mean size (B) of freshly isolated EVs compared to EVs stored overnight at -80°C and 4°C as determined by Nanoparticle Tracking Analysis. Mode and mean size of EVs was not affected by overnight storage at -80°C and 4°C. Data are displayed as mean \pm SD of three replicate experiments. C) Particle numbers decreased slightly after storage at -80°C compared to freshly isolated EVs and EV storage at 4°C. Data are displayed as mean \pm SD of three replicate experiments. D) EV protein expression was determined using Western blotting. Samples were normalized for protein concentration determined after storage. Western blot analysis showed enrichment of common EV proteins CD81, CD63, CD9, and Alix in our EV preparation. EV markers were expressed similarly between EV storage conditions. β -actin was expressed in all EV conditions and in cell lysate. As expected, ER marker calnexin was only expressed in cell lysate. CL = cell lysate

Since CPC-EVs have been described to stimulate endothelial cell migration and activate endothelial cell signaling pathways, we used these two functional read-outs to compare the effect of storage conditions on EV functionality *in vitro*. HMEC-1 showed increased ERK 1/2 and Akt phosphorylation upon stimulation with EVs compared to PBS stimulation, regardless of storage condition (Figure 2A+B, full, uncropped blots in Supplemental Figure 2).

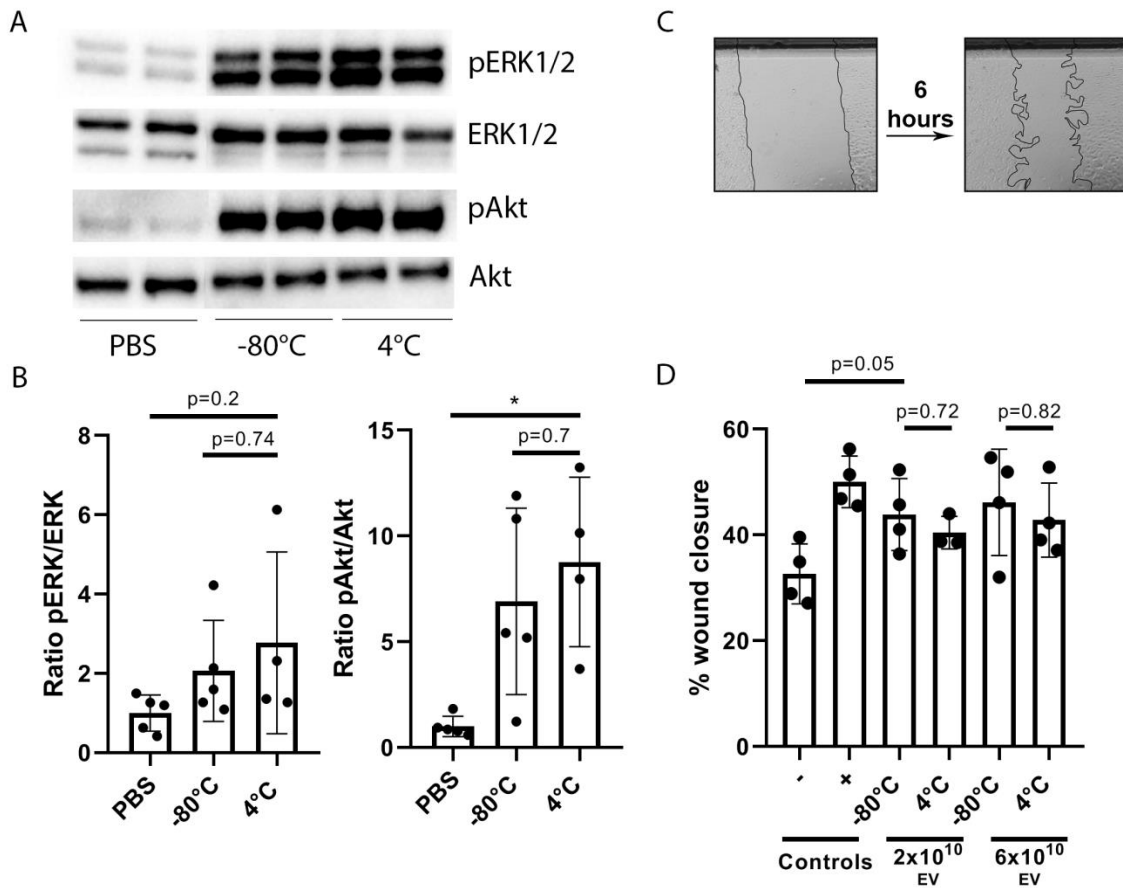


Figure 2 EVs, stored at 4°C and -80°C, showed no difference in functionality *in vitro*. A) HMECs were stimulated with 2×10^{10} EVs for 30 min, after which phosphorylated ERK1/2 and Akt as well as total ERK1/2 and Akt protein levels were determined using western blotting. (B) Ratios of pERK/ERK and pAkt/Akt were increased upon stimulation with EVs. No marked difference was observed between -80°C and 4°C stored EVs. (C) Scratch migration assay showed increased wound closure upon EV stimulation with no marked storage-mediated differences.

The second angiogenic assay we used to study the effect of storage temperature on EV functionality *in vitro* was a scratch migration assay. Percentage of wound closure was determined at baseline and after 6 hours follow-up (Figure 2C). After low dose EV stimulation (2×10^{10}), the percentage of wound closure increased to $40.5\% \pm 3.1\%$ for 4°C-stored EVs and $43.9 \pm 6.8\%$ in the presence of -80°C-stored EVs, as compared to the negative control ($32.6\% \pm 5.7\%$, $p=0.05$) (Figure 2D). Thus, no apparent differences between -80°C and 4°C storage could be observed ($p=0.72$). When stimulating with a higher EV dose (6×10^{10}), no additional increase in wound closure was observed compared to stimulation with a low EV dose ($43.9 \pm 6.8\% \pm$ for low

dose -80°C vs $46,17 \pm 10,06$ for high dose -80°C ($p=0.996$). Moreover, also here no difference could be observed between the -80°C and 4°C stored EVs ($p=0.82$).

Moving towards therapeutic applications of EVs, the effect of storage temperature on EV functionality should be studied *in vivo*, especially as the field increasingly recognizes that *in vitro* potency assays do not predict *in vivo* efficacy yet. Here, we investigated *in vivo* functionality of stored EVs using a subcutaneous Matrigel plug assay. Their angiogenic effect was assessed by determining hemoglobin levels in the plugs and infiltration of CD31+ cells after 14 days. Unfortunately, hemoglobin levels in all plugs did not exceed background levels, indicating that only low levels of hemoglobin were present inside the plugs (Supplemental Figure 3). Angiogenesis is marked by the *in-situ* proliferation and migration of resident endothelial cells. Therefore, CD31+ cell infiltration was used as a gauge for endothelial cell infiltration. Interestingly, the number of CD31+ cells per hpf was similar for EV-loaded (1.6 fold for -80°C stored EVs, $p=0.54$, 1.2 fold for 4°C stored EVs, $p=0.94$) and PBS-loaded Matrigel plugs (normalized to 1), although some plugs did show higher numbers of CD31+ cells when loaded with EVs compared to PBS (Figure 3B). Furthermore, there was no difference in the number of CD31+ cells between EVs stored at 4°C and -80°C ($p=0.70$). We also assessed total cell infiltration in Matrigel plugs, as we observed visual differences in cell counts between plugs. A non-homogenous increase of total number of cells was observed in plugs loaded with 4°C stored EVs (1.5 fold, $p = 0.1$) and in plugs loaded with -80°C stored EVs (1.3 fold, $p = 0.39$) when compared to PBS control (normalized to 1) (Figure 3C). No apparent difference was observed between the two storage conditions ($p=0.61$). Images of all Matrigel plugs are depicted in Supplemental Figure 4.

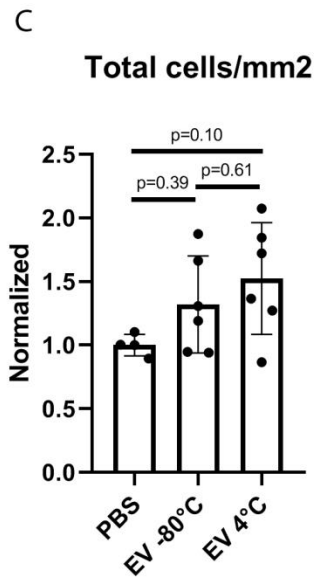
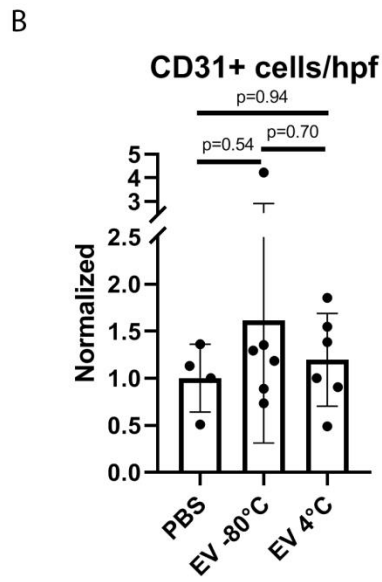
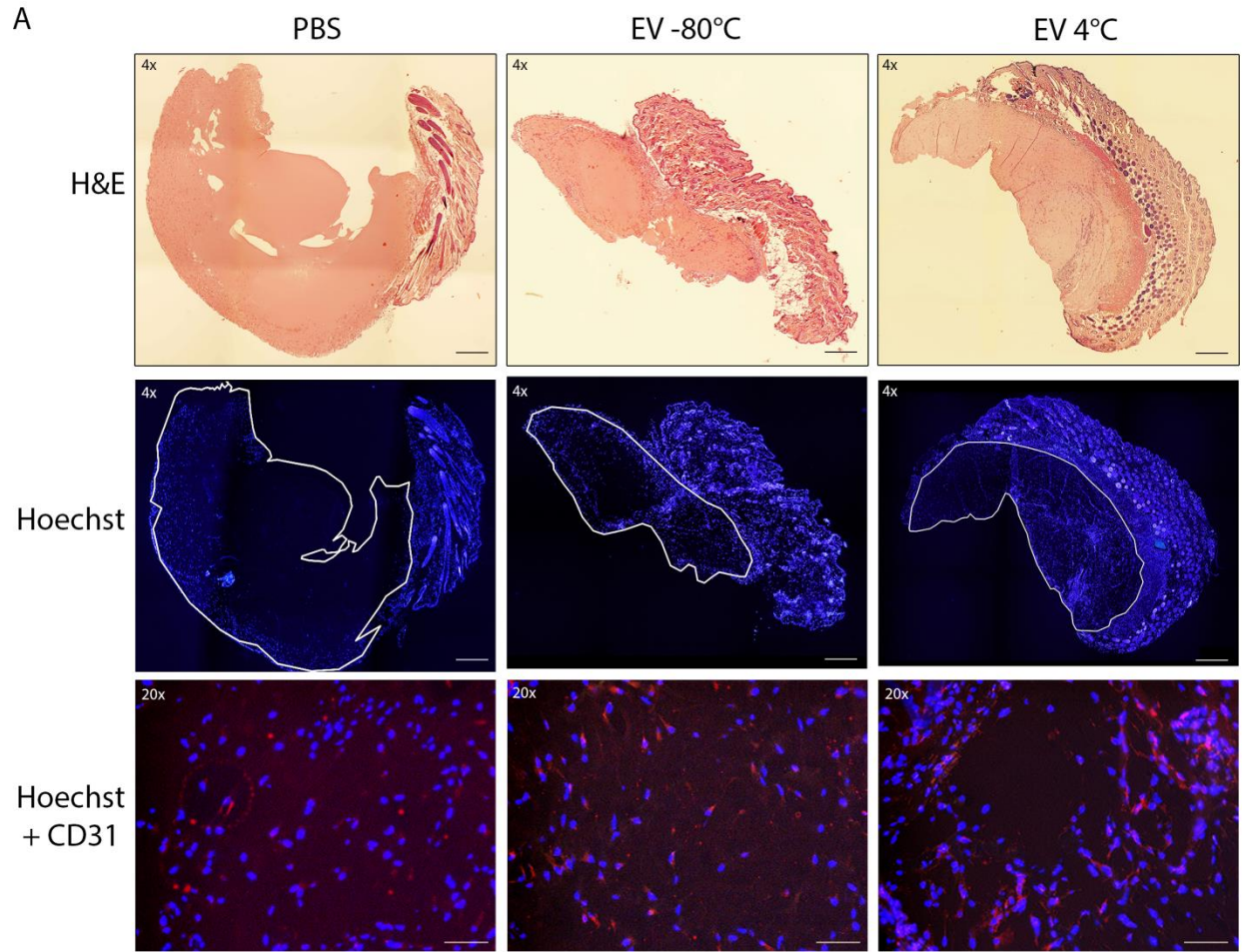


Figure 3 EVs increase cell infiltration into Matrigel plugs *in vivo* independently of storage condition. A) Representative images of Matrigel plugs loaded with PBS, 4°C stored EVs, and -80°C stored EVs. H&E staining was performed to visualize the Matrigel plugs. Immunofluorescent images were taken at 4x magnification to assess cell infiltration per mm² in the plug using whole slide scanning. Scale bar = 500 µm. The borders of the plugs are indicated with a white line. The amount of CD31+ cells are displayed per hpf at 20x magnification in red. Scale bar = 50 µm. B) Quantification of the number of CD31+ cells per hpf. The number of CD31+ cells was similar between all groups. C) Quantification of total cells per mm². The amount of total cell infiltration in the plugs was higher when loaded with EVs stored at 4°C and -80°C compared to PBS-loaded Matrigel plugs. There was no marked difference in total cell infiltration between storage conditions.

Discussion

EVs are endogenous messengers that have been implicated to contribute to various physiological and pathological processes. Therefore, EVs are increasingly being studied for both therapeutic and diagnostic purposes. Currently reported studies use EVs either fresh, stored at 4°C, frozen at -20°C or -80°C and thawed, or lyophilized for experiments, indicating that a golden standard is lacking. Recent studies have shown that storage temperature can influence EV characteristics such as size, number, and biological function, as assessed by *in vitro* studies⁹⁻¹¹. To ensure consistency between studies, it is important to assess the effect of EV storage condition on EV functionality for future work. The aim of this study was to directly compare characteristics and functionality of CPC-EVs, stored at 4°C and -80°C, using both *in vitro* and *in vivo* angiogenesis assays.

When assessing storage-mediated effects on EV characteristics, we observed that average EV sizes remained similar after storage at 4°C and -80°C, as compared to freshly isolated EVs. This finding is comparable to other studies that also showed no difference in EV size 1 day post storage at 4°C or -80°C^{10,11}. However, when stored for a period of 4 days at 4°C and -80°C, Maroto et al. observed a size shift towards larger EVs⁹. This could indicate that swelling, fusion or aggregation occurs when EVs are stored for longer time periods. Park et al., on the other hand, showed that median EV size decreased over time when stored for longer periods at 4°C and -80°C¹⁰. The reason for this apparent discrepancy is unclear, therefore future studies should determine if storage for longer periods of time affects size of other EV types, or that specifically used buffers are affecting EVs, and if this would have an effect on EV functionality *in vitro* and *in vivo*.

Next, we determined particle numbers directly after isolation and compared those to particle numbers after storage at 4°C and -80°C. Particle numbers slightly decreased after -80°C storage, although some variation was observed between individual isolations. A decrease in particle number could be the result of aggregation upon storage at -80°C, however, this should be reflected in a larger average EV size, which was not observed in our study. Other explanations may be that EVs adhere to the Eppendorf storage tubes, resulting in an apparent quantitative loss, or that EVs completely destabilize during the freeze-thawing process. There is some controversy regarding EV numbers after storage in current literature.

While some studies do show reduced particle numbers 1 day after 4°C storage, but not at -80°C¹¹, others do not detect differences in particle number when stored for longer periods at both 4°C and -80°C¹⁰. Ideally, when experimental dosing is based on particle number, particle numbers should be assessed on the day of experiments, to avoid inaccurate dosing due to under- or overestimation of particle count.

When comparing the expression of EV marker proteins CD81, CD9, Alix, and CD63, we found that protein marker expression was not different between 4°C and -80°C stored EVs nor when compared to freshly isolated EVs. Similarly, Park et al. observed preservation of the EV markers CD63 and CD81 at 4°C and -80°C for up to 25 days after EV storage¹⁰. Our results indicate that storage temperature at 4°C or -80°C for 1 day resulted in a maintained protein marker expression.

We used known angiogenic properties of CPC-EVs to investigate the effect of storage temperatures on EV functionality *in vitro*^{4,6,12,13}. Our findings show no apparent difference between 4°C and -80°C stored EVs, as assessed by ERK1/2 and Akt activation upon stimulation with EVs. In addition, the increase in wound closure after stimulation with EVs was similar for both storage conditions, suggesting preserved functionality after EV storage. We, however, did not observe a dose-dependent increase in wound closure upon stimulation with higher EV doses. This could indicate that the maximum EV dose to induce angiogenic effects is already reached at a lower dose. The study by Park et al. supports our findings, as maintained functionality of Kaposi's sarcoma-associated herpesvirus infected human endothelial cell-derived EVs on complement activation 1 day after storage at 4°C and -80°C was shown, with slightly higher biological activity of 4°C stored EVs¹⁰. In contrast, the antibacterial capacity of human neutrophilic granulocyte-derived EVs on *S. aureus* was impaired 1 day after storage at 4°C compared to fresh EVs¹¹. Also for -80°C stored EVs, a trend towards reduced antibacterial capacity was observed over time. These discrepancies between EV preparations from different cell sources suggest that EV functionality should be individually assessed for different cell-derived EVs, since the effect of storage temperatures on different biological functions could be varying between EV types due to different mechanisms of action. Our results indicate that, at least for a short period, CPC-EVs' pro-angiogenic functionality does not appear to be altered upon storage at 4°C or -80°C.

To our knowledge, we are the first to perform a direct comparative study of different storage conditions on EV functionality *in vivo*. We found no difference in the number of CD31+ cells between PBS-loaded and EV-loaded Matrigel plugs. Some EV-loaded plugs, however, did show higher numbers of CD31+ cells when compared to PBS-loaded plugs. Furthermore, we observed elevated non-homogenous cell infiltration in Matrigel plugs loaded with EVs compared to PBS, indicating no apparent differences between 4°C and -80°C stored EVs. This finding supports prior studies that have shown functional benefits after treatment with CPC-EVs stored at -80°C post-MI, although in these studies efficacy was not directly compared to freshly isolated EVs or EVs stored at 4°C^{3,5}.

The observation that increased total cell numbers in our study did not correlate with increased numbers of CD31+ cells may be explained by differences in experimental procedures. We assessed the number of CD31+ cells using representative images within the total plug area, while for quantification of total cell numbers we used whole slide scanning. As the highest number of infiltrating cells were detected at the borders of the plugs, the largest difference in infiltrating CD31+ cells might also be expected in these areas. Also, we observed only weak fluorescent staining of CD31, which might indicate we assessed CD31 expression close to the detection limit. Although this should be resembled in all conditions, it may have affected our ability to detect small differences. Other quantification methods have become available which allow for fast and straightforward quantification of cellular infiltrates in Matrigel plugs using multiple markers simultaneously¹⁵. Thus, future research should focus on optimization of the staining protocol or the quantification method.

Even though CD31 is often used as endothelial marker, it is not the only available marker for endothelial cells. Other proteins that are expressed in vascular networks and are regularly used as markers to assess cell infiltration in Matrigel plugs are CD34, α Smooth Muscle Actin, VE cadherin, and Von Willebrand factor^{6,15-18}. Furthermore, an interesting study has shown that early infiltrating cells in FGF2-loaded Matrigel plugs removed after 5 days represented a population of pericytes (based on expression of NG2, desmin, and PDGFbR), rather than an endothelial cell population (based on CD31 expression)¹⁷. After 9 days they found the majority of infiltrating cells formed vessel-like structures positive for NG2 and CD31, markers for cell types that together form mature blood vessels. Although we assessed the number of infiltrating cells at a relatively late time point (14 days), we could speculate that the increased cellular infiltrate in EV-loaded plugs may represent an early angiogenic infiltrating population rather than a mature population. Therefore, assessing multiple different vascular markers would be useful to better identify infiltrating cell types.

A different explanation for the observed increase in total cell infiltration, but not in absolute numbers of CD31+ cells, could be that the infiltrating cells are of different, non-vascular origin. In this study, we performed xenotransplantation of human-derived EVs in an immunocompetent mouse, raising the question whether the increased cell populations might be inflammatory cells. Proteomics analysis of our EV preparation indeed showed presence of human leukocyte antigens (HLA) class I proteins (data not shown), however, whether these proteins are functionally capable to allocate an immune reaction remains to be investigated. Future studies should focus on determining expression of additional markers to characterize angiogenic or other cell populations that infiltrate into EV-loaded Matrigel plugs in our study.

In conclusion, our results showed similar physiochemical properties for EVs stored at 4°C and -80°C when compared to freshly isolated EVs, and no apparent difference in EV functionality *in vitro* and *in vivo*. Thus, our findings provide useful information for appropriate short-term storage of CPC-EVs, which could contribute to faster clinical adoption of EV therapeutics.

Acknowledgements

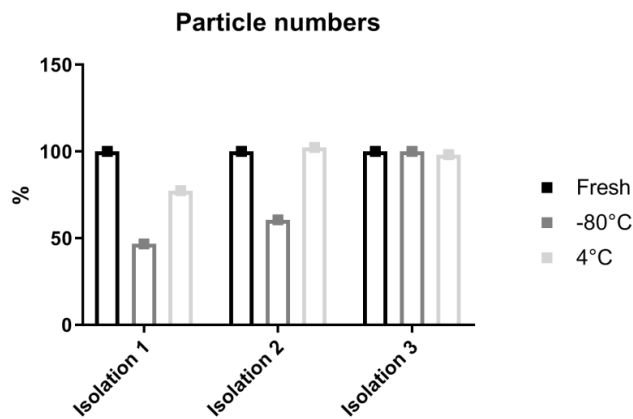
The authors thank M. Brans (UMC Utrecht) and P. van de Kraak (UMC Utrecht) for their excellent technical support. This work is supported by the Project EVICARE (#725229) of the European Research Council (ERC) to JS, co-funded by the Project SMARTCARE-II of the BioMedicalMaterials institute to JS/MJG, the ZonMw-TAS program (#116002016) to JS/MJG, the Dutch Ministry of Economic Affairs, Agriculture and Innovation and the Netherlands CardioVascular Research Initiative (CVON): the Dutch Heart Foundation to JS/MJG, Dutch Federations of University Medical Centers, the Netherlands Organization for Health Research and Development, and the Royal Netherlands Academy of Sciences.

References

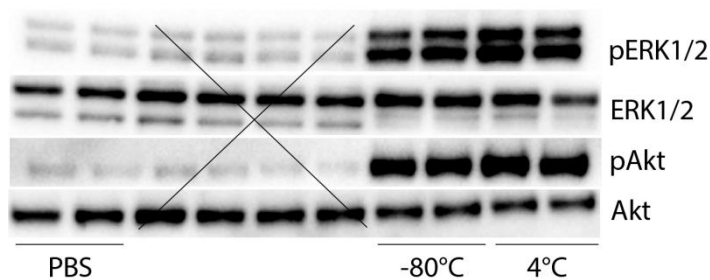
1. Lässer, C. Exosomes in diagnostic and therapeutic applications: biomarker, vaccine and RNA interference delivery vehicle. *Expert Opin. Biol. Ther.* **15**, 103–17 (2015).
2. Urbanelli, L. *et al.* Exosome-based strategies for diagnosis and therapy. *Recent Pat. CNS Drug Discov.* **10**, 10–27 (2015).
3. Barile, L. *et al.* Extracellular vesicles from human cardiac progenitor cells inhibit cardiomyocyte apoptosis and improve cardiac function after myocardial infarction. *Cardiovasc. Res.* **103**, 530–541 (2014).
4. Maring, J. A. *et al.* Cardiac progenitor cell-derived extracellular vesicles reduce infarct size and associate with increased cardiovascular cell proliferation. *J. Cardiovasc. Transl. Res.* **12**, 5–17 (2019).
5. Chen, L. *et al.* Cardiac progenitor-derived exosomes protect ischemic myocardium from acute ischemia/reperfusion injury. *Biochem. Biophys. Res. Commun.* **431**, 566–71 (2013).
6. Vrijssen, K. R. *et al.* Exosomes from Cardiomyocyte Progenitor Cells and Mesenchymal Stem Cells Stimulate Angiogenesis Via EMMPRIN. *Adv. Healthc. Mater.* **5**, 2555–2565 (2016).
7. Sahoo, S. *et al.* Exosomes from human CD34(+) stem cells mediate their proangiogenic paracrine activity. *Circ. Res.* **109**, 724–8 (2011).
8. Vandergriff, A. C. *et al.* Intravenous Cardiac Stem Cell-Derived Exosomes Ameliorate Cardiac Dysfunction in Doxorubicin Induced Dilated Cardiomyopathy. **2015**, (2015).
9. Maroto, R., Zhao, Y., Jamaluddin, M., Popov, V. L. & Wang, H. Effects of storage temperature on airway exosome integrity for diagnostic and functional analyses. *J. Extracell. Vesicles* **6**, (2017).
10. Park, S. J., Jeon, H., Yoo, S. & Lee, M. The effect of storage temperature on the biological activity of extracellular vesicles for the complement system. *In Vitro Cell. Dev. Biol. Anim.* **54**, 423–429 (2018).
11. Lőrincz, Á. M. *et al.* Effect of storage on physical and functional properties of extracellular vesicles derived from neutrophilic granulocytes. *J. Extracell. vesicles* **3**, 25465 (2014).
12. Vrijssen, K. R. *et al.* Cardiomyocyte progenitor cell-derived exosomes stimulate migration of endothelial cells. *J. Cell. Mol. Med.* **14**, 1064–1070 (2010).
13. Mol, E. A., Goumans, M. J., Doevendans, P. A., Sluijter, J. P. G. & Vader, P. Higher functionality of extracellular vesicles isolated using size-exclusion chromatography compared to ultracentrifugation. *Nanomedicine Nanotechnology, Biol. Med.* **13**, 2061–2065 (2017).
14. Smits, A. M. *et al.* Human cardiomyocyte progenitor cells differentiate into functional mature cardiomyocytes: an in vitro model for studying human cardiac physiology and pathophysiology. *Nat. Protoc.* **4**, 232–243 (2009).
15. Coltrini, D. *et al.* Matrigel plug assay: evaluation of the angiogenic response by reverse transcription-quantitative PCR. *Angiogenesis* **16**, 469–77 (2013).

16. Mikirova, N. A., Casciari, J. J. & Riordan, N. H. Ascorbate inhibition of angiogenesis in aortic rings ex vivo and subcutaneous Matrigel plugs in vivo. *J. Angiogenes. Res.* **2**, 2–7 (2010).
17. Tigges, U., Hyer, E. G., Scharf, J. & Stallcup, W. B. FGF2-dependent neovascularization of subcutaneous Matrigel plugs is initiated by bone marrow-derived pericytes and macrophages. *Development* **135**, 523–32 (2008).
18. O'Brien, M. J. *et al.* A unique role for galectin-9 in angiogenesis and inflammatory arthritis. *Arthritis Res. Ther.* **20**, 1–8 (2018).

Supplemental material

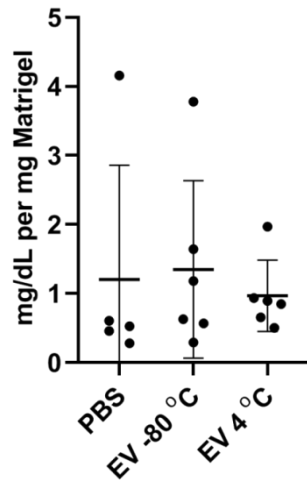


Supplemental Figure 1 Particle numbers of individual EV isolations. Mean particle numbers decreased upon storage at -80°C compared to freshly isolated EVs, although this varied between individual isolations.

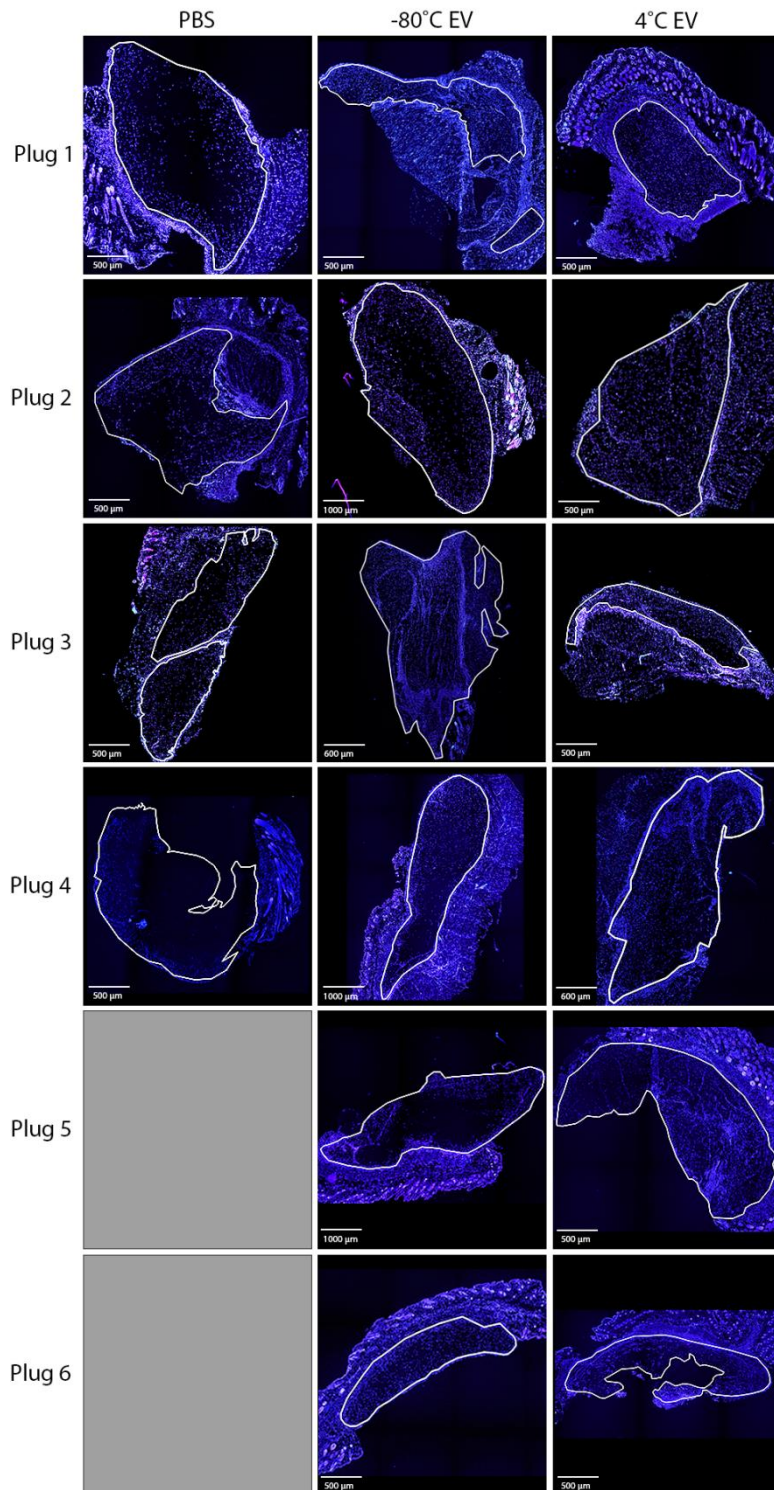


Supplemental Figure 2 Original image of western blot. Original image of western blot showing increased ERK1/2 and Akt activation upon stimulation with EVs.

Hemoglobin levels



Supplemental Figure 3 Hemoglobin levels in the Matrigel plugs. Hemoglobin levels were too low to detect differences between EV-loaded and PBS-loaded Matrigel plugs.



Supplemental Figure 4 Fluorescent images of all Matrigel plugs stained for nuclei.

Summary and general discussion

Extracellular vesicles for cardiac repair

Cardiovascular disease (CVD) is the number one cause of death worldwide, accounting for 32% of death worldwide¹. Ischemic heart disease has an estimated death rate of >9 million people a year. Over the last decade, acute mortality after MI has decreased due to better strategies including timely reperfusion. However, at the same time, approximately 25% of people that survive this initial ischemic event will develop heart failure (HF), which is characterized by the inability of the heart to provide a sufficient amount of blood to the body^{2,3}. For this chronically ill patient population, no curative treatments are available besides heart transplantation. Therefore, other treatment options are needed and being explored that either focus on preventing the development towards HF, or, focus on treatment of this chronic HF-patient population. The use of progenitor cells as a regenerative therapy to restore the initial cell loss after MI has been a huge focus area for the last decade.

Different types of progenitor cells have been considered as potential mediators of cardiac repair. Cardiac-derived progenitor cells (CPC) could be an attractive cell type to induce cardiac repair, since they originate from the heart itself and might be predisposed to activate internal cardiac reparative pathways. Furthermore, CPC are able to differentiate in all needed cardiac cell types^{4,5}. Interestingly, direct injection of CPC into the damaged myocardium resulted in improved cardiac function after MI, despite only 3-4% engraftment of these transplanted cells⁶. An immediate wash-out of cells through the venous drainage system was observed, indicating involvement of paracrine factors⁷. When injecting conditioned medium from mesenchymal stromal cells (MSC), Timmers et al. found the same benefit in infarct reduction as compared to cell injection⁸. After separating the conditioned medium into fractions smaller and larger than 1000 kDa, it was observed that only fractions larger than 1000 kDa were responsible for infarct reduction upon MI⁹. In depth research on the secretome of progenitor cells identified extracellular vesicles (EVs) as important components of conditioned medium carrying reparative properties¹⁰. EVs are nanosized, lipid bilayer-enclosed particles that play important roles in intercellular communication in both health and disease, which makes them an interesting source for therapeutic applications. Progenitor-cell derived EVs have been shown to provide endogenous protection after MI by transferring their cargo, *e.g.* miRNAs, lipids, and proteins, to cardiac cell types, thereby stimulating repair processes in the ischemic myocardium¹¹⁻¹⁵. An overview describing the potential of cardiac progenitor cell-derived extracellular vesicles (CPC-EVs) as therapeutics post MI was provided in **chapter 1**.

This thesis described the potential use of these cardiac progenitor-derived extracellular vesicles for cardiac repair and focused on translational aspects that could accelerate clinical implementation of EV-based therapeutics.

Optimization of EV production processes

EV isolation method

While EVs are increasingly being considered as potential therapeutics, some important aspects have to be addressed before their use as a product in clinical studies. First, one of the prerequisites for clinical application of EVs is a standardized, reproducible, and scalable isolation method^{16,17}. The most widely used EV isolation method and the current golden standard is differential ultracentrifugation (UC). However, this method is time consuming, has a limited scalability, and EV yield is operator-dependent^{18,19}. Furthermore, recent literature suggested that high speed centrifugation may induce aggregation and/or disruption of EVs due to high shearing forces, which might affect EV functionality^{20,21}. For this reason, alternative EV isolation methods are currently being explored, one of which is ultrafiltration combined with size-exclusion chromatography (SEC)²². This size-based separation of EVs from other media components is more standardized and highly scalable for clinical production. In order to assess if EV isolation method leads to differences in EV functionality, we compared EVs isolated with ultracentrifugation (UC-EV) to EVs isolated with chromatography (SEC-EV) *in vitro* in **chapter 2**. Here, we used CPC-EV-induced extracellular signal regulated kinase (ERK) phosphorylation in endothelial cells as read-out to investigate possible differences in EV functionality¹³. We found that SEC-EV resulted in higher functionality compared to UC-EV, indicated by more pronounced ERK activation in endothelial cells. This may be a consequence of the high shear forces that UC-EV have to withstand during high speed centrifugation. Consequently, signaling molecules on the UC-EV surface may be destroyed, thereby preventing their ability to activate, bind, or be taken up by recipient cells.

In order to validate our *in vitro* results in an *in vivo* model, we compared functionality of EVs obtained using different isolation methods, in a permanent ligation model, as well as an I/R injury model (**chapter 3**). To our surprise, we observed no difference in infarct size between PBS, UC-EV, and SEC-EV treated groups after permanent ligation nor after I/R injury, indicating the absence of a therapeutic effect upon EV injection. As a result, we were not able to assess if EV isolation influenced EV functionality *in vivo*. Our data is in contrast with previously reported studies that did observe reduced infarct size upon treatment with CPC-derived EVs²³⁻²⁵. A recent meta-analysis of controlled animal studies showed that EVs derived from several types of progenitor cells reduced infarct size and improved cardiac function²⁶. Therefore, finding the primary driving factor for this difference is of great importance for future employment of EV-based therapeutics. There are several possible explanations for the observed discrepancy, which will be discussed in separate subheadings below.

Cell source

As mentioned before, EVs derived from different progenitor cells have been used for cardiac repair²⁶. MSC-derived EVs have been shown to exert beneficial effects after MI in multiple

studies^{8-10,27}. MSCs can be obtained from bone-marrow or blood, allowing for clinical translation. However, MSC-EV have their own technical limitations, as, in our hands, MSCs cultured in serum-free medium fail to produce sufficient numbers of EVs for further analysis. Furthermore, a cell population originating from the heart itself, such as CPCs, might be more inclined to excrete beneficial mediators for the heart. Thus, although MSCs could be an interesting cell source, in this thesis we have focused on the use of CPC-EVs for cardiac repair.

CPCs can be isolated from human biopsies using different methodologies that are either based on surface markers (Sca1⁺-CPC or c-kit⁺-CPC) directly, or via explant culture (cardiosphere-derived cells (CDC))^{4,28,29}. When comparing the gene expression profiles of multiple CPC types, isolated using these different methodologies, no major differences were found between these CPC types³⁰. Interestingly, small differences were mainly related to individual CPC clones rather than CPC isolation methodology. One main difference between our study and a previously reported study by Maring et al. was the use of a different Sca1⁺ CPC clone for the *in vivo* studies²³. Within the heart, multiple Sca1⁺ CPC subpopulations have been discovered, which can be detected using different antibodies recognizing a glycosylation variant of their respective epitopes³¹. As different subpopulations may have different therapeutic efficacy, we compared the CPC clone used in our study to the CPC clone from the study by Maring et al. in a mouse study with long-term follow-up²³. However, treatment with neither of the CPC clones was able to improve cardiac function 1 and 4 weeks after MI, suggesting this possibility is unlikely to explain the different outcomes (data not shown).

Culture methods

Another potential explanation could be differences in culture methods. In order to purify our EV population and optimize our culture procedure for future human application, we cultured our cells in serum-free culture media before EV collection, whereas cells were previously cultured in 'EV-depleted' FBS-containing medium²³. EV-depleted serum is obtained via overnight ultracentrifugation of serum in order to deplete it from serum-derived EVs. It has been suggested that ultracentrifugation of serum does not deplete all serum-derived EVs, RNAs, and proteins³²⁻³⁵. Therefore, a possible explanation could be that serum-derived EVs, proteins and/or RNA are co-isolated when EV-depleted medium is used. This may, on its turn, be responsible for the observed functional difference of both EV types.

In order to investigate if differences in the presence of serum components could be the key explanation for the observed differences, we performed a pilot study. Here, we isolated CPC-EVs from either EV-depleted serum-containing medium (EV + serum) or serum-free medium (EV - serum) using ultracentrifugation and assessed EV purity and their biological effects using two *in vitro* angiogenesis assays (see Appendix). Our data suggest at least similar purity of EV + serum and EV - serum, as assessed by a similar ratio in particle number per 1 µg protein³⁶. In terms of function, biological activity of EV - serum was slightly increased when

compared to EV + serum, as assessed by two different *in vitro* angiogenesis assays. Therefore, these data are in contrast to our hypothesis that co-isolation of EV-depleted serum components could explain the observed differences in functional outcome *in vivo*. Yet, we may question the predictive value of these *in vitro* assays for therapeutic efficacy *in vivo*, since we observed no therapeutic benefits when injecting EVs derived from serum-free cultured cells after MI.

One important aspect that remains to be addressed, however, is the possibility that serum-free culturing might alter the composition and content of EVs, leading to reduced therapeutic efficacy *in vivo*. It has been described that EV content can be altered after stimulation of cells with different environmental cues, for example hypoxia, TNF- α stimulation, high glucose concentrations, or serum-free culturing³⁷⁻³⁹. Thus, serum-free culturing of CPC may alter the content of CPC-EVs, reducing levels of key components needed to exert functional effects in post-MI models *in vivo*. Proteomic analysis of EV - serum and EV + serum could reveal possible differences in protein composition between EVs obtained from cells with different culture methods and could provide insights on how intracellular signaling pathways are potentially affected by serum-free cell culture, which eventually might lead to altered EV protein content.

There is much more diversity in culture and isolation methods when we examined studies in literature. One of these differences is the time after which conditioned medium is being collected. While we collected conditioned medium after culturing cells for 24 hours, other studies cultured cells in serum-free medium for 48 hours, or for even longer periods of 7 or 15 days^{11,14,24,25,40}. Culturing cells in serum-free medium for such a long period of time should raise concerns about whether these cells are alive and healthy, and whether the EV isolates do not comprise apoptotic bodies. Furthermore, a variety of EV isolation methods are currently used to isolate EVs. Most studies either use ultracentrifugation, which is the current golden standard, or ultrafiltration to isolate EVs for assessing their therapeutic efficacy in *in vivo* studies^{9,14,23,40}. However, some reported studies have used ExoQuick or similar polyethylene glycol (PEG) solutions to precipitate EVs^{11,24}. While this method is simple and quick, there are concerns that this isolation method does not yield a pure population of EVs⁴¹. Moreover, differences can even be found within one isolation method. Although 1 hour of ultracentrifugation is sufficient to pellet EVs, some studies collect EVs after 4 hours of centrifugation¹⁴, which should also raise concerns on the purity of the isolated EV population. Altogether, as there are many different methods to obtain EVs, examining their effect on functionality *in vivo* is key to accelerate clinical adoption of EV therapeutics.

In conclusion, a variety of culture methods are used to culture cells before EV collection. Although our data do not support the hypothesis that co-isolation of EV-depleted serum components would explain our differences in therapeutic efficacy *in vivo*, we should examine whether serum-free culturing alters EV composition and content. Furthermore, future studies

should focus on the effect of different culture methods on EV functionality *in vivo* before clinical application of EVs.

MI model

An alternative explanation could be provided by differences in the experimentally induced MI model. Currently, we lack a standardized MI model to evaluate efficacy of new therapeutic strategies. As a result, reported studies that assess CPC-EVs' therapeutic efficacy have used a variety of MI models. For example, experiments have been performed in different animal species, have used a ligation or cryoinjury to induce cardiac damage, have used a permanent ligation model or I/R injury model, have been using different times of ischemia before reperfusion, or have been using a different time window or dosing regime. In addition, a plethora of different read-outs have been used to assess therapeutic efficacy, for example based on cardiac function or infarct size, which have in addition been assessed after different periods of time. Comparing all those different studies with one another and assessing the most potent therapeutic strategy is therefore a huge challenge.

In our study, we observed high variability in infarct sizes within the PBS treated group. We could speculate that picking up small differences is difficult with such high variations in initial infarct sizes. However, similar variabilities in infarct size have been observed in other studies^{25,42-44}. Therefore, technical differences in the experimentally induced MI model might not be the most likely explanation for the observed lack of therapeutic efficacy.

Dosing and timing of treatment

One of the challenges in EV research is to accurately quantify the number of EVs after isolation, which has resulted in the development of a large variety of technologies for EV quantification. Consequently, this has led to differences between studies with regards to the quantification method of EV dosing. Thus, while some studies applied an EV dose based on only the number of producing cells and not by a quantitative analysis, others based EV dosing on the number of particles, or amount of protein. The EV dose we employed differs from previously reported mouse studies using CPC-EV treatment after MI. Some examples are an EV dose of 2.8×10^9 particles¹¹, 6.5×10^8 particles⁴⁵, or an EV dose based on protein levels²³. Generally, when comparing our EV dosing (10×10^{10} particles per injection) to previous studies, we used higher particle numbers. Thus, in our study we may have administered too high doses, thereby failing to achieve therapeutic benefits post-MI. Reduced therapeutic effects have previously been observed *in vitro* when using a high EV dose of CPC-EVs when compared to a lower EV dose¹⁴. Although dose-dependency was only tested *in vitro*, this could indicate that overdosing may be important issue *in vivo* as well. However, a critical note is that particle numbers and protein concentration of EV preparations are dependent on their purity upon isolation, making a direct comparison very challenging.

Another explanation could be differences in the time of EV administration after MI. In our study, we performed intramyocardial injection of EVs 15 min after permanent ligation, while

others perform intramyocardial injections after 60 minutes^{14,25}. In our I/R model, we applied EV treatment at the moment of reperfusion, which is similar to one study¹⁴, but differs from another study that administered EVs 30 minutes after reperfusion²⁴. The optimal EV dose and timing of treatment needed for therapeutic efficacy post-MI has not been adequately covered by previous studies, and is therefore an important topic for future research. These variables can only be eliminated when performing dose-response experiments and investigating differences in timing of treatment in *in vivo* models of MI.

Altogether, several variables could be explaining the observed differences in therapeutic efficacy among studies. Future studies should focus on whether cell culture method, dosing, or timing of treatment could explain these apparent discrepancies. Once we have identified these key factor(s), we can proceed to validate if EV isolation methods lead to differences in EV functionality *in vivo*. For further investigation of EVs' therapeutic potential we propose to isolate EVs using SEC, although we were not able to assess if SEC-EVs have a beneficial therapeutic potential *in vivo* when compared to UC-EVs yet. Nevertheless, the biological activity of SEC-EVs has shown to be beneficial when compared to UC-EVs in multiple *in vitro* assays. Furthermore, EV isolation using SEC is a highly standardized, reproducible, and scalable method, which is essential to pursue EV therapeutics for clinical use.

EV storage

For therapeutic application, EVs have to be stored after isolation in order to use them immediately when required. The ability to store EVs upon isolation while maintaining their functionality is indispensable for future clinical application of EVs. Therefore, another important aspect to address within the EV production process is the effect of storage conditions on EV functionality. Currently, most studies describing the effect of storage on EVs have focused on physiochemical properties, while few studies are available that have assessed the effect of storage on EV functionality^{46,47}. Therefore, in **chapter 5** we investigated the effect of storage conditions on EV physiochemical properties such as size and concentration, and EV functionality *in vitro* and *in vivo*. Physiochemical characteristics of 4°C or -80°C stored EVs were similar 1 day after storage when compared to freshly isolated EVs. Furthermore, we found no apparent differences between 4°C stored EVs and -80°C stored EVs, as assessed by *in vitro* angiogenesis assays. In contrast, other studies showed altered physiochemical properties and impaired function of EVs *in vitro* after storage at 4°C or -80°C for periods varying between 1 to 25 days⁴⁶⁻⁴⁸. These differences may have been the result of differences in storage buffers, freeze-thawing procedures, or cellular mechanisms of action when using EVs derived from different cell types. Moving towards therapeutic applications of EVs, the effect of storage temperature on EV functionality should be studied *in vivo*, especially as the field increasingly recognizes that *in vitro* potency assays do not predict *in vivo* efficacy yet. We studied the effect of different storage conditions on EV functionality *in vivo* using a Matrigel plug assay. We found no statistically significant difference in the number of CD31+ cells between PBS-loaded and EV-loaded Matrigel plugs although some

EV-loaded plugs did show higher numbers of CD31+ cells. Furthermore, we observed elevated non-homogenous cell infiltration in Matrigel plugs loaded with 4°C or -80°C stored EVs when compared to PBS, indicating no apparent differences between 4°C and -80°C stored EVs. We have previously shown that CPC-EVs have strong pro-angiogenic effects, both *in vitro* and *in vivo*^{13,49}. However, the increased total cell numbers in our study did not correlate with increased numbers of CD31+ cells. Possible explanations for this disparity could be that the infiltration cells are vascular cells, but we do not detect them as such due to technical limitations, or that the infiltrating cells express other vascular markers. Alternatively, these infiltrating cells could be of a different, non-vascular, origin. We should first investigate these two potential explanations and validate our *in vivo* findings in a larger number of animals to be able to draw definite conclusions. However, altogether, our data suggest that short-term storage of EVs at -80°C does not affect functionality of CPC-EVs when compared to storage at 4°C, which is useful information that could eventually contribute to faster clinical adoption of EV therapeutics.

EV retention

The injection of cellular therapeutics has often demonstrated only modest beneficial effects in different patients groups, as a result of retention problems⁵⁰⁻⁵³. Similarly, strategies to enhance EV delivery in chronically diseased patients and prolong exposure of EV therapeutics have yet to be optimized to achieve their full potential for therapeutic efficacy. Given the immediate flush-out of cells after intramyocardial injection⁷, which may also be expected for EVs, strategies are being developed aiming to increase retention of therapeutics. A potential method for sustained EV release and to prolong therapeutic exposure is provided in **chapter 4**. Here, we evaluated the use of a hydrogel based on ureido-pyrimidinone (UPy) units coupled to poly(ethylene glycol) chains (UPy-hydrogel) as potential gradual release system for EVs. We found that UPy-hydrogels provide gradual release of EVs *in vitro* measured over a period of 4 days and that EVs retained their biological activity after release from UPy-hydrogel. In addition, we showed that UPy-hydrogel enhanced local EV retention *in vivo* after subcutaneous application. Another potential delivery platform for EVs are porcine-derived decellularized extracellular matrix (ECM) hydrogels⁵⁴. Here, the majority of released EVs were detected 1 day after encapsulation⁵⁵. Ultimately, we aim to investigate if EV-loaded hydrogels can enhance retention of EVs upon intramyocardial delivery and whether sustained EV release could increase therapeutic efficacy after MI compared to a single EV dose. However, examining EV retention in the mouse heart is still limited by the fact that accurate injection of such a small volume is challenging. Thus, when exploring the use of UPy-hydrogel to enhance EV retention upon intramyocardial delivery in future studies, we might be dependent on controllable infusion pumps that can accurately administer small volumes into the myocardium or on the use of larger animal models. Ultimately, this could contribute to improved efficacy upon local delivery of EV therapeutics.

Challenges in the translation of EV therapeutics

Since the discovery that EVs have potential reparative and/or regenerative capacity in multiple fields, the interest in EV therapeutics has expanded rapidly. However, as we move towards standardization and optimization of EV production processes and have successfully increased purity of our EV preparations, we are facing several challenges in translating these optimized preparations into therapeutically effective products on at least two different levels (Figure 1). Successful clinical translation starts with the discovery and assessment of EVs' biological effect using *in vitro* assays, followed by validation of these findings in preclinical animal models. In **chapter 3**, we showed that CPC-EVs were not able to reduce infarct size in two mouse models of MI. However, when assessing the functionality of the used CPC-EVs *in vitro*, we found that EVs were still able to activate ERK in endothelial cells, indicating some level of functionality *in vitro*. Therefore, one could question the predictive value of this *in vitro* assay. This lack of correlation between *in vitro* and *in vivo* functionality is one of the major challenges in the field of EV therapeutics, as we are currently not aware of an *in vitro* assay that is able to predict EV functionality *in vivo* for myocardial repair. Therefore, more effort in developing *in vitro* assays that are able to predict whether EVs induce cardiac repair *in vivo* is essential. Given that the therapeutic mode of action will likely be different and specific for each disease condition, we may need distinct *in vitro* assays for different therapeutic applications. Improving our understanding of CPC-EVs' mechanism of action (MoA) is essential for this. Functional assays are fundamental in order to proceed towards clinical use of EVs, as we must establish standardized validation methods of EVs' biological activity to be able to assess EV quality and batch-to-batch differences. To address these issues, members of four societies (SOCRATES, ISEV, ISCT, ISBT) proposed a potential quantifiable metrics to harmonize the definition of MSC-EVs and provide a guide to enable the comparison of EV manufacturing and define key physical and biological characteristics of MSC-EVs⁵⁶. These criteria included that the MSC-EV preparation must be defined according to their cellular origin, the presence of membrane lipid vesicles, physical and biochemical integrity of the vesicles, and biological activity. The development of such standardized quality assurance assays is fundamental to characterize and compare EV preparations and to ensure further translation of EV therapeutics.

An additional challenge in the translation of EV therapeutics is that EVs' therapeutic effect may not be as robust as was initially anticipated on²⁶, as it may be dependent on factors as culture methods, MI models, or dosages. This scenario might remind us of the stem cell therapy 'hype'. The major initial promise of stem cells to favorably alter the clinical course of major cardiovascular disease has quickly led to progression into huge and costly clinical trials, without proper understanding of their biological mechanism. Although stem cell therapy was found to be safe, these studies mostly found contradictory results in terms of efficacy⁵⁷⁻⁶⁰. Thus, as EV-based therapeutics are of somewhat similar complexity as stem cell therapeutics, we may take this as an example and improve understanding of CPC-EVs' mechanism of action before moving forward into clinical trials.

Moreover, exploring EVs' mechanism of action is essential for further clinical translation with respect to regulatory aspects⁶¹. With regards to the pharmaceutical classification of EV therapeutics derived from unmodified cells, EV therapeutics can be defined as biological medicines. Regulatory classification of drugs and most biological products is dependent on their pharmaceutically active substance. In contrast to pharmaceutical drugs, the active substance of cellular therapeutics does not necessarily have to be a defined molecule, but it can be defined as the cells themselves⁶². In that respect, the same definition could be applied to EV-based therapeutics. Although the MoA of EV-based therapeutics does not have to be sorted out completely before the start of the first clinical trials, an overview of a plausible hypothesized MoA must be provided when EV-based therapeutics are applied in the clinic^{63,64}. Therefore, although EV therapeutics still hold enormous potential, we must improve upon our understanding of their biology and mechanism of action in order to further pursue use of EV-therapeutics in clinical trials.

Future perspectives

Unraveling CPC-EVs' mechanism of action

As touched upon in the previous paragraph, understanding the mechanism by which CPC-EVs exert therapeutic benefits after MI is essential for moving towards translational use of EVs. In **chapter 1**, we have described four processes that can be targeted by new therapeutic strategies to stimulate cardiac repair after MI, which are: preventing cardiomyocyte apoptosis, regulating the immune response, stimulating vessel formation/angiogenesis, and reducing fibrosis. Furthermore, we mentioned the key mechanisms by which CPC-EVs are able to stimulate cardiac repair, of which the most well studied mechanisms of action are inhibition of cardiomyocyte apoptosis and stimulation of angiogenesis.

More recently, a few new studies were reported that showed the potential cardioprotective capacity of CPC-EVs. One of those studies showed that CPC-EVs were able to suppress proliferation of activated T cells, indicating their potential to balance the immune response after MI⁶⁵. Furthermore, the ability of CPC-EVs to lower cardiac fibroblast activation was shown in a 3D human fibrotic model⁶⁶. Lastly, a surface protein with anti-apoptotic properties was recently discovered in CPC-EVs called pregnancy associated plasma protein A (PAPP-A). PAPP-A is a protease and has been demonstrated to release bioactive insulin growth factor-1 (IGF-1) via proteolytic cleavage of IGF-binding protein-4 (IGFBP-4)¹⁴. The release of IGF-1 subsequently activates the IGF-1 receptor, which triggers intracellular ERK1/2 and Akt activation in HL-1 cardiomyocytes, leading to decreased caspase activity and reduced cardiomyocyte apoptosis. siRNA-knockdown of PAPP-A in CPC-EVs reduced the functional benefit after permanent MI in rats when compared to control CPC-EVs, indicating a cardioprotective role for PAPP-A¹⁴.

It is generally assumed that EVs exert their therapeutic effect via a combination of bioactive molecules, including *e.g.* miRNAs and proteins. However, an interesting study by Toh et al.

showed that it is not likely that the MoA of EVs is regulated via miRNAs, as the number of functional miRNA copies per EV is probably too low to exert a therapeutic effect⁶⁷. In contrast, proteins are usually present in a biologically relevant concentration, indicating that it is more likely that EVs exert their effect via a protein-based MoA. Therefore, future studies should focus more on this aspect. To date, most information on EVs' mechanism has been gathered by using proteomics or miRNA enrichment analysis, however, these analyses are usually limited by a lack of causal relation between the presence of the protein or miRNA and functional efficacy *in vitro* and *in vivo*. Two exceptions are studies on PAPP-A and on EMMPRIN that used knock-down experiments to show a causal relation between these proteins and a therapeutic effect^{13,14}. Ultimately, we are aiming to unravel the MoA by which CPC-EVs provide cardioprotection after MI. For that reason, we developed a protocol to perform single cell sequencing of the mouse heart which may potentially be used to identify the specific cardiac cell types and affected mechanisms upon EV uptake. This could provide insights into the MoA of CPC-EVs' upon MI.

EV-mimetic therapeutics

Interestingly, we have the ability to engineer EVs' surface and cargo through chemical and biological techniques, which is already extensively explored in the drug delivery field^{68,69}. If we are able to identify EVs' effector molecules in the coming years, we could use this knowledge to engineer EVs with more favorable characteristics. Furthermore, engineering cardiac homing peptides on EVs could lead to improved targeting to cardiac tissue. Ultimately, this may allow us to create unique EV-mimetic populations e.g. by engineering liposomes to carry cardioprotective molecules and targeting moieties. By using EV-mimetics, we could eliminate effects induced by culture conditions as a factor that can influence EV cargo. Furthermore, EV-mimetic therapeutics would contribute to enhanced standardization, scalability, and reproducibility for clinical application.

Importance of standardization in science

Chapter 3 in this thesis described results with an unexpected negative outcome. A potential contributor to this outcome may have been lack of standardization of experimental processes. This thesis described many discrepancies between reported studies on cell culture method, culturing time, EV isolation method, and MI models. As there are so many different variables introduced by using different experimental methods that could alter therapeutic outcome, this stresses the need to improve upon standardization of these processes.

Thus, when exploring innovative EV-based therapeutics for cardiac repair, we should standardize our EV production methods and establish a standardized and widely accepted MI model. Although this concept is widely acknowledged by others^{61,70}, major complications include the lack of understanding of the optimal culture conditions for EV collection, or the most optimal MI model. A worldwide collaboration of key opinion leaders would be required to develop such standardized recommendations. For EVs, first steps have already been made

by the International Society for Extracellular Vesicles to improve standardization by introducing guidelines on e.g. EV characterization, EV separation, and concentration^{17,71}. More effort must be put in development of - and adherence to those guidelines for cell culture methods, EV isolation method, purity, quantity, and MI models. Eventually, this could contribute to improved translation of innovative EV-based therapeutic strategies towards future clinical application.

Conclusions

In this thesis, the first steps have been made in optimizing EV production processes such as EV isolation and storage, in order to accelerate clinical adoption of EV therapeutics. However, we did not observe therapeutic efficacy of our CPC-EV treatment after MI, which is in contrast to previously reported studies. Thus, future studies should focus on exploring the cause of this discrepancy. While CPC-EVs hold great potential to serve as cell-free therapeutic for cardiac repair, more effort must be put in understanding EVs’ mechanism of action and increasing standardization of EV production processes in order to allow for further employment of EV-based therapeutics.

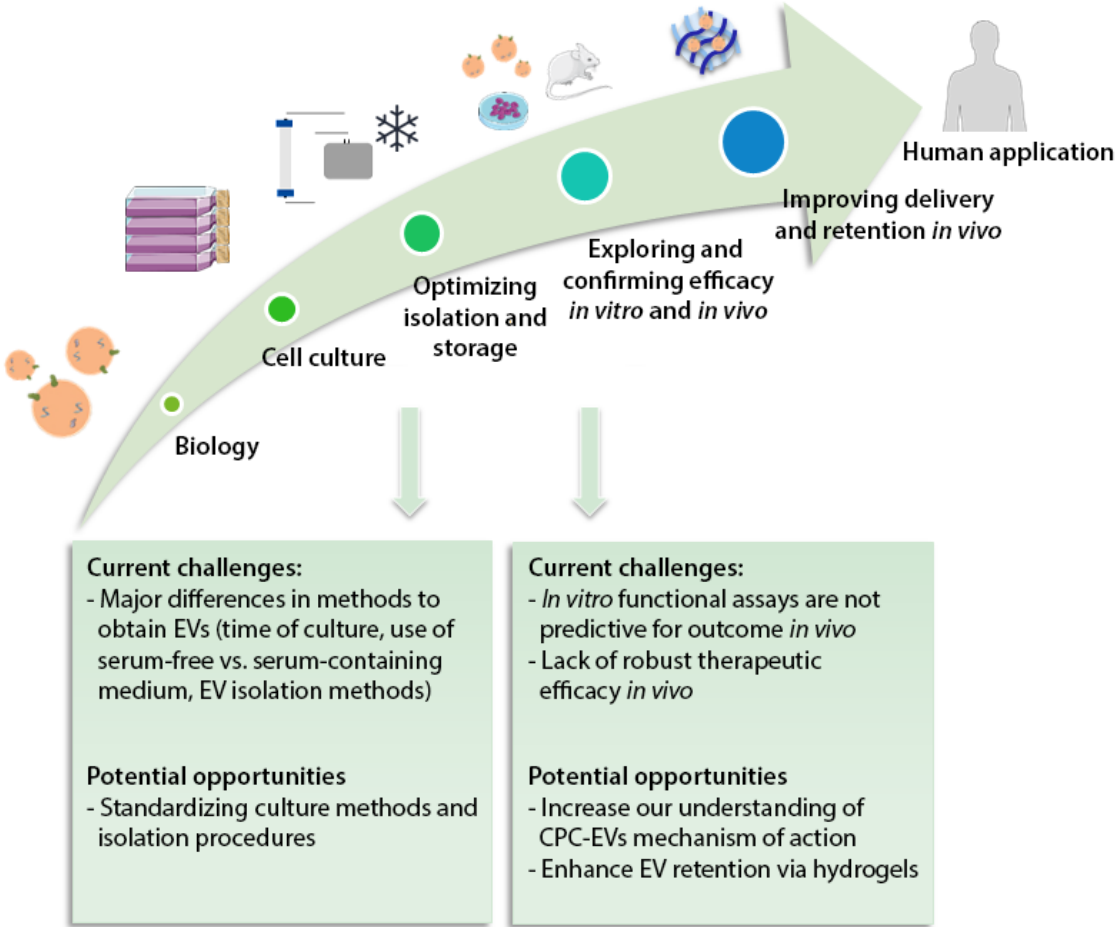
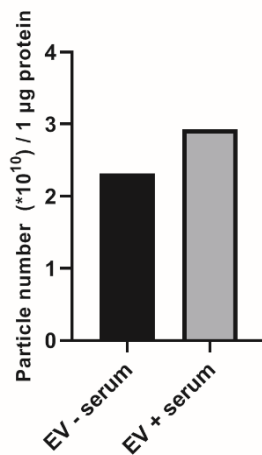


Figure 1 A translational perspective on EV therapeutics.

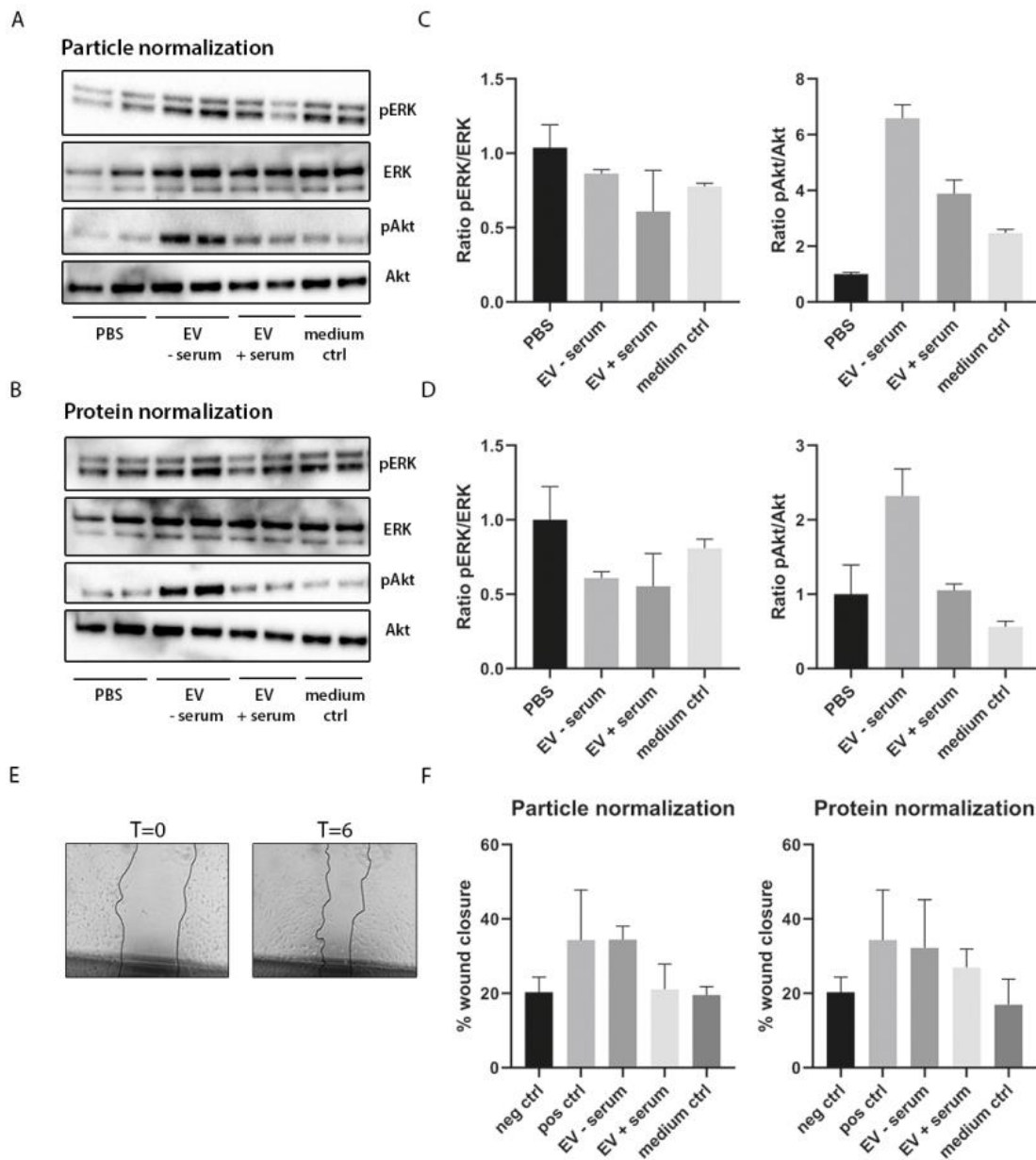
Appendix

In this pilot study, we aimed to investigate if co-isolation of serum-derived components when using EV-depleted serum-containing culture medium could explain the differences in therapeutic efficacy we found in comparison to the previous reported study by Maring et al²³. Therefore, we isolated CPC-EVs either from cells cultured in EV-depleted serum-containing medium (EV + serum) or serum-free medium (EV - serum) using ultracentrifugation. To assess if serum components are isolated from EV-depleted culture medium, we used non-conditioned EV-depleted serum-containing medium (medium ctrl) that underwent ultracentrifugation steps similar to conditioned medium as additional control. First, we assessed the purity of EV - serum and EV + serum, expressed by the ratio of the number of EV particles in 1 μg EV protein, as described before³⁶. EV + serum and EV - serum displayed no major difference in ratio between particle number per 1 μg protein, indicating comparable EV purity.



Supplemental Figure 1 Assessment of EV purity. EV purity of serum-free medium derived EVs (EV - serum) and EV-depleted serum-containing derived EVs (EV + serum), expressed as particle number per 1 μg EV protein.

To compare EV functionality of both preparations of EVs, we used two *in vitro* angiogenesis assays. We assessed the ability of EV + serum and EV - serum to activate both ERK and Akt and performed a scratch migration assay in endothelial cells. As shown in Figure 2, EV - serum activated ERK and Akt to a higher extent than EV + serum and medium ctrl (Figure 2A-D). Similarly, EV - serum treatment resulted in higher percentage of wound closure when compared to EV + serum and medium ctrl (Figure 2E+F). Therefore, biological activity of EV - serum was higher when compared to EV + serum and medium ctrl. These results indicate that, despite our expectation, co-isolation of serum components after culturing with EV-depleted medium would not explain the observed differences in functional outcome *in vivo*.



Supplemental Figure 2 Comparison of serum-free medium derived EVs (EV - serum) and EV-depleted serum-containing medium derived EVs (EV + serum) using *in vitro* angiogenesis assays. Non-conditioned serum-containing medium (medium ctrl) was used as additional control. A-B) HMEC-1 were stimulated with EVs, after which phosphorylation of ERK and Akt as well as total ERK and Akt were assessed using Western blotting. EVs were either normalized for similar number of particles (A) or similar protein content (B). C-D) Quantification of ratio pERK/ERK and pAkt/Akt for both particle and protein EV normalization. E) A scratch migration assay was performed in HMEC-1 and percentage of wound closure was assessed at baseline (T=0) and after 6 hours (T=6). F) Quantification of percentage of wound closure.

Supplemental methods

Cell culture

Human fetal heart tissue was obtained by individual permission using standard procedures for written informed consent and prior approval of the ethics committee of the University Medical Center Utrecht, the Netherlands. This is in accordance with the principles outlined in the Declaration of Helsinki for the use of human tissue. Cells were cultured on 0.1% gelatin-coated culture flasks. Human cardiac progenitor cells (CPCs) were cultured using EGM-2 (Lonza, CC-3162), with M199 (Gibco, 31150-030) supplemented with 10% fetal bovine serum (Biowest, S1810-500), 1% Penicillin-Streptomycin (Gibco, 15140-122), and 1x MEM Non-Essential Amino Acids Solution (Gibco, 11140-035), as described before⁵. Human microvascular endothelial cells (HMEC-1) were cultured in MCDB-131 (Gibco, 10372-019) with 10 ng/mL human Epidermal Growth Factor (EGF) (Peprotech/ Invitrogen 016100-15-A), 1 µg/mL Hydrocortisone (Sigma H6909-10), supplemented with 10% fetal bovine serum (Biowest, S1810-500), and 10 mM L-Glutamine (Gibco, 25030-024). HL-1 mouse cardiomyocytes were cultured using Claycomb medium (Sigma, 51800C), supplemented with 10% FBS, 1% Glutamax, 1% Penicillin-Streptomycin (Gibco, 15140-122), 0.3 mM Vitamin C (Sigma, A4034), and 0.1 mM Phenylephrine. Cells were incubated at 37°C with 5% CO₂ and 20% O₂ and passaged at 80-90% confluency after digestion with 0.25% trypsin.

Collection of conditioned medium

Conditioned medium (CM) was collected either from CPCs cultured in serum-free medium for 24 hours or from CPCs cultured in EV-depleted FBS-containing medium for 3 days. EV-depleted FBS-containing medium was prepared as follows. First, 33% FBS was mixed with 67% Medium 199, followed by centrifugation at 120.000 x *g* using a type 50.2 Ti fixed-angle rotor for 16 hours. Next, additional M199, EGM2, 1% Penicillin-Streptomycin and 1% MEM Non-Essential Amino Acids Solution were added. As an additional control, non-conditioned EV-depleted FBS-containing medium was kept for 3 days at 37°C, followed by similar isolation procedures, to assess if additional media components were isolated.

EV isolation

EVs were isolated using ultracentrifugation. First, conditioned medium was centrifuged for 15 min at 2000 x *g* and 0.45 µm filtered (0.45 Nalgene filter bottles) to remove cell debris. Next, EVs were pelleted by a 1 hour centrifugation at 100.000 x *g* using a type 50.2 Ti fixed-angle rotor. EVs were filtered (0.45 µm) and washed by a second 100.000 x *g* centrifugation step. EV pellets were dissolved in PBS, after which particle count was determined using Nanoparticle Tracking Analysis (Nanosight NS500, Malvern), using a camera level of 15 and a detection threshold of 5. EV protein levels were determined using a microBCA assay kit (Thermo Scientific, 23235).

Angiogenesis assays

Methods of the ERK/Akt activation assay and scratch migration assay are described in **chapter 5**.

References

1. WHO. *Global Health Observatory data*. (2019).
2. Hellermann, J. P. *et al.* Heart failure after myocardial infarction: a review. *Am. J. Med.* **113**, 324–30 (2002).
3. Kemp, C. D. & Conte, J. V. The pathophysiology of heart failure. *Cardiovasc. Pathol.* **21**, 365–371 (2012).
4. van Vliet, P. *et al.* Progenitor cells isolated from the human heart: a potential cell source for regenerative therapy. *Neth. Heart J.* **16**, 163–9 (2008).
5. Smits, A. M. *et al.* Human cardiomyocyte progenitor cells differentiate into functional mature cardiomyocytes: an in vitro model for studying human cardiac physiology and pathophysiology. *Nat. Protoc.* **4**, 232–243 (2009).
6. Smits, A. M. *et al.* Human cardiomyocyte progenitor cell transplantation preserves long-term function of the infarcted mouse myocardium. *Cardiovasc. Res.* **83**, 527–35 (2009).
7. van den Akker, F. *et al.* Intramyocardial stem cell injection: go(ne) with the flow. *Eur. Heart J.* **38**, 184–186 (2017).
8. Timmers, L. *et al.* Human mesenchymal stem cell-conditioned medium improves cardiac function following myocardial infarction. *Stem Cell Res.* **6**, 206–14 (2011).
9. Lai, R. C. *et al.* Exosome secreted by MSC reduces myocardial ischemia/reperfusion injury. *Stem Cell Res.* **4**, 214–22 (2010).
10. Arslan, F. *et al.* Mesenchymal stem cell-derived exosomes increase ATP levels, decrease oxidative stress and activate PI3K/Akt pathway to enhance myocardial viability and prevent adverse remodeling after myocardial ischemia/reperfusion injury. *Stem Cell Res.* **10**, 301–312 (2013).
11. Ibrahim, A. G. E., Cheng, K. & Marbán, E. Exosomes as critical agents of cardiac regeneration triggered by cell therapy. *Stem Cell Reports* **2**, 606–619 (2014).
12. Mackie, A. R. *et al.* Sonic hedgehog-modified human CD34+ cells preserve cardiac function after acute myocardial infarction. *Circ. Res.* **111**, 312–21 (2012).
13. Vrijssen, K. R. *et al.* Exosomes from cardiomyocyte progenitor cells and mesenchymal stem cells stimulate angiogenesis via EMMPRIN. *Adv. Healthc. Mater.* **5**, 2555–2565 (2016).
14. Barile, L. *et al.* Cardioprotection by cardiac progenitor cell-secreted exosomes: Role of pregnancy-associated plasma protein-A. *Cardiovasc. Res.* **114**, 992–1005 (2018).
15. Sahoo, S. *et al.* Exosomes from human CD34(+) stem cells mediate their proangiogenic paracrine activity. *Circ. Res.* **109**, 724–8 (2011).
16. Sluijter, J. P. G. *et al.* Extracellular vesicles in diagnostics and therapy of the ischaemic heart: Position Paper from the Working Group on Cellular Biology of the Heart of the European Society of Cardiology. *Cardiovasc. Res.* **114**, 19–34 (2018).
17. Théry, C. *et al.* Minimal information for studies of extracellular vesicles 2018 (MISEV2018): a position statement of the International Society for Extracellular Vesicles and update of the MISEV2014 guidelines. *J. Extracell. Vesicles* **7**, (2018).
18. Linares, R., Tan, S., Gounou, C., Arraud, N. & Brisson, A. R. High-speed centrifugation induces aggregation of extracellular vesicles. **1**, 1–7 (2015).
19. Bobrie, A., Colombo, M., Krumeich, S., Raposo, G. & Théry, C. Diverse subpopulations of vesicles secreted by different intracellular mechanisms are present in exosome preparations obtained by differential ultracentrifugation. *J. Extracell. vesicles* **1**, (2012).

20. Taylor, D. D. & Shah, S. Methods of isolating extracellular vesicles impact down-stream analyses of their cargoes. *Methods* **87**, 3–10 (2015).
21. Lamparski, H. G. *et al.* Production and characterization of clinical grade exosomes derived from dendritic cells. *J. Immunol. Methods* **270**, 211–226 (2002).
22. Nordin, J. Z. *et al.* Ultrafiltration with size-exclusion liquid chromatography for high yield isolation of extracellular vesicles preserving intact biophysical and functional properties. *Nanomedicine* **11**, 879–83 (2015).
23. Maring, J. A. *et al.* Cardiac progenitor cell-derived extracellular vesicles reduce infarct size and associate with increased cardiovascular cell proliferation. *J. Cardiovasc. Transl. Res.* **12**, 5–17 (2019).
24. Gallet, R. *et al.* Exosomes secreted by cardiosphere-derived cells reduce scarring, attenuate adverse remodelling, and improve function in acute and chronic porcine myocardial infarction. *Eur. Heart J.* **38**, 201–211 (2017).
25. Barile, L. *et al.* Extracellular vesicles from human cardiac progenitor cells inhibit cardiomyocyte apoptosis and improve cardiac function after myocardial infarction. *Cardiovasc. Res.* **103**, 530–541 (2014).
26. Yang, L. *et al.* Stem cell-derived extracellular vesicles for myocardial infarction: A meta-analysis of controlled animal studies. *Aging (Albany, NY)*. **11**, 1129–1150 (2019).
27. Zhao, Y. *et al.* Exosomes derived from human umbilical cord mesenchymal stem cells relieve acute myocardial ischemic injury. *Stem Cells Int.* **2015**, 761643 (2015).
28. Smith, R. R. *et al.* Regenerative potential of cardiosphere-derived cells expanded from percutaneous endomyocardial biopsy specimens. *Circulation* **115**, 896–908 (2007).
29. Beltrami, A. P. *et al.* Adult cardiac stem cells are multipotent and support myocardial regeneration. *Cell* **114**, 763–776 (2003).
30. Gaetani, R. *et al.* Different types of cultured human adult cardiac progenitor cells have a high degree of transcriptome similarity. *J. Cell. Mol. Med.* **18**, 2147–51 (2014).
31. Moerkamp, A. T. *et al.* Glycosylated cell surface markers for the isolation of human cardiac progenitors. **26**, 1552–1565 (2017).
32. Wei, Z., Batagov, A. O., Carter, D. R. F. & Krichevsky, A. M. Fetal bovine serum RNA interferes with the cell culture derived extracellular RNA. *Sci. Rep.* **6**, 31175 (2016).
33. Driedonks, T. A. P., Nijen Twilhaar, M. K. & Nolte-'t Hoen, E. N. M. Technical approaches to reduce interference of Fetal calf serum derived RNA in the analysis of extracellular vesicle RNA from cultured cells. *J. Extracell. vesicles* **8**, 1552059 (2019).
34. Shelke, G. V., Lässer, C., Gho, Y. S. & Lötvall, J. O. Importance of exosome depletion protocols to eliminate functional and RNA-containing extracellular vesicles from fetal bovine serum. **3078**, (2014).
35. Kornilov, R. *et al.* Efficient ultrafiltration-based protocol to deplete extracellular vesicles from fetal bovine serum. *J. Extracell. vesicles* **7**, 1422674 (2018).
36. Webber, J. & Clayton, A. How pure are your vesicles? *J. Extracell. Vesicles* **2**, 1–6 (2013).
37. Li, J. *et al.* Serum-free culture alters the quantity and protein composition of neuroblastoma-derived extracellular vesicles. **1**, 1–12 (2015).
38. Sluijter, J. P. G., Verhage, V., Deddens, J. C., van den Akker, F. & Doevendans, P. A. Microvesicles and exosomes for intracardiac communication. *Cardiovasc. Res.* **102**, 302–311 (2014).
39. de Jong, O. G. *et al.* Cellular stress conditions are reflected in the protein and RNA content of endothelial cell-derived exosomes. *J. Extracell. vesicles* **1**, (2012).
40. Vandergriff, A. C. *et al.* Intravenous cardiac stem cell-derived exosomes ameliorate cardiac dysfunction in doxorubicin induced dilated cardiomyopathy. **2015**, (2015).
41. Tang, Y. T. *et al.* Comparison of isolation methods of exosomes and exosomal RNA from cell culture medium and serum. *Int. J. Mol. Med.* **40**, 834–844 (2017).
42. Deddens, J. C. *et al.* Targeting chronic cardiac remodeling with cardiac progenitor cells in a murine model of ischemia / reperfusion injury. 1–17 (2017).
43. Ellenbroek, G. H. J. M. *et al.* Leukocyte-Associated Immunoglobulin-like Receptor-1 is

- regulated in human myocardial infarction but its absence does not affect infarct size in mice. *Sci. Rep.* **7**, 18039 (2017).
44. Frobert, A., Valentin, J., Magnin, J., Riedo, E. & Cook, S. Prognostic value of Troponin I for infarct size to improve preclinical myocardial infarction small animal models. **6**, 1–10 (2015).
 45. Kervadec, A. *et al.* Cardiovascular progenitor-derived extracellular vesicles recapitulate the beneficial effects of their parent cells in the treatment of chronic heart failure. *J. Hear. Lung Transplant.* **35**, 795–807 (2016).
 46. Maroto, R. *et al.* Effects of storage temperature on airway exosome integrity for diagnostic and functional analyses. *J. Extracell. vesicles* **6**, 1359478 (2017).
 47. Park, S. J., Jeon, H., Yoo, S., Lee, M. & Al, P. E. T. The effect of storage temperature on the biological activity of extracellular vesicles for the complement system. 423–429 (2018).
 48. Lorincz, A. *et al.* Effect of storage on physical and functional properties of extracellular vesicles derived from neutrophilic granulocytes. **1**, 1–8 (2014).
 49. Vrijssen, K. R. *et al.* Cardiomyocyte progenitor cell-derived exosomes stimulate migration of endothelial cells. *J. Cell. Mol. Med.* **14**, 1064–1070 (2010).
 50. Perin, E. C. *et al.* Evaluation of cell therapy on exercise performance and limb perfusion in peripheral artery disease. *Circulation* **135**, 1417–1428 (2017).
 51. Rigato, M., Monami, M. & Fadini, G. P. Autologous cell therapy for peripheral arterial disease: systematic review and meta-analysis of randomized, nonrandomized, and noncontrolled Studies. *Circ. Res.* **120**, 1326–1340 (2017).
 52. Meyer, G. P. *et al.* Intracoronary bone marrow cell transfer after myocardial infarction. *Circulation* **113**, 1287–1294 (2006).
 53. Schachinger, V. *et al.* Improved clinical outcome after intracoronary administration of bone-marrow-derived progenitor cells in acute myocardial infarction: final 1-year results of the REPAIR-AMI trial. *Eur. Heart J.* **27**, 2775–2783 (2006).
 54. Wang, R. M. & Christman, K. L. Decellularized myocardial matrix hydrogels: In basic research and preclinical studies. *Adv. Drug Deliv. Rev.* **96**, 77–82 (2016).
 55. Hernandez, M. J. *et al.* Decellularized extracellular matrix hydrogels as a delivery platform for microRNA and extracellular vesicle therapeutics. *Adv. Ther.* **1**, 1800032 (2018).
 56. Witwer, K. W. *et al.* Defining mesenchymal stromal cell (MSC)-derived small extracellular vesicles for therapeutic applications. *J. Extracell. vesicles* **8**, 1609206 (2019).
 57. Malliaras, K. *et al.* Intracoronary cardiosphere-derived cells after myocardial infarction: evidence of therapeutic regeneration in the final 1-year results of the CADUCEUS trial (CARDiosphere-Derived aUtologous stem CELls to reverse ventricUlar dySfunction). *J. Am. Coll. Cardiol.* **63**, 110–22 (2014).
 58. Perin, E. C. *et al.* Effect of transendocardial delivery of autologous bone marrow mononuclear cells on functional capacity, left ventricular function, and perfusion in chronic heart failure: the FOCUS-CCTRN trial. *JAMA* **307**, 1717–26 (2012).
 59. Rosen, M. R., Myerburg, R. J., Francis, D. P., Cole, G. D. & Marbán, E. Translating stem cell research to cardiac disease therapies: Pitfalls and prospects for improvement three sections with opinions separately and independently expressed by. *J. Am. Coll. Cardiol.* **64**, 922–937 (2014).
 60. Bolli, R. *et al.* Cardiac stem cells in patients with ischaemic cardiomyopathy (SCIPIO): Initial results of a randomised phase 1 trial. *Lancet* **378**, 1847–1857 (2011).
 61. Lener, T. *et al.* Applying extracellular vesicles based therapeutics in clinical trials - An ISEV position paper. *J. Extracell. Vesicles* **4**, 1–31 (2015).
 62. The European Parliament and the Council of the European Union. Directive 2009/83/EC on the Community code relating to medicinal products for human use. *Off. J. Eur. Communities* **269**, 1–188 (2000).
 63. EMA. Guideline on the requirements for quality documentation concerning biological investigational medicinal products in clinical trials. *Chinese J. New Drugs* **21**, 1–21 (2012).
 64. EMA. Guideline on the requirements to the chemical and pharmaceutical quality

- documentation concerning investigational medicinal products in clinical trials. **2**, 1–15 (2006).
65. van den Akker, F. *et al.* Suppression of T cells by mesenchymal and cardiac progenitor cells is partly mediated via extracellular vesicles. *Heliyon* **4**, (2018).
 66. Bracco Gartner, T. *et al.* Anti-fibrotic effects of cardiac progenitor cells in a 3D-model of human cardiac fibrosis. *Cardiovasc. Res.* **114**, S37–S37 (2018).
 67. Toh, W. S., Lai, R. C., Zhang, B. & Lim, S. K. MSC exosome works through a protein-based mechanism of action. *Biochem. Soc. Trans.* **46**, 843–853 (2018).
 68. Vader, P., Mol, E. A., Pasterkamp, G. & Schiffelers, R. M. Extracellular vesicles for drug delivery. *Adv. Drug Deliv. Rev.* **106**, 148–156 (2016).
 69. de Jong, O. G. *et al.* Drug delivery with extracellular vesicles: from imagination to innovation. *Acc. Chem. Res.* **52**, 1761–1770 (2019).
 70. Lecour, S. *et al.* ESC working group cellular biology of the heart: Position paper: Improving the preclinical assessment of novel cardioprotective therapies. *Cardiovasc. Res.* **104**, 399–411 (2014).
 71. Lötvall, J. *et al.* Minimal experimental requirements for definition of extracellular vesicles and their functions: A position statement from the International Society for Extracellular Vesicles. *J. Extracell. Vesicles* **3**, 1–6 (2014).